THE MESSENGER

EL MENSAJERO

Munich
La Silla
La Serena
Santiago

No. 39 – March 1985

New Infrared Photometer and F/35 Chopping Secondary at the 3.6 m Telescope

A. Moorwood and A. van Dijsseldonk, ESO

An F/35 chopping secondary mirror was installed and tested on the 3.6 m telescope in November 1984 together with a new infrared photometer which incorporates the TV acquisition and guiding system. In future, this system will replace the "F/8" photometer used until now. After a brief description of the chopper and photometer, we report here on the performance achieved during this first test using detector units essentially identical to those used with the old system and described by Moorwood in an earlier *Messenger* article (**27,** 11, 1982).

Chopping Secondary

Fig. 1 is a photograph of the 3.6 m telescope with the chopping secondary installed. As the mirror has a diameter of only 33 cm, it is rather more difficult to see than the normal F/8 secondary! It is attached to a unit, providing for chopping, focussing and rotation, which is supported by the special infrared top ring and spider assembly mounted in place of the usual optical top ring. The mirror is driven by magnetic actuators which are servo-controlled to provide either square wave chopping (for photometry) or a linear sweep on the sky (for speckle interferometry). Immediately behind it, a metal compensating plate having a similar moment of inertia is driven in opposition to the mirror by the same control system. This substantially improves the overall performance by suppressing any vibration of both the position sensor and the support spider. Chopping amplitude, frequency, centre position, angle and the focus are all remotely controlled via an HP terminal in the control room.

For the test, the servo system was adjusted to give a 5 ms rise time (90 % duty cycle at the frequencies around 10 Hz normally used for photometry) and yielded an end position stability of $\simeq$ 0.5 % of the amplitude up to values of 2 arcminutes on the sky.

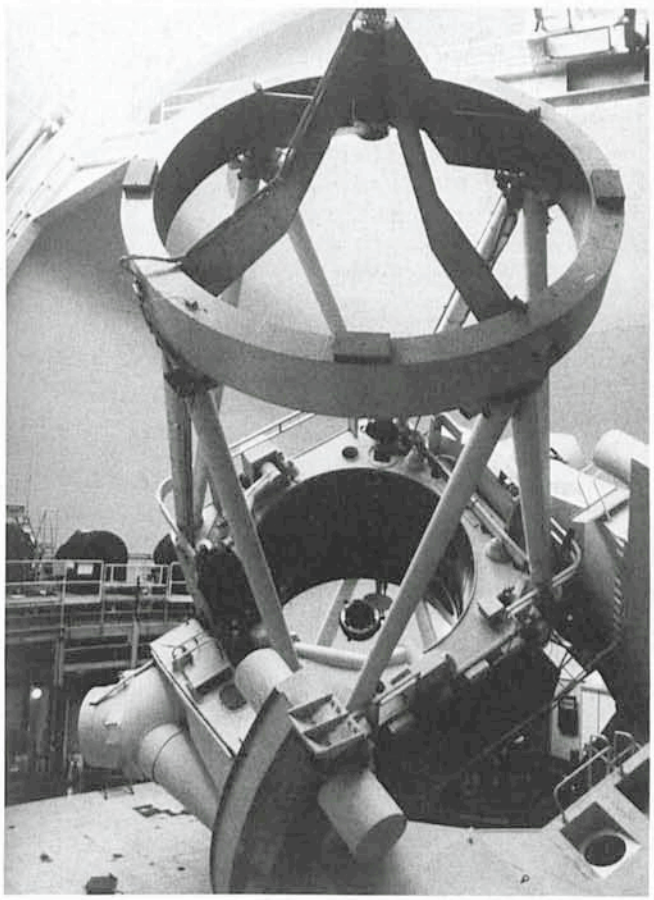

Fig. 1: *F/35 top ring and chopping secondary mounted on the 3.6 m telescope.*

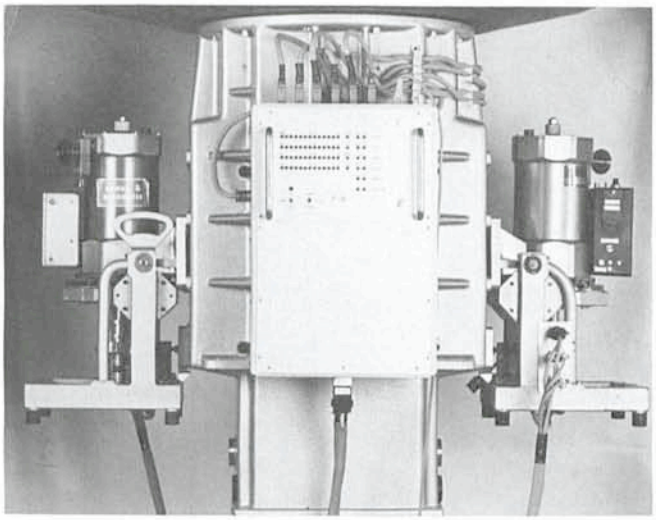

Fig. 2: *The new F/35 photometer.*

Photometer

Fig. 2 is a photograph of the new photometer mount shown supporting InSb and bolometer detector units equipped with standard photometric and CVF filters. The new speckle detector has also been designed to be compatible with this mount. Fig. 3 is a schematic of the optical layout and contains some basic data for the 3.6 m and also the 2.2 m telescope where it is planned to install an identical photometer for use with an F/35 chopping secondary unit to be built by the Max-Planck-Institut für Astronomie in Heidelberg. Although only one is shown, the detector units are in fact fed by separate dichroic mirrors which are supported in such a way that the centre of the field is either occupied by one of the dichroics or is completely unobstructed to allow acquisition of faint objects.

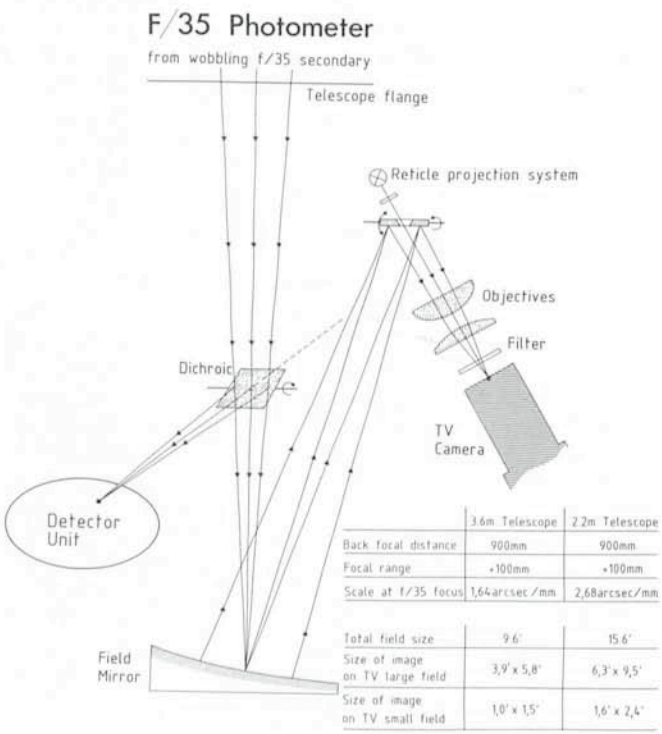

Fig. 3: *Optical schematic of the photometer illustrating the principle of the TV acquisition/guiding system.*

The TV camera is fixed and views the field via the field mirror, a small flat mirror located at the pupil image formed by the field mirror and one of two objectives which determine the instantaneous field sizes given in Fig. 3. The large field offers higher sensitivity for acquisition while the small field has a more optimum scale for guiding. For the latter purpose, offset guide stars can be located by scanning the instantaneous fields over the total field by tilting the small flat mirror. To the observer, this is equivalent to a normal X, Y movement of either the camera or a more conventional guide probe. With this mirror at its "centre field" position, the optical cross projected onto the camera is centred on the infrared beam and, to facilitate centring guide stars, its size is matched to the small field and hence shows the extent of the latter within the large field. For acquisition, the observer has the choice of viewing the chopped or a single image (with the chopper stationary in either beam or centred) which can either be direct or through the dichroic. Similarly, the telescope can be guided directly on the object being observed through the dichroic or on an offset guide star. In practice, these choices are determined by the object brightness. During the test, the dark sky limits were $m_v \simeq 19$ (direct), 16.5 (bolometer dichroic) and 14.5 (InSb dichroic) but it is hoped to improve these limits in future by cooling the camera which was not possible on this occasion for technical reasons. Provision for daytime observing has also been made by installing a second, infrared sensitive, TV camera such that it or the normal camera can be selected by simply moving a mechanical slide to which both cameras are permanently attached. Unfortunately, this first test of its performance was somewhat disappointing. At about 45° from the Sun it is possible to see stars down to m_H (1.65 μm) $\simeq 5$. This is better than the normal camera and should help ease the problem of pointing (by checking the telescope pointing on bright stars) but is inadequate for guiding.

As with the chopper, all the photometer functions (except switching between TV cameras) are remotely controlled from the control room.

Performance

Magnitude limits (1σ, 30 min., $\Phi = 7.5''$) determined during the test are summarized in Table 1 together with the improvements gained relative to the old "F/8" system. These are consistent with the increased throughput of the telescope plus photometer ($\simeq$ 40 % at 1.2 μm to $\simeq$ 25 % at 20 μm) and the reduction in thermal background emission. At 3.8 μm, an effective emissivity of 0.15 was measured for the telescope plus photometer compared with a value of about twice this determined for the old system using the same technique. The wavelength dependence of the sensitivity gain is determined by the relative contributions of the noise from the detector (dominant at J, H), the telescope thermal emission (L, N) and the thermal sky emission (M, Q). Variable noise at N and Q coupled with rapidly varying humidity on the nights available

TABLE 1: *Limiting magnitudes and improvement relative to the F/8 system*

BAND	J	H	K	L	M	N	Q
Centre Wavelength (μm)	1.25	1.65	2.2	3.8	4.8	10.3	18.6
Limiting Magnitude*	20.6	19.8	19	14.7	11.7	8.8	≃4.5
Improvement w.r.t. F/8	0.5	0.4	0.6	0.8	0.3	0.4	≃0.2

* Limits correspond to the 1σ noise measured through a 7.5" diameter diaphragm with a total integration time of 30 min.

for performance tests suggests that the magnitude limits quoted for these bands may have been somewhat degraded by an additional sky noise component.

The new system also offers several other performance advantages which are less directly obvious. No significant chopping offset signals are generated for example and there is thus no baseline drifting due to telescope flexure during long integrations. The possibility of direct guiding through the dichroics avoids the loss of time required to find offset guide stars and the availability of an optically generated reference cross permits accurate optical centring independently of the electronic stability of the TV system. Some observational flexibility has also been gained by virtue of the fact that switching between detectors, changing the chopping amplitude and direction, etc. are now relatively easy operations from the control room.

A Word of Thanks

Many ESO staff have been involved in the project at various stages. For their technical support in Garching we would like particularly to thank D. Enard, G. Hess, G. Huster, B. Jensen, J.-L. Lizon, M. Moresmau, W. Nees, J. Paureau and G. Raffi. During the installation and test we were also ably assisted by the La Silla staff and are particularly grateful for the invaluable help given by T. Bohl, P. Bouchet, F. Gutierrez, G. Ihle, J. Roucher and K. Teschner.

Tentative Time-table of Council Sessions and Committee Meetings in 1985

May 20	Users Committee
May 21	Scientific Technical Committee
May 22–23	Finance Committee
May 30	Committee of Council, Berlin
May 30–31	Council, Berlin
June 4–5	Observing Programmes Committee, Zürich
November 12	Scientific Technical Committee
November 13–14	Finance Committee
December 11–12	Observing Programmes Committee
December 16	Committee of Council
December 17	Council

All meetings will take place at ESO in Garching unless stated otherwise.

AS 338 in Outburst, or How I Found my "Pet Symbiotic"

R. Schulte-Ladbeck, Landessternwarte Heidelberg-Königstuhl

Until some months ago, I used to envy those of my colleagues who were always talking and writing with tremendous enthusiasm about *their favourite object*. My recent observations of the symbiotic star AS 338 enable me now to tell an exciting story as well.

Did I Observe the Right Object?

Symbiotic systems contain late-type (bright) giants or Miras and, in addition, a hot radiation source. They are surrounded by gaseous and dusty envelopes. Therefore, their radiation should be polarized due to scattering in the atmospheres of the late-type stars and/or the circumstellar nebulae. In October 1983, I started a multifilter linear polarization survey of 16 symbiotic stars, using the 1.23 m telescope of the German-Spanish Astronomical Centre. Only four stars showed sufficiently large intrinsic polarization that could be separated from the interstellar component. These were such fashionable symbiotics as HM Sge, V1016 Cyg and R Aqr and, last not least, AS 338. The wavelength dependence of the polarization and the position angle of AS 338 as displayed in Fig. 1 show some interesting properties: a pronounced maximum of the polarization in the B-filter and a significant, sharp rotation of the position angle at H_α. In a forthcoming article in *Astronomy and Astrophysics* I shall show in detail that the polarization of AS 338 can be explained by two scattering regions: Mie scattering by solid particles in the extended atmosphere of the M star and Thomson scattering in an asymmetric circumstellar nebula (possibly an accretion disk around a companion star). Encouraged by this result I decided that AS 338 merits a more thorough investigation. Luckily, the low declination of AS 338 allows its observation from the southern hemisphere as well. In July/August 1983, I had observing time at ESO's 1.5 m and 50 cm telescopes for spectroscopic and photometric studies of southern symbiotic stars. During this observing run, I had already secured one IDS spectrum in the range 4500 to 6800 Å and UBVRI photometry of AS 338. Subsequently, I could convince my colleague F. J. Zickgraf of the importance of getting JHKL photometry of AS 338 during his own observing run at the ESO 1 m telescope in April 1984; and J. Bouvier, in July 1984, took another IDS spectrum at the 1.5 m telescope, covering from about 3650 to 8050 Å. The 1983 and 1984 spectrograms are presented in Fig. 2. They show strong emission lines of the Balmer series and HeI and numerous weaker emission lines of singly ionized iron. Only a trace of the underlying late-type continuum is visible longward from H_α in the 1984 spectrogram. David Allen's recently published new "Catalogue of Symbiotic Stars" also contains a spectrum of AS 338, dated August 1978 (see Fig. 2). Even a quick look at this spectrogram shows it to be quite different from my own ones: In Allen's spectrogram, the Balmer lines and the HeI lines are stronger and, in addition, there are emission lines of higer ionized species such as HeII, [OIII] and [FeVII]. The M-type absorption spectrum is prominent with strong TiO bands. My surprise changed into fear when I recalled that, for identifying AS 338, I had not used a finding chart, but the description of its position given by P. Merrill and C. Burwell in 1950 (*Astrophysical Journal*, **112,** 72). Did I really observe the right object? Fortunately, during the observations, I had made a quick freehand drawing of the field around AS 338 as it appeared on the TV guider screen. A comparison of this "finding chart" with the one published now by Allen not only proves that I actually did observe the right object, but, in 1983, the star seemed to be much brighter compared to other field stars than on the POSS print used by Allen.

An Outburst?

The spectral changes and the brightening of AS 338 become explainable if we assume that it has undergone an outburst as sometimes observed in symbiotic stars. The published and new near IR data of AS 338 from 1974, 1980 and

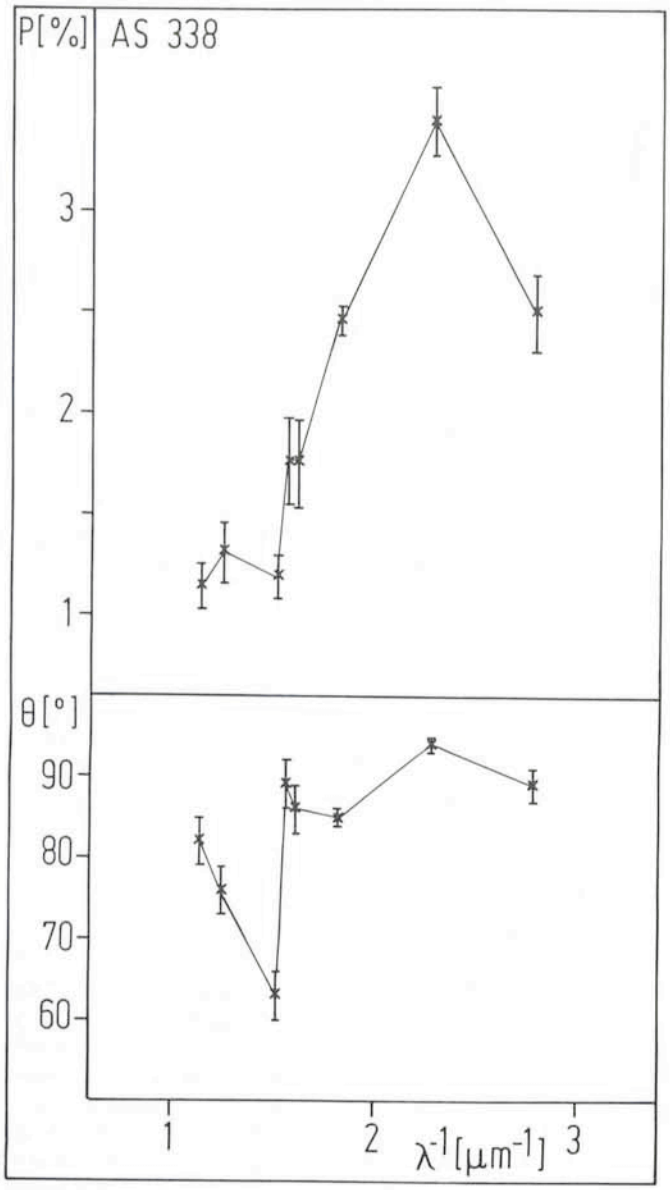

Fig. 1: *Observed percentage polarization P and equatorial position angle θ as a function of inverse wavelength λ^{-1} for AS 338. The outstanding features of the polarization spectrum are: a pronounced maximum of the percentage polarization in the B filter and a significant, sharp rotation of the position angle at H_α.*

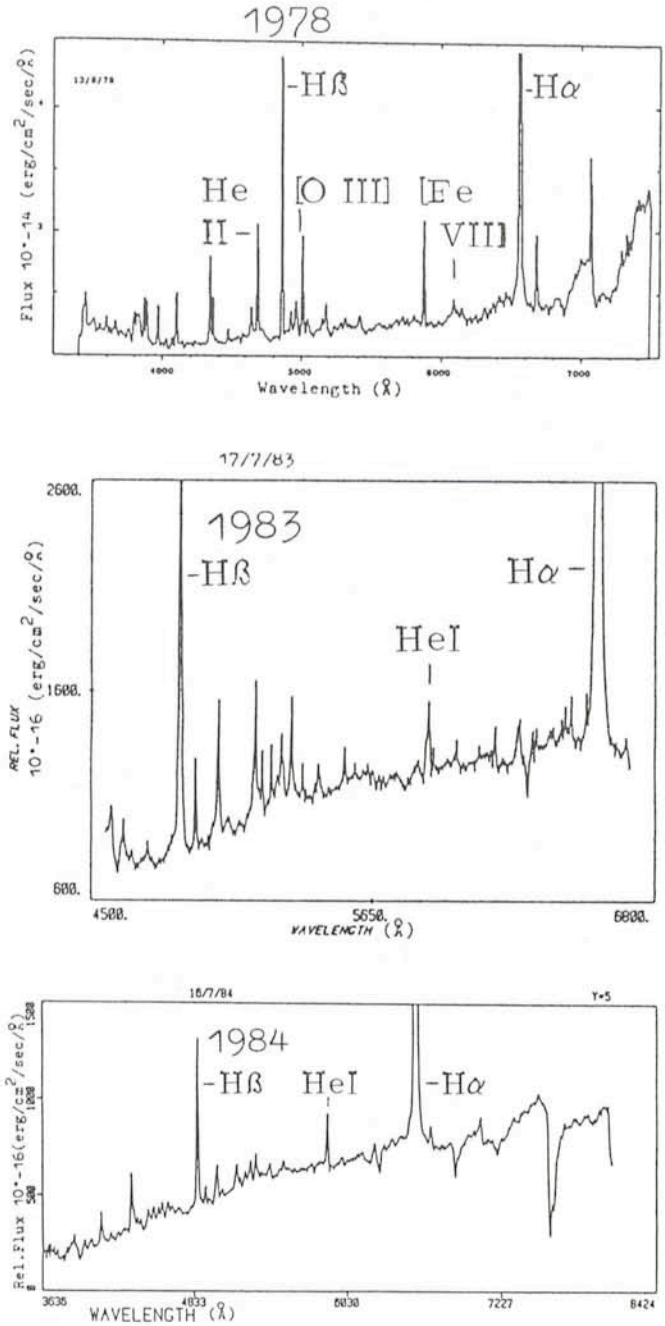

Fig. 2: *Available spectroscopic information on AS 338. Note the strong variability of the emission lines and the continuum. In the 1983 and 1984 spectrograms, the emission lines of HeII, [OIII] and [FeVII] are missing.*

1984 show that the outburst did not significantly alter the late-type star in this system. The constancy of the late-type component therefore lends support to a binary model for AS 338. Binary models for symbiotic stars generally consist of three components: (1) a late-type giant or bright giant, (2) a hot component and (3) a surrounding gaseous nebula ionized by the hot component. I therefore supposed that three sources of radiation contribute to the observed flux distribution of AS 338 in the optical and near IR spectral range. The observed fluxes of AS 338 are displayed in Fig. 3 (solid line). As the M star remained constant, I combined the J, H, K, L measurements from 1984 with the U, B, V, R, I measurements taken in 1983. They have been dereddened using an E(B–V) of $0\overset{m}{.}77$. This value is in agreement with the one derived from the Balmer line ratio of the 1983 spectrum ($0\overset{m}{.}79$) and with the reddening of nearby field stars ($0\overset{m}{.}76$) in the Neckel and Klare field No. 264 at a distance of 7 kpc as given by Allen in 1980. The broad-band fluxes are of course heavily contaminated by the strong emission lines. Therefore, an estimate of the contribution by the nebular spectrum has been made. The dashed line in Fig. 3 shows the approximate flux distribution of the continuum. The slope of this curve readily shows that it cannot be described by the radiation of a single blackbody. The question then raised whether *two* blackbody energy distributions – corresponding to the two energy sources of a binary system – would render an acceptable result. And indeed, reasonable fits could be obtained with a temperature of 8,250 to 10,250 K for the hot component and temperatures ranging from 2,750 to 3,500 K for the cool component. A typical fit with $T_h = 9{,}750$ K and $T_c = 3{,}250$ K is presented in Fig. 4 a. At a distance of 7 kpc for AS 338, the radii turn out to be 39 to 59 $R_\odot$ for the hot source and 151 to 206 $R_\odot$ for the cool source. Assuming that the two

energy sources are stars, the derived temperatures and radii would lead to a spectral classification as A supergiant plus M giant. The most critical points of the model described here are the reddening and the distance. Other combinations of distance and E (B–V) are possible according to the Neckel and Klare fields No. 264 and 266. The use of these values of the fits inevitably led to radii for the cool component which were by a factor of 10 too small for a giant. But at least a giant is necessary to provide the circumstellar gas whose presence is observed in the strong emission lines. On the other hand, assuming that the model yields a fair description of nature, a consistent interpretation of all present data is readily at hand. During an outburst, the spectra of other symbiotic stars, like e.g. Z And, were observed to change from an M giant with a high-excitation emission line spectrum to an A–F supergiant with a shell-like emission line spectrum of HI and HeI. In AS 338 I observed the following characteristic outburst properties:

(1) The development of the emission lines as illustrated by Fig. 2, i.e. strong lines of HeII, [OIII] and [FeVII], are present at minimum, but absent at maximum.

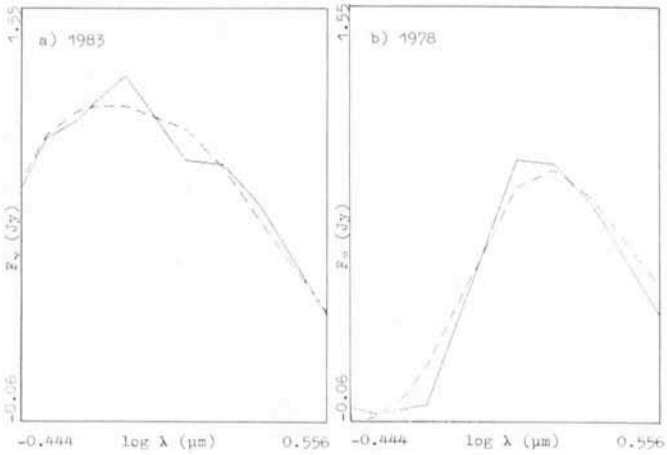

Fig. 4: *The continuum flux distribution of AS 338 during 1983 (4a) and 1978 (4b) is illustrated by the solid lines. The dashed lines are models. For details about the parameters of these models, see the explanations in the text. Note the strong variability of the continuum of AS 338 in the optical spectral range.*

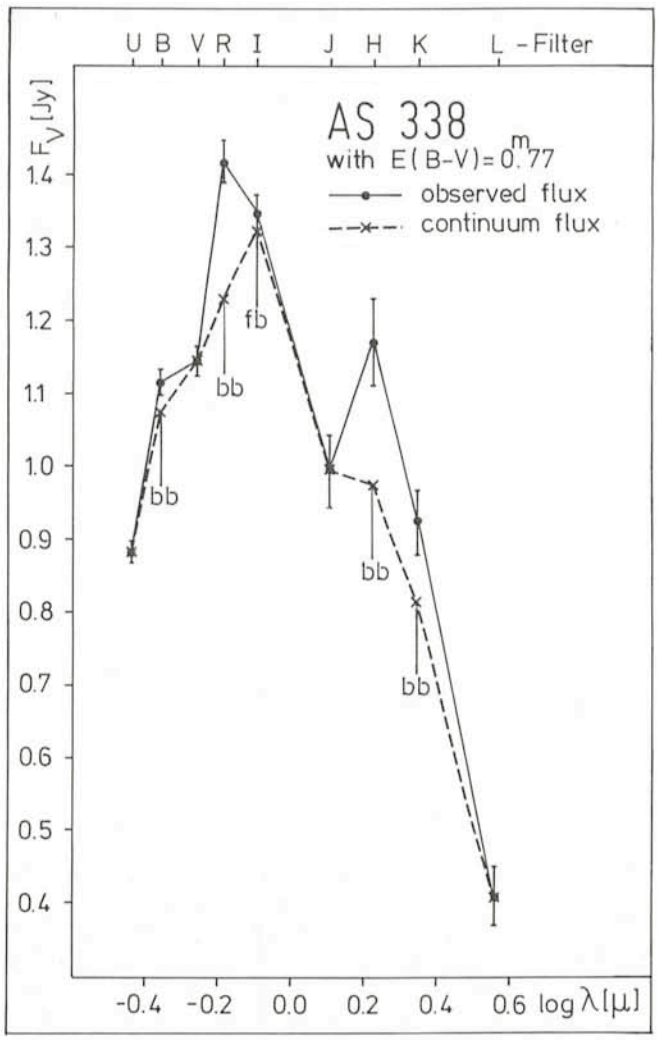

Fig. 3: *The dereddened flux distribution of AS 338. The solid line shows the observed flux, derived by combining the U, B, V, R, I photometry obtained in 1983 at the ESO 50 cm telescope with the J, H, K, L measurements, carried out in 1984 at the ESO 1 m telescope. The flux distribution has been dereddened using a value of E (B–V) = 0.m77. An estimate of the contribution by the nebular spectrum has been made and the dashed line is believed to show approximate continuum fluxes.*

(2) The brightening by $\Delta V \approx 3.^m5$. The development of the emission lines furthermore indicates that AS 338 has undergone at least two outbursts during this century. The amplitude and the timescales of the outbursts also closely resemble those of Z And.

(3) The presence of an A supergiant continuum during 1983, when the high-excitation emission lines were absent.

A Little Bit of Theory

Since the late-type component in AS 338 has remained virtually constant, the outburst must be related to the hot component in the system. I have used the 1978 spectrophotometry published in the new Allen catalogue to derive approximate U, B, V and R continuum magnitudes. Evidently at this time, the star was close to minimum state. Again, these magnitudes have been combined with the J, H, K, L magnitudes measured in 1984. The resulting flux distribution of AS 338 close to minimum is presented in Fig. 4b. The A supergiant continuum is clearly absent here. Instead, reasonable fits could be obtained by combining the late-type star with a very hot (~ 100,000 K) and small ($\lesssim 1\ R_\odot$ companion. Such a star would emit most of its radiation in the UV spectral range and its contribution to the optical spectrum would be low.

There are two principal outburst models for symbiotic binaries: the thermonuclear outburst model (e.g. Paczyński and Rudak, 1980, *Astronomy and Astrophysics* **82,** 349) and the accretion event model (e.g. Bath, 1977, *Mon. Not. R. Astr. Soc.***178,** 203). The basic requests to the outburst models are common to all. A late-type continuum has to be present in the IR during quiescence as well as during outburst. During outburst, the optical spectral range must simulate an A–F supergiant. The main differences between the proposed models are the nature of the hot components and the mechanisms which, during outburst, redistribute the radiation of the hot companion to optical wavelengths. According to the recently computed synthetic spectra from 0.1 to 3.5 μm (Kenyon and Webbing, 1984, *Astrophysical Journal* **279,** 252), the typical A–F supergiant continuum during outburst may be produced by either (a) a blackbody at $T_{eff} \approx 6{,}000-10{,}000$ K), (b) a white dwarf accreting matter at a rate above the Eddington limit ($\dot{M} > 10^{-5} M_\odot yr^{-1}$), or (c) a main sequence star accreting matter near the Eddington limit ($\dot{M} \sim 10^{-3} M_\odot yr^{-1}$). An observational diagnostic is proposed by these authors, which allows to

discriminate among possible hot components in symbiotic systems. Obviously, the data required to apply this method are continuum magnitudes in the UV spectral range. Since the symbiotic star AS 338 is presently bright enough to make its continuum accessible to the IUE low-dispersion mode, I have applied for observing time with the IUE satellite, to make use of this opportunity. In addition, the observers of the Sterken group (*The Messenger,* **33,** 10) are going to monitor the optical brightness variations of AS 338, using one of ESO's photometric telescopes.

Although my story ends here, it is not at all finished. A hint in favour of the accretion event model is given by the polarimetric observations. But, for the time being, we have to wait for the ultraviolet observations to derive, as I hope, the nature of the hot component in my pet symbiotic system.

A Near Infrared Survey of the Southern Galactic Plane

N. Epchtein, Observatoire de Meudon

1. Infrared Sky Surveys

Beyond the photographic spectral range, three major infrared sky surveys have been performed till now: (i) the Two Micron Sky Survey (TMSS) achieved by Neugebauer and Leighton (1969) which provided a catalogue (IRC) containing about 5,600 sources brighter than K ~ 3.5 at declination north of –35°; (ii) the Air Force Geophysical Laboratory (AFGL) survey at 4, 11, 20 and 27 micron (Price and Walker, 1974), a rocket-borne survey covering large parts of the sky but suffering many gaps, mostly in the southern sky, and (iii) the Infrared Astronomical Satellite (IRAS) mission, mainly dedicated to a complete and deep sky survey at 10, 20, 60 and 120 micron whose results have just been released to the astronomical community.

The first two surveys, even though they were sensitivity-limited and incomplete, have led to a large amount of follow-up observing programmes in the optical, infrared and radio ranges. For many years, they have been the unique sources of homogeneous data on a large number of infrared objects. They revealed new important classes of dusty celestial objects such as the so-called OH-IR sources, an extreme class of late-type stars and the compact infrared objects, which are probably very young massive stars still embedded in their protostellar envelopes.

Mostly sensitive to cool stars (1,000–4,000 K), the TMSS has shown that the appearance of the sky in the infrared and in the visible are definitely different. It has revealed many extremely luminous, but invisible or optically very faint stars.

The reddest IRC sources (see list in Kleinmann and Payne-Gaposchkin, 1979), such as +10216, +10011, +10401, have been shown to be extreme late carbon or oxygen-rich stars surrounded by a dense cool (500 to 1,500 K) expanding envelope of dust and gas, revealed by the infrared spectral signatures of grains. Many of them are long-period variable stars and exhibit thermal and maser molecular emission lines in the millimetre range (see, e.g., Nguyen-Q-Rieu et al., 1983). They still deserve further observations to be fully understood and modelized.

Unfortunately there has been no attempt to complete the TMSS in the southern sky during the last 15 years. Even after the completion of the IRAS mission, which does not cover the near infrared spectral range, a large part of the sky still remains essentially unknown in the 1–10 micron range.

2. The Valinhos Survey

In order to partly fill up this gap, we have undertaken, in collaboration with astronomers at Instituto Astronomico e Geofisico (IAG) of the University of São Paulo (USP), a 2.2 micron survey of the southernmost part of the galactic plane. The primary aim of the project is to show up the brightest near IR point sources for future observations at longer infrared and radio wavelengths, which will be possible thanks to the developments of powerful infrared and millimetre telescopes and instrumentation in the southern hemisphere, more specifically at La Silla.

The achievement of a survey, even within a limited area, needs the availability of a telescope for a long period and a "staff" of observers, ready to spend many nights observing. By the beginning of the 80s, several opportunities were favourable to a completion of the TMSS in the south. I was involved in a joint programme with astronomers at USP and was told that this University was operating a modern 60 cm telescope at A. de Moraes Observatory located 80 km north of the large city, atop a 1,000 m high hill, above the small city of Valinhos.

An increasing amount of commercial and industrial lights around the observatory was making optical observations more and more difficult, and therefore this telescope was little used. Since infrared observations are much less sensitive to light pollution, the telescope could be almost full time dedicated to IR observations. Actually, owing to the Brazilian climate, observations were undertaken only during the (relatively) dry winter season, from May to October, which, fortunately, corresponds to the night transit of the galactic plane.

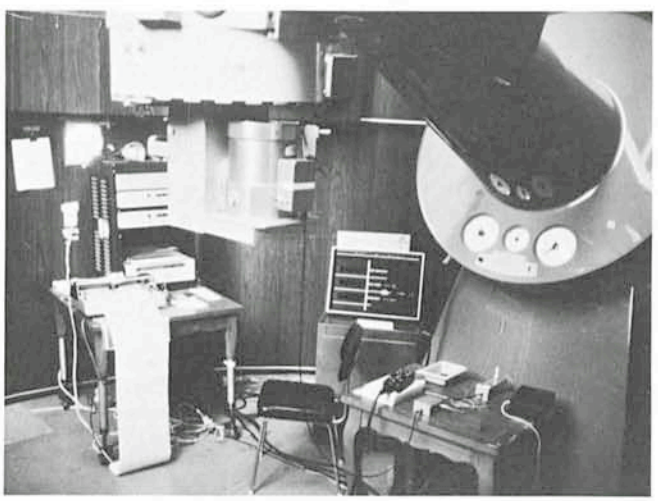

Fig. 1: *The large field infrared photometer installed at the Cassegrain focus of the 60 cm telescope of the University of São Paulo at Valinhos. This very simple device has been used since June 1982 to survey the southern galactic plane at 2.2 micron with a 3.5 arcminute diaphragm. So far, more than 1,500 sources have been detected.*

Moreover, a large field InSb photometer was left unused by the Institut d'Astrophysique de Paris. In a short time it was decided, jointly with astronomers at USP, to design a mechanical and optical interface and to apply for a bilateral agreement between French CNRS and Brazilian CNPq to finance this project. The first step of the project was to scan an area of 100° of galactic longitude on 10° of latitude, limited by 260° $< l <$ 360° and $|b| < 5°$. With a small amount of money and a lot of perseverance, the project turned out to be viable. On the Brazilian side O.T. Matsuura, J. Lépine, E. Picazzio, M.A. Braz, P. Marques Dos Santos and P. Boscolo participated in the observations while T. Le Bertre, A. Roussel and I came several times from France, sometimes on the way to La Silla, to observe at Valinhos.

The instrument is as simple as it can be. A room temperature box holds the dewar at the Cassegrain focus of the telescope, it contains two 45° plane mirrors, one is used to send the telescope beam to the detector, the other, removable, to an eyepiece (Fig. 1). The liquid nitrogen cooled dewar contains a 2 millimetre diameter Indium antimonide cell equipped with a K band filter (λ = 2.2 μm, $\Delta\lambda$ = .5 μm), a Germanium Fabry lens and a field diaphragm of 3.5 arcminutes diameter. The photometer is used in a direct mode of detection, without chopping nor lock-in amplifier. The signal is only filtered in order to eliminate the DC component and recorded on a chart recorder. The coordinates of the telescope are given by the numeric read-out of the telescope. The scanning of the sky is achieved by moving the telescope in RA in "set" mode at a rate of approximately 3 arcmin/sec. During the best nights, the 3 σ limiting magnitude in this mode was K ~ 4.5. In order to discriminate between sources and spurious signal generated by clouds or other atmospheric perturbations, a second scan, close to the position where a signal was detected, was performed for confirmation, making the final results quite reliable.

3. Results and Follow-up Programme at La Silla

So far, the area extending between Carina and Scorpius (l = 285° to l = 360°) has been almost fully surveyed. A few gaps still remain which will be filled up in 1985. More than 1,500 sources have been detected. Their position accuracy is 2 arcminutes rms and only a rough estimate of their flux density can be derived from the observed signal. The selection of objects for further observations requires more information on their nature and more accurate positions. Therefore, a complementary programme is carried out with the ESO 1 m telescope and its standard infrared photometer. Since the objects are rather bright, it is a very suitable programme for day-time use of this telescope. Positions to within 10 arcseconds rms and JHKLM photometry of 338 objects selected among the sources with faint or without optical counterparts (as seen in the 10 cm finder of the 60 cm telescope) have been obtained during two runs at La Silla in September 1983 and September 1984. Identifications with catalogued stars is achieved with the help of the "Centre de Données Stellaires" at Strasbourg. More than two thirds of the subsample remain unidentified and can be considered as "new" objects. They

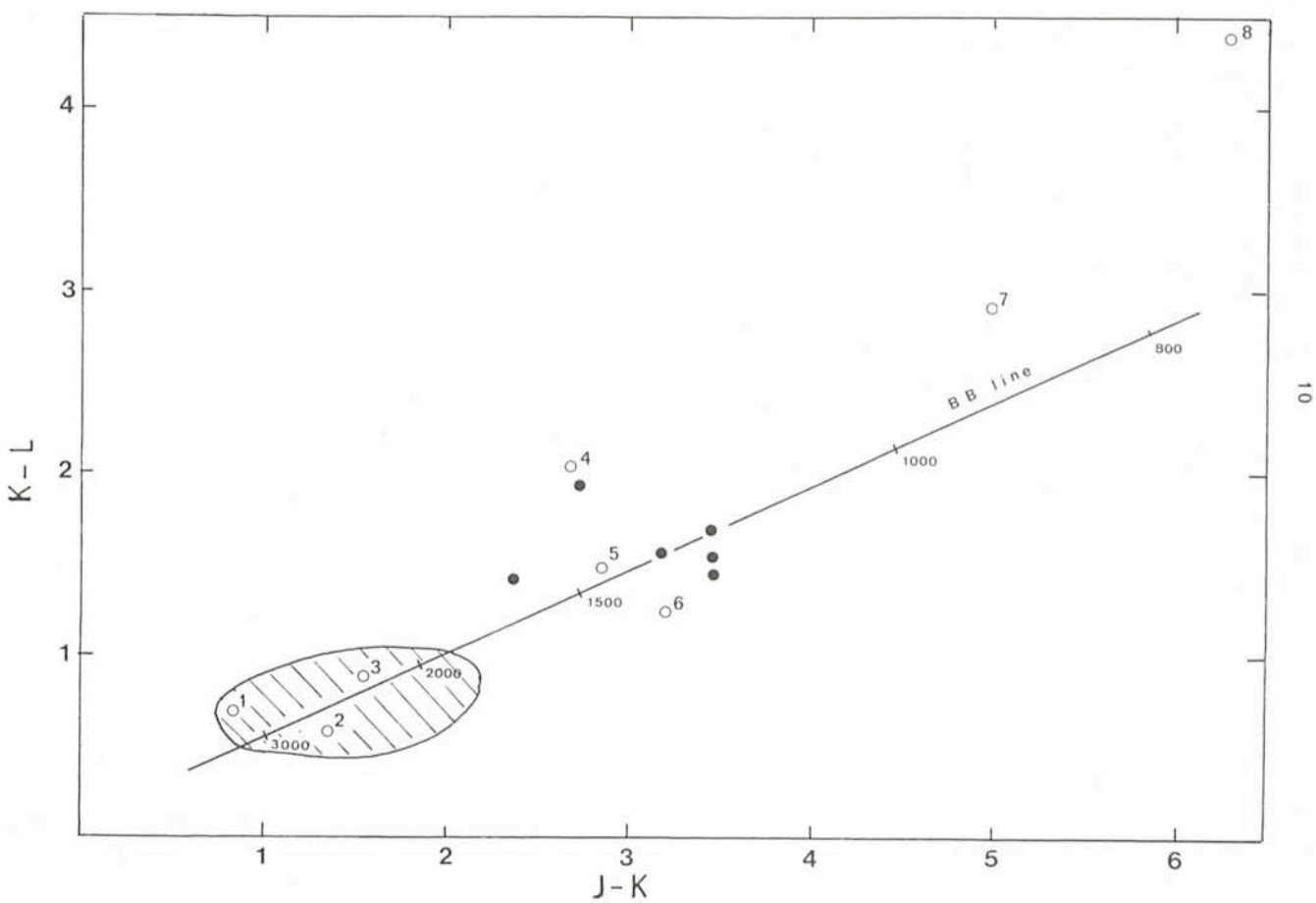

Fig. 2: *In this near infrared colour diagram, we have plotted the reddest objects found in the Valinhos survey as filled dots. Circles represent the position of several well-known infrared stars (1: o Cet, 2: R Leo, 3: R Cae, 4: VY CMa, 5: WX Ser, 6: V Cyg, 7: IRC + 10401, 8: IRC + 10216). The dashed area represents the location of the oxygen-rich Mira stars.*

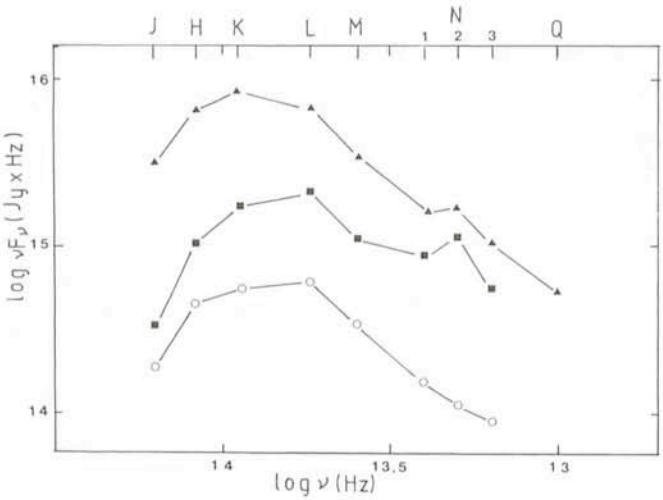

Fig. 3: *Infrared energy distribution of 3 among the reddest objects found in the Valinhos survey: IRSV 1145–6245 (▲), IRSV 1246–6418 (■) and IRSV 1412–5845 (÷ 10) (○). The first two objects clearly exhibit a silicate emission feature at 9.7 micron. They are likely to be oxygen-rich LPVs (observations carried out by T. Le Bertre in December 1984).*

have been designated as IRSV (i.e. Infrared Survey Valinhos) followed by their equatorial coordinates (1950). The complete list and photometric data will be published shortly (Epchtein et al., 1985) and can be supplied on request.

Most of the newly found objects are likely to be late-type stars surrounded by a dust shell. Several objects observed at different epochs have shown a definite variation in the IR bands. They are likely to be long-period variable stars (LPVs). Others, not variable, are more probably very reddened giant or supergiant stars. The reddest objects are represented in a (J–K), (K–L) colour diagram (Fig. 2) together with some well-known infrared stars. No object as red as IRC +10216 has been found yet, but the reddest stars exhibit near IR colours similar to those of sources such as VY CMa (a star which displays a non-spherically symmetric envelope), or V Cyg (a carbon star). It is still rather hazardous on this basis to claim that we have discovered new carbon stars or asymmetrical envelopes, but it is clear that many new variable late-type stars have been found thanks to this survey. They deserve further observations in the visible and in the infrared in order to determine their spectral types, luminosity classes and variability types. Recently, T. Le Bertre observed about 30 very red new objects with the bolometer in the 10 micron bands on La Silla. In several sources he found the typical silicate emission feature at 9.7 micron which characterized oxygen-rich LPVs (Fig. 3); they will be worth observing in radio molecular lines. Finally, the results of the Valinhos survey, combined with the IRC will allow a study of the distribution of the brightest late-type stars in the whole galactic plane. It is also expected to identify some IRAS sources in the region where the space mission was suffering a maximum of confusion.

4. Next Step: A Deep, Complete Near IR Survey?

In a statistical study of the AFGL survey data, Grasdalen et al. (1983) have shown that the stellar populations detected at near IR wavelengths (2–4 μm) and at 10 μm are distinct. For a large class of optically invisible or very faint stellar sources at temperatures ranging between 800 and 2,000 K, ground-based near IR surveys may easily overcome space missions such as IRAS. In the near future, the large gap which separates IR photographical and the 10 μm IRAS surveys could be filled. Our complement to the TMSS was limited in area and sensitivity due to the use of a single detector and the direct mode of detection, but it is expected that a complete ground-based sky survey at 2–3 μm with a limiting K magnitude of 10–12 could be shortly achievable with a multidetector such as an InSb CID array and a 1 metre class telescope.

Acknowledgements

I warmly thank the head of the Astronomy Department at Instituto Astronomico e Geofisico of São Paulo University for the generous allotment of their telescope time, all Brazilian astronomers who participated in the survey under the responsibility of Oscar T. Matsuura, and the ESO staff for their efficient assistance.

The Valinhos survey is supported in Brazil by FAPESP under grants nos. 82055–4 and 82273–4 and in France by INAG, CNRS and Observatoire de Paris.

References

Epchtein, N., Matsuura O.T., Lépine, J.R.D., Braz, M.A., Picazzio, E., Marques Dos Santos, P., Boscolo, P., Le Bertre, T., Roussel, A., Turon, P.: 1985, *Astron. Astrophys. Suppl. Ser.*, submitted.

Grasdalen, G.L., Gehrz, R.D., Hackwell, J.A., Castelaz, M., Gullixson, C.: 1983, *Astrophys. J. Suppl. Ser.*, **53,** 413.

Kleinmann, S.G., Payne-Gaposchkin, C., 1979: *Earth and Extraterr. Sci.*, **3,** 161.

Neugebauer, G., Leighton, R.B., 1969: Two Micron Sky Survey, (NASA SP–3047).

Nguyen-Q-Rieu, Epchtein, N., Le Bertre, T., 1983: *The Messenger* No. **34,** 16.

Price, S.D., Walker, R.G., 1976, The AFGL Four Color Infrared Sky Survey (AFGL–TR–76–0208).

List of Preprints Published at ESO Scientific Group

December 1984 – February 1985

355. M.-P. Véron-Cetty and P. Véron: NGC 1808: A Nearby Galaxy with a Faint Seyfert Nucleus. *Astronomy and Astrophysics.* December 1984.
356. A.F.J. Moffat, J. Breysacher and W. Seggewiss: Wolf-Rayet Stars in the Magellanic Clouds. III. The WO4+O4V Binary Sk 188 in the SMC. *Astrophysical Journal.* December 1984.
357. G. Contopoulos: Bifurcations and Stability in Three-Dimensional Systems. Proc. of the Summer School in Dynamical Astronomy, Cortina, August 1984. December 1984.
358. L. Woltjer: Problems of Supernova Remnants. Proc. of the Workshop on Supernovae and their Remnants, Bangalore, India. February 1985.
359. M.R.S. Hawkins and L. Woltjer: Evidence for Underlying Galaxies in a Complete Sample of Variable Quasars. *Monthly Notices of the Royal Astronomical Society.* February 1985.
360. M.-P. Véron-Cetty, P. Véron and L. Woltjer: Optical Observations of the Jet of the Crab Nebula. *Astronomy and Astrophysics.* February 1985.
361. E.M. Sadler and O.E. Gerhard: How Common are "Dust-Lanes" in Early-Type Galaxies? *Monthly Notices of the Royal Astronomical Society.* February 1985.
362. M.-H. Ulrich, A. Altamore, A. Boksenberg, G.E. Bromage, J. Clavel, A. Elvius, M.V. Penston, G.C. Perola and M.A.J. Snijders: Discovery of Narrow and Variable Lines in the Ultraviolet Spectrum of the Seyfert Galaxy NGC4151. *Nature.* February 1985.
363. J. Roland, R.J. Hanisch, P. Véron and E. Fomalont: WSRT and VLA Observations of Very Steep Spectrum Radio Galaxies in Clusters. *Astronomy and Astrophysics.* February 1985.

Coordinated Multiband Observations of Stellar Flares

M. Rodonò[1], B. H. Foing[2], J. L. Linsky[3], J. C. Butler[4], B. M. Haisch[5], D. E. Gary[6] and D. M. Gibson[7]

[1] *University of Catania, Italy*
[2] *European Southern Observatory, La Silla, Chile*
[3] *Joint Institute for Laboratory Astrophysics, Boulder, USA.*
[4] *Armagh Observatory, Northern Ireland, U.K.*
[5] *Lockheed Research Laboratory, Palo Alto, USA*
[6] *California Institute of Technology, Pasadena, USA*
[7] *New Mexico Institute of Mining and Technology, Socorro, USA*

Activity and Flare Stars

Dedicated observations of active stars have suggested a solar-type scenario with activity levels up to several orders of magnitudes higher than the Sun. Activity phenomena have been observed particularly in red dwarfs and subgiants (Byrne and Rodonò 1983): photospheric spots, overlying plages, coronal structures, flaring events, have been inferred from the modelling of the observations, in analogy with solar phenomena. In particular, the U Ceti-type stars (or dwarf M stars presenting the Balmer lines in emission, Fig. 1) show that even at quiescent phases their chromospheres, transition regions and hot coronae, are enhanced in comparison to the Sun. These stars also show evidence of flare events involving variations in the continuum and emission line fluxes over a wide range of wavelengths, from all the levels on the atmosphere, from the photosphere to the corona, and with typical rise and decay times of 10 and 10^3s respectively. Simultaneous photometry and spectroscopy of flares have shown emission line enhancements of different species to take place on different time scales and to last 10–100 times longer than the continuum flash-phase at flare maximum. Line broadening indicating a turbulent motion of 10^2–10^3 km s^{-1} have been inferred from spectroscopic observations. However, many questions remain unanswered about the vertical structure in temperature and pressue of the quiescent, active and flaring chromosphere and corona. The basic physical processes of flares which have been exhaustively studied for the Sun, such as the triggering, the energy budget, the dynamics of the cooling (by radiation, conduction or expansion) have not been elucidated in the stellar case.

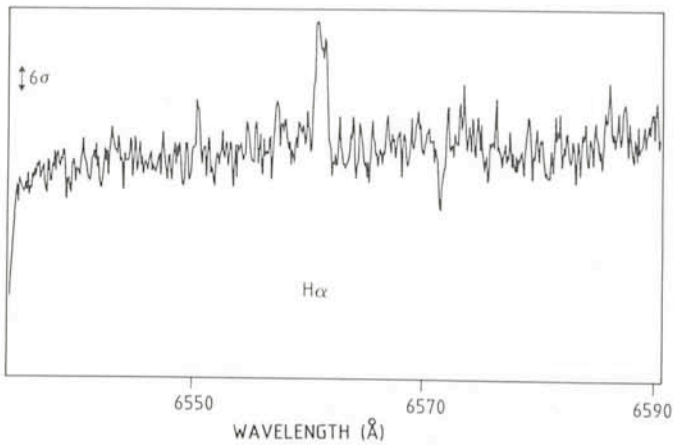

Fig. 1: *High-resolution spectra of the Hα line for Prox Cen taken at the CES, obtained by combination of 8 spectra of exposure 15 min obtained during the monitoring of the star out of any noticeable flare.*

Coordinated Multiband International Campaign

To answer these basic questions, a few years ago four groups, at Catania University, JILA (Boulder), Armagh Observatory and Lockheed Research Laboratory (Palo Alto) jointly organized international observation campaigns of flare stars from both satellite and ground-based observatories. Such were the simultaneous IUE and Einstein observations of a major flare of Prox Cen on August 20, 1983 (Haisch et al., 1983). The first time ESO took part in the observation campaign was in October 1983, then in March 1984 and in December 1984, this included simultaneous coverage at IUE, VLA and other ground-based facilities (Rodonò 1983), and in December 1984 concurrent EXOSAT observations were also obtained.

The March 1984 campaign involved IUE, VLA and four telescopes at La Silla: the 3.6 m telescope was equipped with the Boller & Chivens spectrograph with the IDS in the 3600–4300 Å range, to allow coverage from the Balmer discontinuity to the Hγ line, with a time resolution of 1 minute and with a spectral resolution that enables measurement of possible shifts and the broadening of emission lines; the CES connected to the 1.4 m CAT telescope provided high spectral resolution of the Hα line with 15-min time resolution; the infrared photometer at the 1 m telescope was operated in fast-speed photometry mode in the K band and, finally, the 50 cm photometer in the U-band and Hα ($\Delta\lambda$ = 20 Å) was used with 10-s time resolution.

The IUE satellite, operated round the clock continuously by European and American collaborators, alternated multiple exposures on the short and long wavelength cameras.

We were fortunate to obtain telescope time at ESO before the IUE observations which permitted us to have a dress rehearsal before the actor/observers went on stage. All the collaborators in the campaign were to follow a schedule for observing the selected active stars. We began with the 50 cm photometer and, as we saw the pen of the strip-chart recorder suddenly rise, we felt the first surge of excitement. "This is a flare", the expert stated.

The excitement increased the following nights as we also recorded simultaneous flare events at the other ESO telescopes. Then the international campaign began. Several flares were observed during the course of our coordinated observations on YZ CMi, Prox Cen and AD Leo.

The 1984, March 28 Flare of AD Leo

On 1984, March 28, we recorded an intense flare on AD Leo at 03^h22^m UT. The observing facilities covered a range from 2000 Å to 20 cm (cf. Fig. 2), including, for the first time, infrared observations at $>1\,\mu$m wavelength. As shown by the U-band, 10-s integration light curve, the flare has a complex structure and a relatively long duration (>30 min). The brightness peak (with magnitude excess $\Delta U = 2.1$) was followed by several secondary peaks. The infrared K-band (2.2 μm) observations gave the first evidence of faint but definite negative events in coincidence with an optical flare. The Hα narrow-band photometry shows an Hα precursor to the flare and a

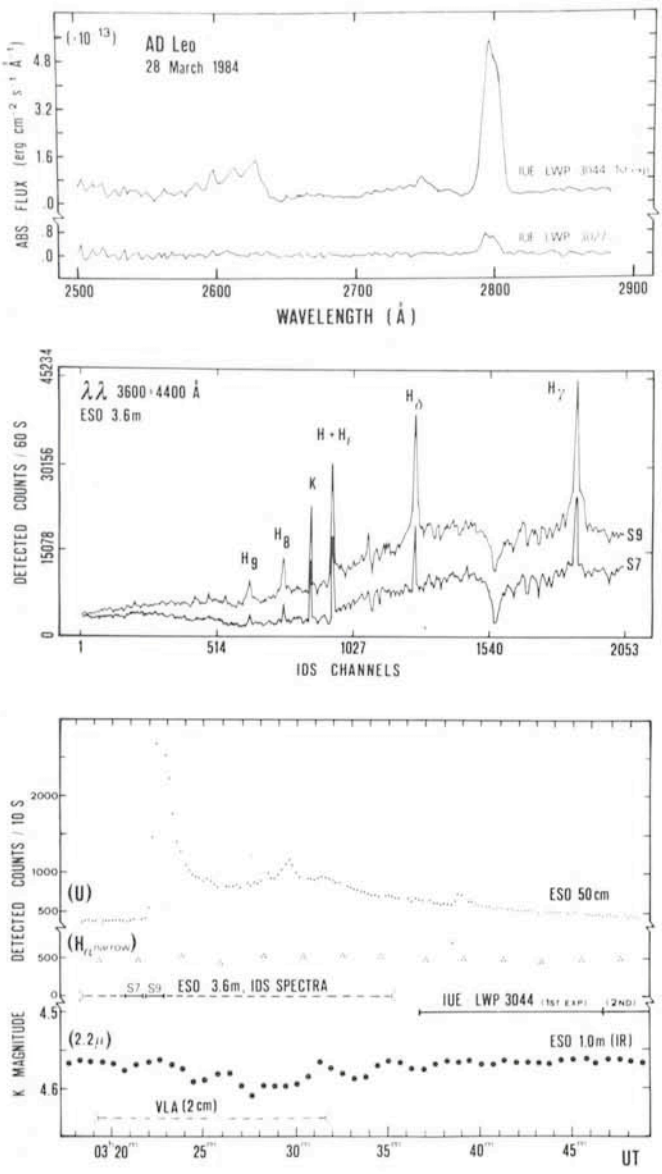

Fig. 2: *The 1984, March 28 flare of AD Leo observed simultaneously with optical and IR photometers (lower panel), optical spectrographs (middle panel) and the IUE. The flare was also detected at 2 cm and 6 cm with the VLA. The IDS spectra S7 and S9 in the middle panel were obtained just before and during the rising phase of the main flare, respectively. In the upper panel, the quiescent IUE spectrum LWP 3027 is also shown for comparison. The IR curve shows the first evidence of a negative event in coincidence with an optical flare.*

longer relaxation of energy release in Hα than in the U-continuum. The comparison between the two selected 60-s exposure uncalibrated IDS spectra, obtained just before and during the flare-rising phase including the flare peak, is striking. They show a strong enhancement in the continuum and line flux, a broadening of CaII and Balmer emission lines, the appearance of higher members of the H Balmer series and an HeI emission line at λ4026 Å. IDS spectra of 60 s were obtained during the whole event and will be presented in a subsequent paper.

The IUE LWP spectrum obtained during the last secondary optical peak shows an enhancement of the continuum, the MgII doublet and of the FeII blend (λ2600 Å) that are remarkable. It is compared in Fig. 2 to a quiescent spectrum taken on March 26.

The microwave observations with the VLA show a flux of 32 mJy at 2 cm and 16 mJy at 6 cm, but no detection at 20 cm. The 2-cm event develops faster than the 6-cm one and follows rather close in time the optical light curve shape with a maximum delay of 1–2 minutes. The 6-cm event is rather slow and the two major peaks occur with 2–3 minutes delay relative to the 2-cm event. Also, the flux maximum at 6 cm is reached during the second major peak, which is fainter at all of the other wavelengths (see Rodonò et al. 1984, for more detail).

In March, 1984, several other stellar flares on AD Leo, Prox Cen and YZ CMi were also observed simultaneously from La Silla, IUE and VLA. In December 1984, we had for the first time simultaneous coverage with EXOSAT of several flares detected also in the Balmer lines with the 3.6 m + IDS. The relationship between the X-ray flux and the Balmer or HeI lines during the flare will be described in a forthcoming paper.

Conclusion

For the first time, multiband data on stellar flares were obtained over a range from 1200 Å to 20 cm. A quantitative analysis of the flare radiation vs. λ, and of its temporal behaviour in the different spectral bands will allow to test the available flare models and to study the dynamical response of the plasma to the flare impulse from the photosphere to coronal levels. Stellar flares being sporadic and non-recurring phenomena, coordinated simultaneous multiband observations involving both satellite and ground-based facilities are essential for their study. With the present report we intend to demonstrate the importance and feasibility of such programmes.

We would like to thank ESO for letting us schedule this coordinated campaign, the La Silla staff for their efficient technical and scientific assistance, and the observers who participated in the campaign.

References

Byrne, P.B. and Rodonò, M., (eds.) 1983, *Activity in Red Dwarf Stars*, IAU Coll. 71, Reidel, Dordrecht.

Haisch et al., 1983, *Astrophysical Journal* **267,** 280.

Rodonò et al., 1983, *Comm. 27, IAU, Inf. Bull. Var. Stars*, No. **2322,** April 1983.

Rodonò et al., 1984, *Coordinated IUE and Ground Based Observations of Active Stars*, 4th European IUE Conference, ESA SP – 218, p. 247.

Visiting Astronomers

(April 1 – October 1, 1985)

Observing time has now been allocated for period 35 (April 1 – October 1, 1985). As usual the demand for telescope time was much greater than the time actually available.

The following list gives the names of the visiting astronomers, by telescope and in chronological order. The complete list, with dates, equipment and programme titles, is available from ESO-Garching.

3.6 m Telescope

April: Appenzeller/Östreicher, D'Odorico/Miley, Hunger/Heber/Schönberner/Drilling, Krautter, Pottasch/Bouchet/Dennefeld/Karoji/Belfort, de Jong/Lub/de Grijp, Mouchet/Bonnet-Bidaud/Motch/Schmider, Larsson S./Larsson B., Ilovaisky/Angebault/Chevalier/Motch, Meikle/Graham/Andrews, Courvoisier.

May: Courvoisier, Pottasch/Bouchet/Dennefeld/Karoji/Belfort, Balkowski/Boisson/Durret/Rocca-Volmerange, van der Hucht/Thé, van der Hucht/de Loore/Hoekstra, Schön-

berner/Hunger, Ulrich/Iye, Finkenzeller/Basri, Kudritzki/Simon/Méndez, Koester/Weidemann, Baade/Danziger, Mathys/Manfroid, Mathys/Stenflo.

June: Mathys/Manfroid, Mathys/Stenflo, Spite, F./François/Spite, M., Gratton/Ortolani, Nesci/Cacciari, Barwig/Schoembs/Kudritzki/Ritter, Moorwood/Cetty-Véron, Azzopardi/Lequeux/Rebeirot, Brahic/Sicardi, Azzopardi/Lequeux/Rebeirot, Oliva/Moorwood.

July: Moorwood/Glass, Le Bertre/Epchtein/Nguyen-Q-Rieu/Sèvre, Habing/Lintel Hekkert/van der Veen, Houziaux/Heck/Manfroid, Grosbøl/Brosch/Greenberg, Azzopardi/Lequeux/Rebeirot, Alcaíno/Liller, Léna/Enard/Lacombe, Zinnecker/Chelli/Perrier, Perrier/Chelli/Léna/de Muizon.

August: Perrier/Chelli/Léna/de Muizon, Preite-Martinez/Persi/Ferrari-T./Pottasch, de Muizon/d'Hendecourt/Perrier, Pietsch/Krautter/Lewin/Pedersen/Sztajno/Trümper/van Paradijs, Danziger/Binette/Matteucci, Jörsäter/Lindblad/Athanassoula, Fosbury/Danziger/Tadhunter, Nelles/Elst, de Grijp/Lub/Miley.

Sept.: Angebault/Chevalier/Hurley/Ilovaisky/Motch/Pedersen, Heckman/Miley, Butcher/Buonanno, Pizzichini/Pedersen, Shaver/Cristiani, Sol, Bergeron, Renzini/D'Odorico/Greggio, Bergeron/D'Odorico, Chmielewski/Jousson.

1.4 m CAT

April: Butcher, Giovannelli/Vittone/Rossi/Bisnovatyi-Kogan/Sheffer/Lamzin, Reimers/Hempe/Toussaint, Ruiz/Melnick/Ortiz, Doazan/Thomas/Boudonneau, Megessier.

May: Megessier, Gredel/Münch, Danks/Lambert, Holweger/Steffen, Wolf/Stahl/Leitherer/Bastian, Spite, M./Spite, F./François.

June: Spite, M./Spite, F./François, Heske/Wendker, Foing/Bonnet/Crivellari/Beckman/Galleguillos/Lemaire/Gouttebroze, Barbuy, Foing/Bonnet/Crivellari/Beckman/Galleguillos/Lemaire/Gouttebroze, Leitherer/Stahl/Wolf/Zickgraf, Baade/Peters/Polidan, Baade/Ferlet.

July: Baade/Ferlet, Ferlet/Vidal-Madjar/Gry/Laurent, Giovannelli/Vittone/Rossi/Bisnovatyi-Kogan/Sheffer/Lamzin, Crane/Mandolesi/Hegyi, Gustafsson/Andersen/Edvardsson/Nissen.

August: Gustafsson/Andersen/Edvardsson/Nissen, Stalio/Porri/Polidan/Smith, Papoular/Catala/Felenbok, Grewing/Baessgen/Barnstedt/Gutekunst/Bianchi.

Sept.: Lührs, Lindgren/Ardeberg/Maurice, Barbieri/Benacchio/Nota.

2.2 m Telescope

April: Pottasch/Bouchet/Dennefeld/Karoji/Belfort, v.d. Hucht/Perryman, Perryman/Jakobsen, Rosa/Benvenuti/Savage, Motch/Courvoisier/Pedersen/Pakull/Ilovaisky, Perryman/Shaver/van Heerde/Macchetto/di Serego Alighieri, Macchetto/Miley/Perryman/Colina/di Serego Alighieri, Miley/Macchetto/di Serego A./Perryman, Bertola/Zeilinger, Ilovaisky/Angebault/Chevalier/Motch, de Waard/Miley/Schilizzi.

May: Colina/Perryman/Kollatschny, Courvoisier, Gratton/Ortolani/Tornambé, van der Kruit/Bottema, Ulrich/Perryman/Collin-Souffrin, Möllenhoff, Krautter/Pietsch, Möllenhoff, Krautter/Frank/Sztajne.

June: Rosa/Mathis, Rosa/Benvenuti/Savage, Véron, Gathier/Atherton/Pottasch/Reay, Dettmar/Wielebinski, Moorwood/Cetty-Véron, Cetty-Véron, MPI.

July: MPI, Lacombe/Léna/Chelli/Rouan.

August: Lacombe/Léna/Chelli/Rouan, Fricke/Kollatschny/Hellwig, Pietsch/Krautter/Lewin/Pedersen/Sztajno/Trümper/van Paradijs, Jörsäter/Lindblad/Athanassoula, Fosbury/Danziger/Tadhunter, Danziger/Binette/Matteucci, Pizzichini/Pedersen, Nelles/Elst, de Grijp/Lub/Miley, Häfner/Metz/Pietsch/Voges.

Sept.: Rafanelli/Schulz/di Serego Alighieri, Macchetto/Miley/Barthel, Courvoisier, Jørgensen/Hansen/Norgaard-Nielsen, Vauclair/Macchetto/Fort/Nieto/Prugniel/Lelièvre/Perryman/di Serego Alighieri, Macchetto/Miley/Barthel, Rafanelli/Schulz/di Serego Alighieri, Jørgensen/Hansen/Nørgaard-Nielsen, Sommer Larsen/Christensen, Buser/Cayrel.

1.5 m Spectrographic Telescope

April: Kroll/Schneider/Voigt, Giovanelli/Vittone/Rossi/Bisnovatyi-Kogan/Sheffer/Lamzin, Gry/Vauclair, Chincarini/de-Souza/Manousoyannaki/Kotanyi, Chincarini, de Souza, Bues/Rupprecht, Fischerström/Liseau.

May: Fischerström/Liseau, Lebertre/Epchtein/Nguyen-Q-Rieu/Sèvre, Wamsteker/Danks/Fricke, Bica/Alloin, Finkenzeller/Basri, Lindgren/Ardeberg/Maurice/Prévot, Pauls/Kohoutek, Molaro/Franco/Morossi/Ramella.

June: Molaro/Franco/Morossi/Ramella, Gerbaldi/Morguleff/Pasinetti/Fracassini/Pastori/Antonello, Bouvier/Bertout, Maciel/Barbuy/Aldrovandi/Faundez, Leitherer/Stahl/Wolf/Zickgraf, Strupat/Drechsel/Haug/Böhnhardt/Rahe.

July: Strupat/Drechsel/Haug/Böhnhardt/Rahe, Giovannelli/Vittone/Rossi/Bisnovatyi-Kogan/Sheffer/Lamzin, Houziaux/Heck/Manfroid, Acker/Stenholm/Lundström, Thé/Westerlund, Acker/Stenholm/Lundström.

August: Acker/Stenholm, Lundström, Lindgren/Ardeberg/Maurice/Prévot, Fricke/Colina, Häfner/Metz/Pietsch/Voges.

Sept.: Richtler/Seggewiss, Heydari-Malayeri/Testor/Lortet, Hahn/Lagerkvist/Rickman.

1 m Photometric Telescope

April: Leene/Goss/Beichmann, Giovannelli/Vittone/Rossi, Bisnovatyi-Kogan/Sheffer/Lamzin, Liller/Alcaíno, Bues/Rupprecht, Westerlund/Jörgensen (UG), Fischerström/Liseau.

May: Fischerström/Liseau, van der Hucht/Thé, Stanga/Natta/Lenzuni, Kollatschny/Loose, Heske/Wendker, Lebertre/Epchtein/Nguyen-Q-Rieu.

June: Lebertre/Epchtein/Nguyen-Q-Rieu, Terzan, Barwig/Schoembs/Kudritzki/Ritter, Brahic/Sicardy, Haug/Drechsel/Strupat/Rahe, Habing/Lintel Hekkert/van der Veen.

July: Habing/Lintel Hekkert/van der Veen, Epchtein/Braz, Giovannelli/Vittone/Rossi/Bisnovatyi-Kogan/Sheffer/Lamzin, Grosbøl/Brosch/Greenberg, Lebertre/Epchtein/Nguyen-Q-Rieu/Sèvre, Heck/Manfroid, Thé/Westerlund.

August: Thé/Westerlund, de Muizon/d'Hendecourt/Perrier, Wargau/Wolterbeek, Olofsson/Bergvall, Clementini/Cacciari/Prévot/Lub/de Bruyn/Lindgren, Arlot/Thuillot/Morando/Lecacheux/Bouchet, di Martino/Zappala/Farinella/Paolicchi/Cacciatori/Barucci.

Sept.: di Martino/Zappala/Farinella/Paolicchi/Cacciatori/Barucci, Poulain, Arlot/Thuillot/Morando/Lecacheux/Bouchet, Poulain, Richtler/Seggewiss, Arlot/Thuillot/Morando/Lecacheux/Bouchet, Hahn/Lagerkvist/Rickman.

50 cm ESO Photometric Telescope

April: Schneider/Pavlovski/Maitzen, Carrasco/Loyola, Scaltriti/Busso/Cellino, Westerlund/Jörgensen (UG).

May: Westerlund/Jörgensen (UG), Lodén LO/Engberg, Schönberner/Hunger, Lodén K., Arlot/Thuillot/Morando/Lecacheux/Bouchet, Lodén K.

June: Lodén K./Arlot/Thuillot/Morando/Lecacheux/Bouchet, Antonello/Conconi/Mantegazza, Arlot/Thuillot/Morando/

Lecacheux/Bouchet, Antonello/Conconi/Mantegazza, Carrasco/Loyola, Haug/Drechsel/Strupat/Rahe.

July: Haug/Drechsel/Strupat/Rahe, Arlot/Thuillot/Morando/Lecacheux/Bouchet, Thé/Westerlund, Arlot/Thuillot/Morando/Lecacheux/Bouchet.

August: Arlot/Thuillot/Morando/Lecacheux/Bouchet, Carrasco/Loyola, Schober/Surdej A. and J./Michalowski, Häfner/Metz, Pietsch/Voges.

Sept.: Häfner/Metz, Pietsch/Voges, di Martino/Zappala/Farinella/Paolicchi/Cacciatori/Barucci, Arlot/Thuillot/Morando/Lecacheux/Bouchet, di Martino/Zappala/Farinella/Paolicchi/Cacciatori/Barucci, Hahn/Lagerkvist/Rickman, Arlot/Thuillot/Morando, Lecacheux/Bouchet, Debehogne/Zappala/de Sanctis.

GPO 40 cm Astrograph

April: Goossens/Waelkens.

May: Bässgen/Grewing/Kappelmann/Krämer, Goossens/Waelkens.

June: Goossens/Waelkens.

July: Goossens/Waelkens.

Sept.: Debehogne/Machado/Caldeira/Viera/Netto/Zappala/de Sanctis/Lagerkvist/Mourao/Tavares/Nunes, Protitch-B./Bezerra.

1.5 m Danish Telescope

April: Alcaíno/Liller, de Jong/Lub/de Grijp, Motch/Ilovaisky/Chevalier/Pedersen/Pakull/Beuermann, Mouchet/Bonnet-Bidaud/Motch/Schmider, Larsson S./Larsson B., de Souza/Chincarini, Boisson/Reid.

May: Reiz, Teuber/Nielsen/Johansen, Schuster/Nissen.

June: Pedersen, Fusi Pecci/Battistini/Bonoli/Federici, Ortolani/Gratton, Lebertre/Epchtein/Nguyen-Q-Rieu/Sèvre, Rosino/Ortolani, Leitherer/Stahl/Wolf/Zickgraf, Pedersen.

July: Pedersen, Veillet, Acker/Maurice/Prévot, Lindgren/Ardeberg/Maurice/Prévot.

August: Lindgren/Ardeberg/Maurice/Prévot, Andersen/Nordström/Olsen, Mayor/Mermilliod, Clementini/Cacciari/Prévot/Lub/de Bruyn/Lindgren, Andersen/Nordström.

Sept.: Andersen/Nordström, Jørgensen/Hansen/Nørgaard-Nielsen, Imbert/Andersen/Nordström/Ardeberg/Lindgren/Mayor/Maurice/Prévot.

50 cm Danish Telescope

April: Schuster/Nissen

May: Lindgren/Ardeberg/Maurice/Prévot, Foing/Bonnet/Crivellari/Beckman/Galleguillos/Lemaire/Gouttebroze.

June: Foing/Bonnet/Crivellari/Beckman/Galleguillos/Lemaire/Gouttebroze, Baade/Ferlet.

July: Baade/Ferlet.

August: Lindgren/Ardeberg/Maurice/Prévot, Group for Long Term Photometry of Variables.

Sept.: Group for Long Term Photometry of Variables, Grenon/Hög/Petersen.

90 cm Dutch Telescope

April: van Roermund, de Loore/Monderen, Pakull/Beuermann/Weißsieker/Reinsch.

May: Pakull/Beuermann/Weißsieker, Reinsch, Roobeek.

June: Roobeek, Trefzger/Pel/Blaauw, Gathier/Atherton/Pottasch/Reay, de Zeeuw/Lub/de Geus/Blaauw.

July: de Zeeuw/Lub/de Geus/Blaauw, de Geus, van Amerongen.

August: Thé/Westerlund, v. Amerongen/v. Paradijs, Courvoisier.

61 cm Bochum Telescope

April: Hanuschik.

May: Hanuschik, Kohoutek, Group for Long Term Photometry of Variables.

June: Group for Long Term Photometry of Variables.

July: Group for Long Term Photometry of Variables.

August: Group for Long Term Photometry of Variables, Grewing/Bässgen/Barnstedt/Bianchi/Gutekunst.

Sept.: Grewing/Bässgen/Barnstedt/Bianchi/Gutekunst, Kiehling.

Serendipitous Discovery of a High Redshift Quasar

M. Azzopardi, ESO

Within the framework of our survey of carbon stars (C stars) in dwarf spheroidal galaxies (Azzopardi and Westerlund, 1984, *The Messenger* **36,** 12), the Carina galaxy was observed on November 2, 1983 at La Silla. A very good quality 2-hour-exposure plate was obtained at the prime focus of the 3.6 m telescope, using the triplet corrector, the Hoag Grism R35 and a GG435 filter (see Breysacher and Lequeux, 1983, *The Messenger* **33,** 21). The GG435 filter, in combination with the IIIa-J emulsion in order to reduce the instrumental spectral domain to the useful range 4350–5300 Å, allows one to reduce the crowding. The plate was searched systematically using a binocular microscope with small magnification. This allowed us to identify 6 out of the 7 C stars listed by Mould et al. (1982, *Astrophysical Journal* **254,** 500) plus 4 new candidates and one dubious (Azzopardi, Lequeux and Westerlund, 1984, ESO preprint No. 345).

These five newly discovered C star candidates were observed with the Cassegrain Boller and Chivens spectrograph and a CCD camera (CID 53612) at the ESO 3.6 m telescope during the nights of November 23–24, 1984 and January 19–21, 1985. A 400 line/mm grating, blazed at 5400 Å, was used in the first order (171 Å mm^{-1}). The slit aperture measured 2 arcseconds, giving a final resolution of 8 Å (FWHM). The observations allowed us to confirm as C stars the candidates Nos. ALW 1, 2 and 3 and to classify as a late M dwarf the dubious candidate ALW 5 according to the library of stellar spectra by Jacoby et al. (1984, *Astrophysical Journal Suppl.* **56,** 257.

Surprisingly, the object ALW 11, which was somewhat far from the central regions of Carina, turned out to be a quasar. Fig. 1 gives the identification chart. Its 1950.0 position is $\alpha = 6^h42^m13^s.40$, $\delta = -50°38'07''.1$ and a rough estimate of its

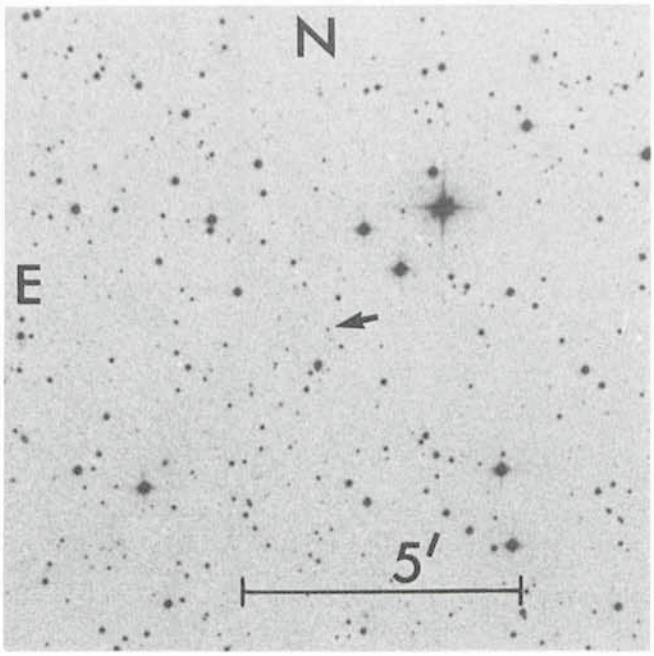

Fig. 1: *Finding chart of the QSO from the ESO Red Sky Survey plate No. 206.*

magnitude is V = 18.5. This object is not listed in the updated Catalogue of Quasars and Active Nuclei by Véron and Véron (1984, *ESO Scientific Report*, No. 1) and as far as we can say is a new high redshift QSO with Z = 3.09. In fact in our very low dispersion spectrum we interpreted the Lyα + NV and CIV

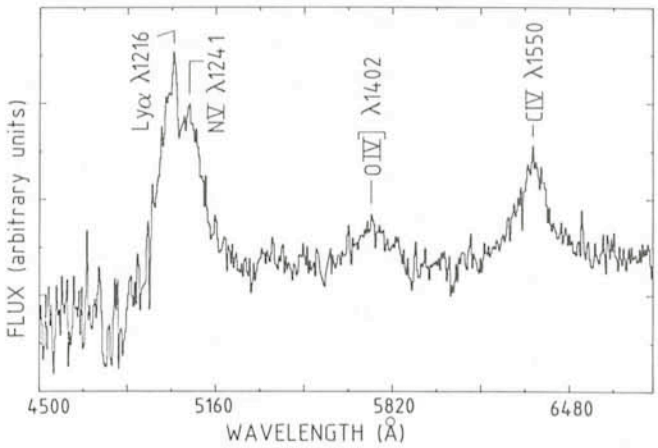

Fig. 2: *Spectrum of the high-redshift QSO obtained with the ESO 3.6 m telescope using the Boller and Chivens spectrograph and a CCD camera. The resolution is 8 Å (FWHM) and the integration time 1 hour.*

λ1550 emission lines as being the continuum on both sides of the λ5165 molecular Swan C_2 band.

Are we lucky or unlucky? We were looking for Wolf-Rayet stars and we found carbon stars; now we are looking for carbon stars and we have found a new high-redshift quasar!

Acknowledgement

I wish to thank P. Angebault for helping me in the reduction of the CCD data.

Circumstellar Shells in the Large Magellanic Cloud

O. Stahl, Landessternwarte Heidelberg-Königstuhl

The brightest stars are known to lose mass at a considerable rate. The most spectacular mass-loss characteristics are exhibited by emission-line stars which are known as P Cyg stars, S Dor variables or as η Car-like objects. It is obvious that these stars are surrounded by circumstellar matter since they have strong emission-lines in their spectra. However, to detect this matter by direct photography may not be easy, but of great interest.

A number of Of and WR stars are known to be surrounded by ring nebulae, several of them in the Large Magellanic Cloud (LMC) (see e.g. Chu and Lasker [1980]). These nebulae have linear diameters of about 20–200 pc. They are probably formed by the interaction between stellar ejecta and the ambient interstellar medium. A few emission-line objects are associated with nebulae of much smaller linear diameter (~1 pc) which probably consist mainly of stellar ejecta. These are the nebulae which we want to discuss here.

A well-known example is the nebulous shell surrounding η Car. It is regarded as the remnant of a great outburst of the star in the last century. Recently Davidson et al. (1984) found a strong overabundance of nitrogen in some knots in the shell which shows that the matter has been processed in the star. That means that the nebula consists of stellar ejecta and not of swept-up interstellar matter. Another case of a nebula surrounding an emission-line supergiant is the shell around the S Dor variable AG Car which was detected by Thackeray (1950).

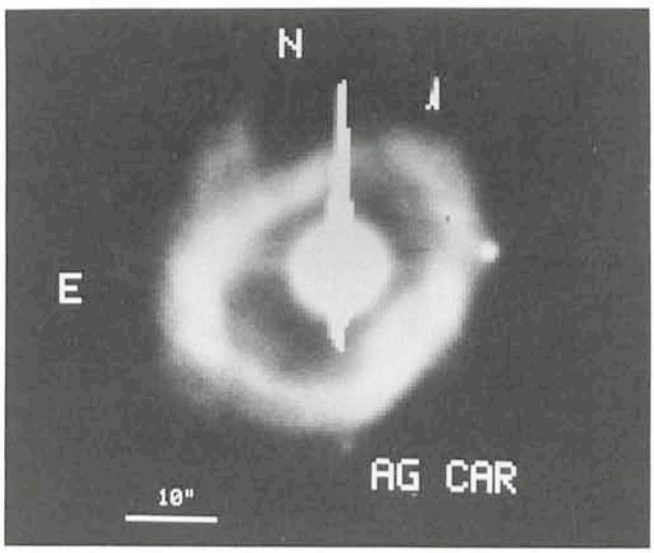

Fig. 1: *CCD image of the ring nebula surrounding the galactic S Dor variable AG Car. A 20 Å wide H_α filter has been used. The exposure time was 30 minutes in a cloudy night. The filamentary structure of the shell can be well seen. The spikes north and south of the central star are* not *jets but due to charge overflow from the overexposed stellar image. The feature at the northwestern boundary of the nebula is a defect on the CCD.*

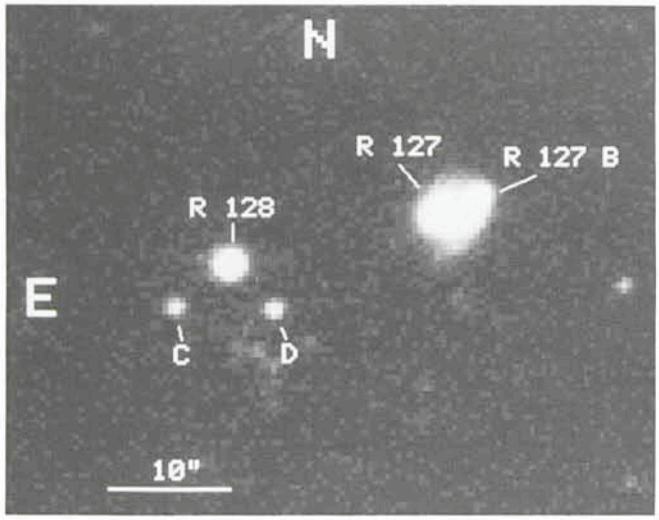

Fig. 2: *CCD image of the field around the S Dor variable R 127 in the LMC. The exposure time was 10 minutes through a 20 Å wide H_α filter. The close companion at a distance of 3 arcsecs – R 127 B – is well separated. The seeing was 1.2 arcsec (FWHM). R 127 appears slightly extended.*

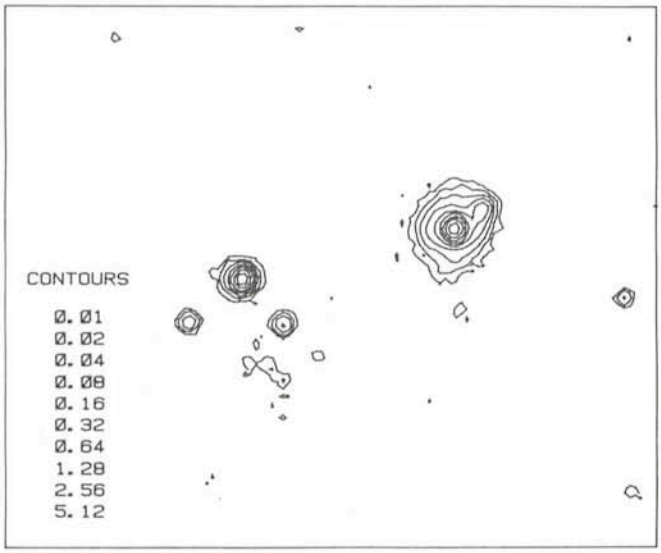

Fig. 3: *An isocontour representation of the field shown in Fig. 2. Note especially the extended structures around R 127.*

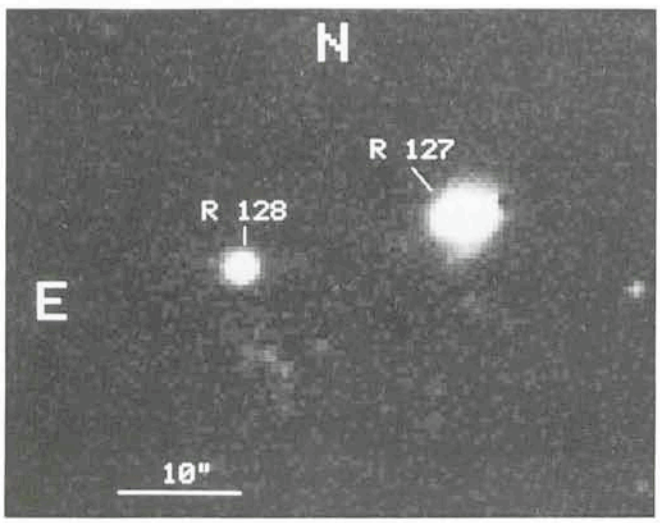

Fig. 4: *Same as Fig. 2 but R 127 B and the two companions of R 128, marked as C and D in Fig. 2, have been removed.*

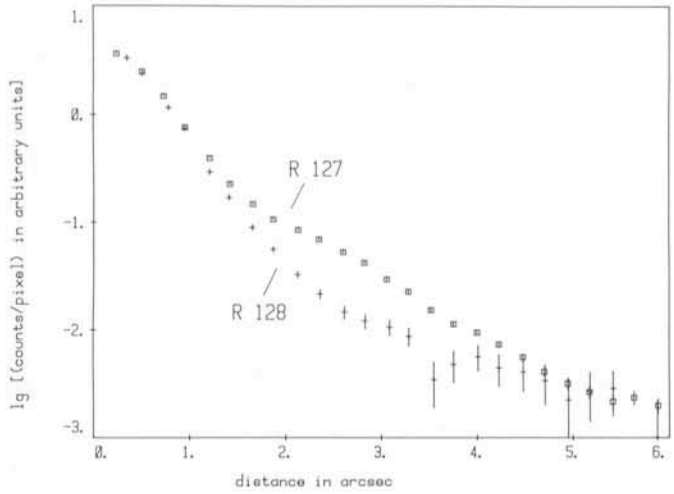

Fig. 5: *Radial brightness profile of R 127 and R 128 as determined from the image shown in Fig. 4. The curve of R 128 has been shifted in order to match the profile of R 127 at the centre. The image of R 127 shows clear evidence for extended structures at distances between 1.5 and 4 arcsecs from the centre of the seeing disk. It is, however, not sure if all of this extension is due to a nebulosity. Part of it may be due to unresolved stars.*

This ring nebula is shown in Fig. 1. In fact, apart from AG Car and η Car there are only very few luminous emission-line stars where such nebulae have been found. Other P Cyg stars in the Galaxy – among them P Cyg itself – have been searched for nebulae, most of them with negative result. When we realized that objects similar to the shell around AG Car should be detectable at the distance of the LMC, we decided to look for similar nebulae in the LMC since there are many luminous emission-line stars of different types found in this neighbouring galaxy. From the investigation of the nebulae we expected to learn something about the mass-loss history of the central stars. In addition, we hoped to get some information about element abundances which are much easier to obtain from nebular lines than from the spectra of the central stars. All this is important for the determination of the evolutionary status of these stars.

However, there are problems. The estimated size of about 1 pc corresponds to only 4 arcsecs at the distance of the LMC, i.e. we have to find a faint nebulosity close to a relatively bright star, typically of magnitude 11. This is only possible if we analyse the image profiles in detail. Such an analysis can only be done with some hope of success if we use a linear detector with a reasonably high dynamic range, such as a CCD. The dynamic range (i.e. the ratio of the strongest to the faintest detectable signal) of a CCD is restricted by two effects. First, every pixel can hold only a limited number of electrons, very roughly 100,000. If a pixel is overexposed, this will result in a charge overflow along a column. This effect can be seen in the image of AG Car, shown in Fig. 1. The results of a charge overflow are of course disastrous if you are looking for small-scale structures. The second effect which limits the dynamic range of a CCD is the noise produced during the read-out process. It corresponds to about 100 electrons per pixel. The dynamic range of a CCD is thus of the Order of 1,000. This means that twe cannot detect nebulae with a surface brightness more than 1,000 times fainter than the seeing disk of the star at its centre. Therefore, it is necessary to use narrow-band filters centred on nebular emission lines to reduce the contribution from the star as far as possible. We wanted to derive the excitation of the nebulae from photographs taken with different filters. We applied for observing time at the Danish

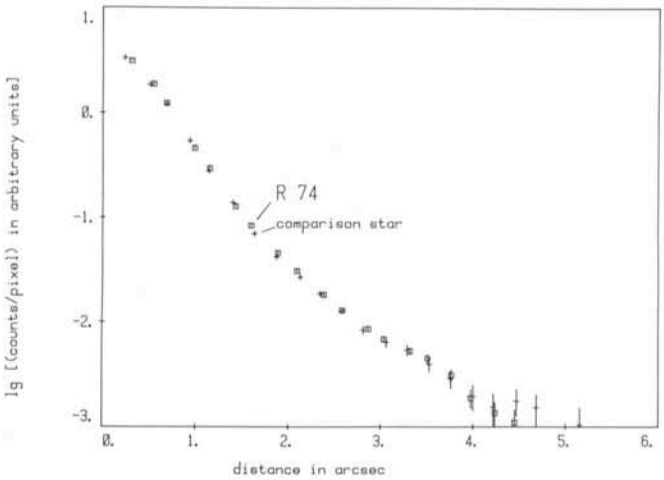

Fig. 6: *Radial brightness profiles of R 74 and a nearby comparison star. The seeing was 1.2 arcsec (FWHM), as in Fig. 4. The profile of the image of R 74 shows no significant deviations from the profile of the comparison star which is supposed to be the point-spread function, i.e. the profile of a point source.*

1.5 m telescope, and 3 nights in January 1984 were allotted to this project.

The weather at La Silla is known to be excellent in January with 90% of photometric nights. This means that about 3 nights in January are not photometric. Unfortunately, it happened that we got these 3 nights; therefore, a calibration of the images was not possible. So we decided to take photographs in one filter – H_α – only, since a determination of line ratios was not possible. In addition, it was a matter of good luck to get properly exposed images, with all these clouds passing. Therefore, we obtained much less useful data than we had anticipated. Useful data of 15 stars have been recorded, but the exposure levels of several pictures is far from ideal.

The analysis of the data is illustrated in Figs. 2, 3, 4 and 5. Fig. 2 shows the field around the S Dor variable R 127 after subtraction of the electronic bias and flat-field correction. Fig. 3 shows the same field in the form of an isocontour plot. In the next step we cleaned the surroundings of the star and an appropriate comparison star – in this case R 128 – from nearby stars by subtracting a properly scaled and centred stellar profile. The cleaned image is shown in Fig. 4. Finally, we determined the radial brightness profile of the star and the comparison star in order to look for a possible extension of the stellar image. The results for R 127 and R 128 are shown in Fig. 5. The curve of R 128 has been shifted to match R 127 in the inner parts. There is a pronounced difference in the two profiles between about 1.5 and 4 arcsecs which we identify with a nebula surrounding R 127.

R 127 has received much interest in recent years. Walborn (1982) described the spectrum as intermediate between Of and WN stars and found velocity-doubled nebular lines. Stahl et al. (1983) detected an S Dor-type outburst of the star, which was also reported in the *Messenger* (Wolf and Stahl, 1983). In addition, Stahl et al. detected nebular emission lines in R 127 B which gave evidence for a spatially resolved emission-line region. Very recently, Lund and Ferlet (1984) reported broad NaI D absorption-line features which they ascribed to an old, cool, ejected shell. It may well be that it is this shell which we see on our direct photographs. Assuming that the nebula is expanding with the velocity indicated by the NaI D absorptions and using a radius of 3 arcsecs, we estimate a kinematic age of about 15,000 years for the nebula around the star.

On most of our other photographs we see little evidence for nebulosities around the stars. As an example we show in Fig. 5 the data for the P Cyg star R 74. We have found, however, extended structures around a few more stars (although in no case as obvious as in the case of R 127). But in these cases it is not clear if the extension of the images is due to a nebula or to nearby unresolved stars. As usual, more observations are needed.

We thank the ESO staff for technical assistance. Comments from Claus Leitherer on the manuscript are gratefully acknowledged.

References

Chu, Y.-H., Lasker, B.M.: 1980, *Publ. Astron. Soc. Pacific* **92,** 730.
Davidson, K., Dufour, R.J., Walborn, N.R., Gull, T.R.: 1984, IAU Symp. No. 105, Reidel, eds. A. Maeder and A. Renzini, p. 261.
Lund, G., Ferlet, R.: 1984, *The Messenger,* No. **36,** 2.
Stahl, O., Wolf, B., Klare, G., Cassatella, A., Krautter, J., Persi, P., Ferrari-Toniolo, M.: 1983, *Astronomy and Astrophysics* **127,** 49.
Thackeray, A.D.: 1950, *Monthly Notices of the Royal Astronomical Society* **110,** 524.
Walborn, N.R.: 1982, *Astrophysical Journal* **256,** 452.
Wolf, B., Stahl, O.: *The Messenger,* No. **33,** 11.

A Possible Nonlinearity in IDS Data

M. Rosa, ST-ECF (ESO), Garching

I. Introduction

Most of the users of the Image Dissector Scanners mounted on the Boller & Chivens Cassegrain spectrographs on La Silla will be aware of the high count rate nonlinearity of the IDS. The typical figure for this saturation effect is a 10 per cent loss at count rates in excess of some 2,000 detected events per channel per second. For a linear dispersion of 1.7 Å per channel (171 Å per mm grating) this corresponds to a 10 mag star at the 3.6 m and an 8 mag star at the 1.5 m telescopes. In the following I will report on another nonlinearity effect present at very low light levels, i.e. for count rates below 100 counts per second and channel, and discuss some of the possible sources and implications.

II. The Observed Nonlinearity

During the process of the analysis and interpretation of a large number of high signal-to-noise IDS spectra of H II regions I have been confronted with the inconsistency of observed values and theoretical predictions for emission line ratios. The line ratios concerned are: [O III] λ5007 versus λ4959, [N II] λ6583 versus λ6548 and the Balmer series from Hα to H12. The two forbidden line ratios are expected to lie around 2.9 (see for example the compilation of C. Mendoza in "Planetary Nebulae", IAU Symposium No. 103, ed. D.R. Flower, p. 143 [1983]). My own data and those of other ESO observers are centred around 3.15 with a sigma of 0.1. It is clear that errors in the reddening corrections, flat fielding and response calibra-

tion cannot be made responsible for this discrepancy. Saturation would decrease the observed line ratios rather than enhancing the stronger lines with respect to the fainter ones. In a detailed analysis of my own data and a large number (> 500) of published observations I demonstrate that the true intensity ratio of the above forbidden lines is likely to be around 3.03 (± 0.03) (to be submitted). Under the assumption of a power law nonlinearity (see below) an index of 0.96 is appropriate to bring the ESO IDS data into agreement with this "true" value for the line ratios.

The Balmer line ratios are affected by interstellar extinction and will obviously suffer from any mismatch between the *absolute* calibration of blue and red spectral ranges as well as any low frequency shift in the spectral response function of the instrument. However, a large fraction of my data has sufficient signal to noise in order to measure the Balmer lines up to H 12. A simultaneous solution of the amount of reddening (using different reddening curves) for all the line ratios available shows that, whatever choices are made, a perfect solution (within the statistical errors) can only be made under the assumption that the stronger lines are enhanced with respect to the fainter ones. A typical example is shown in Table 1 for spectra of the 30 Dor nebula. The first row contains the theoretical values of the Balmer decrements for case B, a density of 100 and an electron temperature of 10,000 K. The second row displays the best solution obtained by giving H3/H4, H5/H4 and H6/H4 the highest weigths and using the extinction curve of Savage and Mathis (*Ann. Rev. Astron. Astrophys.*, **17,** 73, 1979). The last row shows the solution obtained by assuming a power law nonlinearity with index 0.96 under the same choices as above. It is clear that this is scratching uncertainties in the few per cent range and can only be used as an additional indication for nonlinearity effects.

I will not go into more detail in this note but rather summarize my findings. There seems to be a nonlinearity in spectrophotometric data obtained with the IDS detectors at both the 3.6 m and the 1.5 m telescopes. This nonlinearity *increases* the measured intensity ratio of emission lines over the one inherent in the source spectra. The effect occurs at very low light levels, long before nonlinearities due to saturation are important. It seems not to depend on the absolute strength of the signal over a wide range of fluxes (10^{-11} to 10^{-15} erg/sec/cm^2/Å). The effect is present in the raw data and a careful check of the IHAP reduction routines has been made to verify the linearity in the data reduction. The correction formula I suggest to apply to the raw data prior to all reduction is:

$$I(\lambda)/I(\lambda_o) = [i(\lambda)/i(\lambda_o)]^{(0.96 \pm 0.02)}$$

where "i" is the measured intensity (or count rate) and "I" the corrected one. Since it is not clear in which way the nonlinearity works (losses for low count rates or gains for higher count rates) the absolute value of the intensity remains undetermined. Needless to say that observers should check their data before applying this correction blindly.

III. Possible Sources of the Nonlinearity

Since the nonlinearity seems to be inherent in the IDS raw data it is interesting to see whether or not the ESO IDS detectors are peculiar among similar instruments. The above-mentioned analysis of the [O III] line ratios suggests that similar detectors, i.e. the KPNO IIDS, the Lick Observatory ITS, the AAT IIDS and intensified Reticon systems are affected by the same sort of nonlinearity to various degrees. To mention a specific example: In a recent paper J.B. Kaler (1985, preprint Astron. Dept. Univ. of Illinois at Urbana) reports line ratios for 12 planetary nebulae observed with the Red Reticon System at KPNO. The average reddening corrected line intensities are 3.17 for [O III] and 0.43 for H5/H4. Compared with the theoretical values 3.03 and 0.47 respectively and supposing the same power law nonlinearity, an index of 0.91 can be derived.

TABLE 1:

Line ratio H	3/4	5/4	6/4	9/4	10/4	11/4	12/4	[OIII]
Theory	2.86	.469	.259	.073	.053	.040	.031	3.03
C (Hβ) = 0.80	2.78	.457	.250	.065	.040	.035	.040	3.21
C (Hβ) = 0.70 corr. for nonlinearity	2.82	.460	.256	.070	.044	.038	.043	3.07

Comparison of theoretical Balmer line ratios and of the line ratio [O III] 5007/4959 with observations. The overall agreement is better if the data are corrected for nonlinearity effects. Balmer line decrements 7/4 and 8/4 are affected by blends with strong forbidden lines, H12 is hard to resolve.

In order to prove that the nonlinearity is not depending on the absolute value of the signal, I have used He-Ar spectra taken through different neutral density filters, kindly provided by S. Cristiani and G. Palumbo. A straightforeward result is the fact that the exposures can be scaled linearly into each other for count rates between 35 and 0.03 detected counts per second per channel, that is equivalent to the range 60,000 to 50 in IDS data values. A check on the power law nonlinearity is however impossible with these data since it would require the knowledge of very precise values for the attenuation of the neutral density filters or for line ratios in the He-Ar spectra. Similarly, a test in the laboratory would have to record independently the illumination of the photocathode over a dynamic range of at least 100 with an accuracy of better than 5 per cent. The illumination would also have to be comparable to the astronomical reality, i.e. a few photons per second per channel at the photocathode with a high spatial contrast.

Possible sources for the nonlinearity can be sought in the fact that the combination of a three-stage intensifier chain with an image dissector is not working in pulse-counting mode. The principle is to read the temporal buffer (phosphor) at repeated times and accumulate the detected phosphor photons in the memory. The length of this acquisition interval is 1 microsecond and acquisition is repeated for the same location on the phosphor every 4.2 milliseconds. The delta impulses of the photoelectrons released at the first photocathode are broadened considerably in the intensifier chain. The output pulse has a decay law of the form "rate(t) = const. × 1/t" and about 50 per cent of the phosphor output photons are released within 5 milliseconds. Up to this stage the whole process is essentially a convolution of several Poissonian processes, i.e. arrival of photons, release of photoelectrons, particular gain of the intensifiers for each photoelectron and emission of phosphor photons. However, the IDS is sensitive enough to record a given phosphor pulse *on the average* 3.3 times. At this stage one of the requirements for a Poissonian process is violated, i.e. the probability to detect an event at time n×t is coupled with the probability to detect it at (n–1) ×t. Another violation of the ideal counter can be seen in the existence of a discriminator level that is intentionally set to suppress counts from the background (intensifier shot noise, scattered light) and consequently rejects the faint end of the photon event distribution. Furthermore one has to expect the occurrence of aliasing between the sampling frequencies 10^6 cps and 238 cps and the high and low frequency components in the Poissonian distributed input signal. Readers interested in the system performance of intensified IDS detectors are referred to the papers of McNall, Robinson and Wampler (*Publ.A.S.P.*,

82, 488, 1970), Robinson and Wampler (*Publ.A.S.P.*, **84,** 161, 1972), McNall (*Publ.A.S.P.*, **84,** 182, 1972) and Cullum (*ESO Technical Report* No. **11,** 1979).

IV. Implications

At first glance the nonlinearity reported here seems to have little importance for the average observation. Error estimates quoted for line ratios measured in H II region spectra and in the absolute flux calibration are usually of the order of 10 per cent or larger. However, these error estimates concern the random errors. The power law nonlinearity reported here will produce a systematical deviation of 17 per cent for intensity ratios of 100 and 9 per cent for intensity ratios of 10. Though this might be negligible for observations of continuum sources, the effects on H II region line spectra are far reaching. For an electron temperature of 10,000 K and a density of 100 electrons per cubic centimetre the intrinsic ratio of the [O III] lines 5007/4363 is 170. The observed ratio will be 210 and a temperature of 9,350 K will be derived. Together with the overestimated ratios of the strong oxygen lines over Hβ an oxygen abundance too high by a factor of two or more will result. This systematic effect will be present in investigations based on large samples of H II regions or planetary nebulae—for example in abundance gradient studies.

Last but not least I would very much appreciate any comments, in particular to know about similar findings with the detectors on La Silla or anywhere else. The growing confidence in the reality of the nonlinearity reported here has benefitted by discussions with a large number of observers, engineers, technicians and theoreticians, who deserve my thanks.

The Local Stellar Environment (LSE) — The B Emission-Line Stars

V. Doazan, Observatoire de Paris

Observations made during the last decade outside the visual region—in the X-ray, far UV, far IR, and radio regions—have profoundly modified our understanding of the LSE. Historically, from only visual observations, the LSE was considered as either the locale of protostellar material surrounding stars in their early evolutionary stages, or as a product of mass ejection during only the late stages of stellar evolution. However, we know from all these new observations that a mass outflow is observed from a variety of stars, during a variety of evolutionary stages, all across the HR diagram; and that there exists a continuous interaction between the mass outflow at a given epoch, and either (i) the general ISM; (ii) the prestellar nebula; or (iii) the mass outflow at a preceding epoch, i.e. a self-interacting variable mass outflow. Thus, the picture of a static LSE enveloping a thermally structured star is replaced by a dynamic LSE enveloping a nonthermally structured star in continuous interaction with the LSE. From this viewpoint, the outermost layers of the star are to be considered as a major component of the local environment; and the structure of both the outermost layers and the local environment reflects the properties of the mass flux. For this reason, progress in our understanding of the LSE is intimately linked to progress in understanding stellar atmospheric structure and stellar evolution.

The LSE may be either observed directly as nebulosity whose association with star(s) in its vicinity has been established; or inferred from the presence of spectroscopic features that imply the existence of an extended atmosphere. Examples of an observed LSE are: (a) pre-main-sequence (PMS) stars, identified by Herbig (1960), still embedded in the primeval nebulosity—Herbig Ae, Be, T Tauri—(b) the planetary nebulae which, on the contrary, have manufactured their own local environment, and represent late stages of stellar evolution. Examples of inferred LSE come from the presence of low-excitation/ionization emission lines (relative to photospheric conditions) such as observed in the visual spectrum of Be and P Cygni stars. These are to be contrasted with chromospheric-coronal, high-ionization emission lines, such as seen in the Sun and in WR stars. Low-ionization emission, especially in the Balmer lines, implies, for these hot stars, the existence of an extended, cool, outer atmosphere. Our understandig of each of these types of stars, whose LSE is observed or inferred, has strongly evolved during the last decade. But, undoubtedly, it is for the Be stars that our picture has changed the most. Be stars are probably the best observed objects in the Galaxy, after the Sun. In the same way as the Sun has served as a guide for understanding stellar chromospheres and coronae, Be stars may help us to understand that broad class of emission-line objects, observed across the whole HR diagram, which, in addition to having hot, rapidly expanding regions, also possess cool, extended, low-velocity regions which define their peculiarity.

I. The Be Stars as Seen in the Visible— A Variable, Cool, Extended Outer Atmosphere

Be stars show a B-type spectrum of luminosity class III-V accompanied, in the visible region, by emission in the Balmer lines, and often in the singly ionized metallic lines whose presence is expected only at later spectral types.

The origin of emission lines in B-type spectra was attributed by Struve, in 1931, to the presence of an extended, cool atmosphere. The question to be answered, at that epoch, by the existence of Be stars was: Why do only some stars of the B-type class possess an extended atmosphere? On the basis of observed line widths, interpreted as rotational, Struve hypothesized that the presence of emission lines in the spectrum and the rapid rotation of the star were two connected phenomena. At that epoch, rotation at break-up velocity was believed to produce equatorial mass ejection. Thus, a star rotating at such velocity would form an extended, cool, rotating, equatorial gaseous disk. This was the model of Be stars proposed by Struve. Subsequent studies showing that v. sini values are higher, statistically, for Be stars than for normal Bs, strengthened this picture.

However, it was realized that critical rotation by itself could not produce a mass ejection. Moreover, the observations did not provide any basis for justifying the assumption of critical rotation for these stars. Finally, it was recognized that v. sini

values for Be stars are rather uncertain. Given these uncertainties, only ad hoc models of the Be phenomenon have been constructed. They retained the two basic assumptions of Struve's rotation model: (i) Be stars rotate at the critical rotational velocity; and (ii) they possess a mass flux restricted to the equatorial region only.

The rotation model stood up to nearly half a century of new observations; as long as the observations were restricted to the visible or infrared regions, it provided a convenient picture into which a large amount of new data could be fitted.

However, even in the visible region, it was possible to guess that the suggested picture was too narrow for describing the richness and diversity of the properties of the Be stars, especially their striking variable behaviour.

II. The Be Stars in the Far UV—A Variable, Hot, Rapidly Expanding Outer Atmosphere

The real contradiction between the rotation model and the observations comes from the far UV, where there is evidence for a new region in the outer atmosphere of Be stars, which no theory, or model, has predicted. In this spectral region, instead of a cold, low-excitation, low-velocity atmospheric region, one observes a hot, superionized region, with expansion velocity higher than escape. Instead of mass ejection restricted to the equatorial region, one observes high expansion velocities in stars classified as pole-on—that is, in the presumed direction of the axis of rotation—as well as in stars classified as equator-on. Not only was the possible existence of such phenomena ignored in the construction of the models, but the models were actually constructed on the assumption that such a possibility was actually excluded. The hypothesized picture of a cool, rotating equatorial disk is confronted with the actual picture of a hot superionized atmosphere in violent expansion. The rotation model is shaken by these new observations. It is clear now that any Be-star model must represent all the observed atmospheric regions within a coherent, self-consistent framework.

But, such far UV observations have not been genuine surprises for only Be-star models. Those spectral features which indicate the presence of an outer atmosphere of high ionization, and rapid expansion—i.e. the existence of a mass flux and a nonradiative energy flux—are equally observed among both normal B and Be stars. Any distinguishing difference between these 2 types of objects is a matter of degree and temporal behaviour of these 2 nonthermal fluxes rather than existence. It is, thus, in the *presence* of the *cool*, subionized regions and in the *behaviour* of the *hot* superionized regions that B and Be stars differ. Now, the problem raised by the existence of the Be phenomenon is to understand: (i) how do Be stars, and not "normal" B stars, produce, in addition to their superionized regions, slowly moving, subionized, extended atmospheres, (ii) what specific differences exist between the superionized rapidly expanding regions of B and Be stars.

Before trying to find the physical causes of the Be phenomenon, it is first necessary to be more precise on what *is* the Be-behaviour in these various atmospheric regions. Because the outstanding property of Be stars is their variability, it is necessary to observe *simultaneously* such variability in the different atmospheric regions in order to provide the observational basis necessary for modelling the whole atmosphere.

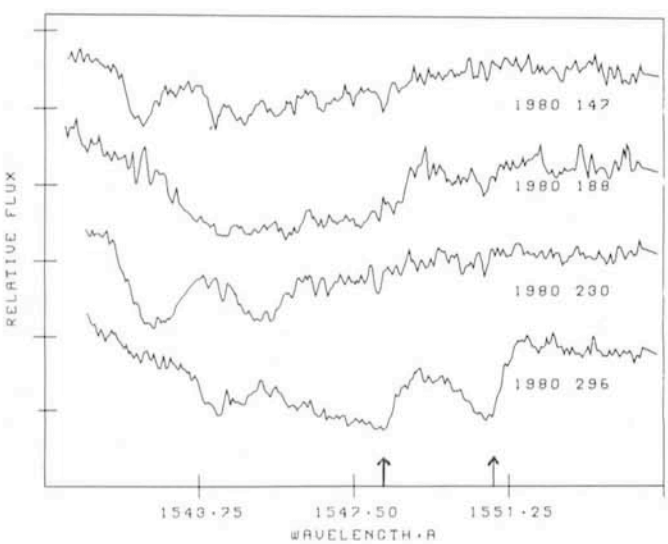

Fig. 1: *Representative C IV line profiles illustrating the striking changes in shape and velocity in the Be star HD 200120. From V. Doazan et al., 1982, IAU Symp. No. 98, p. 415.*

III. Variability of Be Stars—A Variable Mass Flux and/or a Variable Nonradiative Energy Flux

As a general rule, Be stars are variable in their line spectrum, as well as in the continuum, in the visual region. The variability of Be stars can manifest itself in various ways depending on the star in question. In some cases a Be star loses its emission characteristics and becomes a normal B spectrum, and vice versa.

From the first far UV observations, it was quickly recognized that Be stars are also variable in this spectral region. After one decade of far UV observations, it is clear that Be stars are, among the hot stars, those which exhibit the largest, and the most striking, variations there. These large variations are exhibited by the resonance lines of the most highly ionized species present in the IUE spectral range, as C^{+++} and N^{++++}. On the contrary, the Mg II resonance lines in Be stars behave like the Balmer emission lines, in reflecting conditions in the cool regions of the outer atmospheres, and thus do not help in studying the highly ionized rapidly expanding atmospheric regions.

Long-term programmes of simultaneous observations made in the far UV and in the visual, for a few Be stars, have shown that the superionized lines, C IV and N V, are highly variable in velocity, shape and strength—in association with the visual phase. Fig. 1 shows some C IV profiles observed in HD 200120, at an epoch where emission in the Balmer lines begins to develop in the visual. That is, after having shown only absorption lines, the star entered what we have called a "new Be phase". Our regular monitoring of this star during seven years has shown, correlated with changes in the Balmer lines, the most remarkable sequence of changes in the C IV lines ever observed in a Be star. A synthesis of all the data obtained so far shows a striking correlation between the long-term behaviour in the visual and in the far UV. Fig. 2 illustrates another type of variability which affects mainly the strength of the C IV resonance lines: they appear and disappear at varying and irregular time scales. These 2 kinds of variability have been observed in other Be stars of our programme list, so they should not be considered as exceptional. We believe, on the contrary, that the only exceptional aspect of these results is their demonstration of associations between visual and far UV phenomena that became apparent only because of the regularity of our survey during a sufficiently long time.

We have interpreted the large changes of the C IV velocity, measured at maximum depth, as reflecting mainly the variabil-

ity of the mass flux; and the large changes in strength of the C IV lines as reflecting mainly the variability of the nonradiative energy flux. Clearly, it is not possible to decide, from far UV observations alone, which of these fluxes are variable, but the whole set of data obtained so far points toward our interpretation. It is obvious that X-ray, far IR and radio data are necessary to complete the observations.

IV. A Tentative Model for Be and Similar Stars

In a first, wholly empirical, attempt to use all the available observational data on Be and similar hot, emission-line stars, we asked, free from historical preconception: what actually is the outer atmospheric pattern common to all these stars? We recognized, first, what is becoming apparent all across the HR diagram: the outer atmospheric structure is dynamic and nonthermal. Second, that in the Be and similar stars the highly ionized species showed the largest nonthermal velocities, while the subionized ones, formed in the more distant regions of the outer atmosphere, showed the lowest nonthermal velocities. Finally, that variability is always associated to emission-line stars.

Combining far UV and visual observations for Be and similar stars, we concluded that a decelerated outflow, which may occur as close as a few stellar radii from the photosphere, characterizes the stars. We proposed that a deceleration of such a superthermic flow, expanding at velocities higher than the escape velocity, can come only from its interaction/collision with either a preceding slowly moving flow—in the case of a Be star—or with the stellar primeval environment—in the case of Herbig Ae, Be stars; and concluded that mass outflow variability is a sufficient condition to produce a deceleration. If after such a deceleration, the flow velocity is smaller than the escape velocity at that point, then the outflowing material will ultimately fall back on the star. In this picture, both expanding and infalling flows may occur. We did not impose any, a priori, asymmetry to the model. But any asymmetry that the observations may demand may be introduced in a self-consistent way.

The variability of the mass flux is at the basis of our empirical model for Be and similar stars where, after the photosphere, the following radial sequence of atmospheric layers are defined: a chromosphere, a corona with its pre- and post-coronal regions, an Hα-emitting envelope, a cool shell, and a dust shell.

V. The Structure of the LSE—A Reflection of the Nonthermal Properties of the Subatmosphere

The new data (visual observations obtained with highly-performing instruments, and data obtained in the newly observeable spectral regions), synthesized in the NASA-CNRS Monograph Series on Nonthermal Phenomena in Stellar Atmospheres, indicate that nonthermal fluxes (mass flux, nonradiative energy flux) exist, at varying degrees, in a variety of objects, including those associated with an LSE. In our approach for modelling Be and similar stars, we have adopted the suggestion that such nonthermal fluxes are produced by subatmospheric nonthermal modes, due to rotation, convection, pulsation (radial or nonradial). Under such a hypothesis, the structure of the LSE is linked to the nonthermal properties of the subatmosphere.

High-quality observations of variable photospheric line profiles show evidence for nonthermal motions in the subatmospheres of a large variety of stars. From studies of precisely

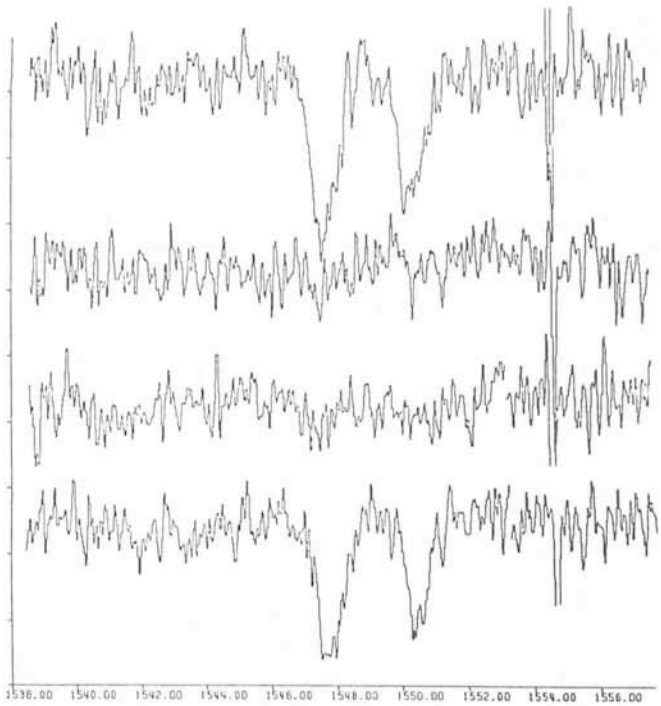

Fig. 2: *Representative C IV line profiles illustrating the changes in strength in the Be star HD 138749. From bottom to top: August 2, 1982; December 17, 1982; January 27, 1983; April 6, 1983. From Doazan et al., 1984,* Astron. Astrophys. **131,** *210.*

that variability of photospheric line profiles, various kinds of photospheric and subphotospheric pulsations have been diagnosed. The next step will be to identify which of these nonthermal modes (rotation, convection, pulsation, or any combination of them) is associated with the observed variety of structures of the LSE. From this viewpoint, any study of the LSE must include a simultaneous investigation of the subatmospheric properties of the stars associated with it. Such a study is currently being made for Be and similar stars.

(The above approach to the study of atmospheric structure and local environment, and the conclusions on the required subatmospheric structure have been abstracted from Volume 2 [B Stars With and Without Emission Lines, by A. B. Underhill and V. Doazan] and Volume 4 [Stellar Atmospheric Structural Patterns, by R. N. Thomas]).

An important collaborative programme based on simultaneous ground-based observations at La Silla, and space observations with EXOSAT and IUE, has been organized recently by Dr. Thé and Dr. Tjin a Djie of Amsterdam for the study of the Herbig star HR 5999. This programme illustrates well the necessity to study simultaneously the whole atmosphere by observing the high- and the low-energy parts of the spectrum. On September 11, 1983, several instruments at La Silla were pointing towards the same star, together with EXOSAT and IUE. We ourselves were observing it in the red and in the blue with the IDS at the 1.5 m telescope. Visual observations alone, which show the presence of Hα emission, and Fe II and Na I shell absorption lines, would only imply the presence of a cool extended atmosphere. But far UV observations, which show the presence of Si IV and C IV resonance lines in the spectrum, and X-ray observations, which imply a hot corona, show that the whole outer atmosphere is composed of multiple, strongly differing, atmospheric regions. These are the data which are needed for modelling the star. But, in order to understand the dynamic interaction of these

several atmospheric regions, further repeated observations are still necessary over a significant time-scale. Finally, in order to link the observed properties of the LSE to the properties of the subatmosphere, we have undertaken at La Silla a study of the behaviour of the photospheric lines of the star with the CES. This programme is currently in progress.

The Multi-Faceted Active Galaxy PKS 0521-36

I.J. Danziger, P.A. Shaver and A.F.M. Moorwood, ESO;
R.A.E. Fosbury, ST-ECF (ESO); W.M. Goss, Kapteyn Astronomical Institute, the Netherlands; and R.D. Ekers, NRAO-VLA, New Mexico

The southern active elliptical galaxy PKS 0521-36 exhibits a range of nuclear and extranuclear phenomena which is remarkable in a single object which has only been observed in any detail over the last few years. Indeed, if it were situated significantly closer than its 330 Mpc (H_0 = 50 km/s/Mpc), it would probably attract more observational and theoretical attention than Centaurus A and M 87 combined. The relationships between its many manifestations of high-energy activity will be the subject of intensive study as new observational techniques become available.

As has so often been the case for southern active objects, attention was first drawn to the galaxy by its optical identification with a Parkes radio source (Bolton, Clarke and Ekers 1965). Higher resolution images suggested an elliptical morphology, but the broad-band colours were anomalously blue, giving the first reason for special interest. The photometric observations of Eggen (1970), showing that it varied by more than one magnitude on a time scale of months, supported the earlier spectroscopic observations of Westerlund and Stokes (1966) and Searle and Bolton (1968), which showed an almost featureless continuum with only very weak emission lines, suggesting a close relationship to BL Lac objects.

Optical Structure

(a) The Jet

Deeper direct imaging obtained by Danziger et al. (1979) showed a jet-like structure extending about 20 kpc towards the north-west. This has a structure somewhat reminiscent of the jet in M87, although a direct comparison is difficult because of the order-of-magnitude difference in linear resolutions available. Sol (1983) has examined the structure of the jet in more detail: as in M87, it consists of condensations of different surface brightness. We are now fairly certain that in the optical region, all sections of the jet are emitting continuum and not line radiation. In deep CCD images of the object in a narrow-band filter isolating redshifted Hα, the jet does not appear. Nor do emission lines appear in the north-west in long-slit spectroscopy aligned along the jet. This spectroscopy does, however, reveal extended emission elsewhere. Nothing is yet known about the polarization of the jet in the optical band although there is associated radio structure which we discuss below.

(b) The Extended Emission

During the course of long-slit spectroscopy of this object with the UCL IPCS on the ESO 3.6 m Boller & Chivens spectrograph, nebular emission was discovered extending about 10 arcseconds to the east and south-east. This is not the source of the relatively weak emission seen in the integrated spectrum, which comes from a compact region at the nucleus.

In Fig. 1, we show the result of a 40-minute exposure taken with the CCD on the Danish 1.5 m telescope on La Silla through an interference filter with a bandwidth of 32 Å and a central wavelength of 6922 Å, corresponding to redshifted Hα. No continuum subtraction has been done. The picture shows a faint filamentary structure extending north of east and then turning towards the south. The reality of this structure has been established by long-slit spectroscopy with the slit in several different positions. In addition to the eastern filament, the picture hints at a more general, irregular filamentary structure. There is perhaps also a very low surface brightness halo extending out to a radius of ~15 arcseconds. These features merit more detailed study with deeper high-resolution imaging and spectroscopy. The picture shows no structure corresponding to the jet.

Spectrophotometry of the eastern filament, Fosbury (1982) and recent unpublished results, show the gas to be in a low state of ionization with [O III] λ 5007 / Hβ ≲ 1.5. This contrasts

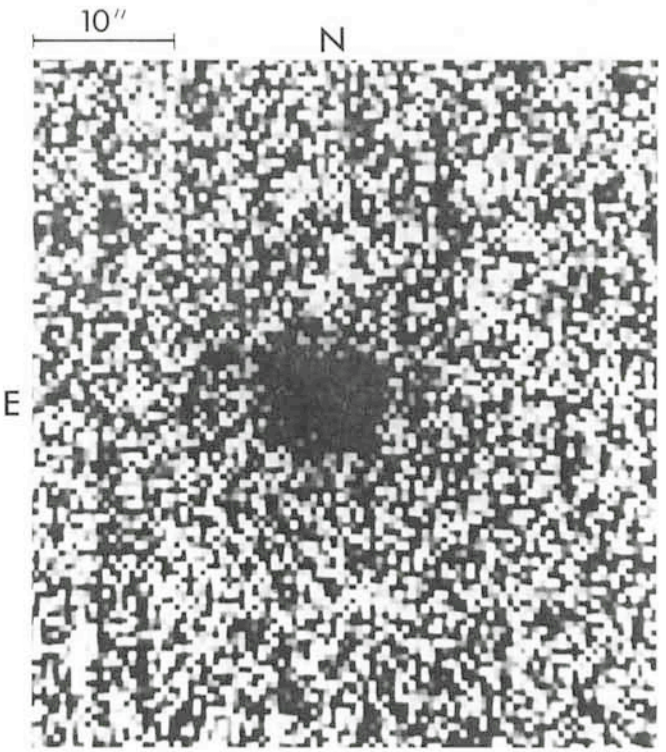

Fig. 1: *A 40-minute CCD exposure of PKS 0521-36 taken with the Danish 1.5 m telescope on La Silla. The filter was a narrow band centred on redshifted Hα (6922 Å). It shows the filament to the east of the galaxy but no feature corresponding to the jet visible on broad-band images in the blue.*

with the nuclear spectrum where this ratio for the narrow line component is close to 3. Little is known yet about the dynamical state of the filamentary gas other than that its internal velocity spread and its velocity relative to the nucleus is less than a few hundred km/s. Attempts to diagnose the ionization mechanism in these outlying regions are hampered by the low signal-to-noise of the spectroscopic observations although we can say that the [OII] λ 3727 / [OIII] λ 5007 ratio is $\gtrsim 2$.

(c) The Nucleus

Apart from the stellar component, characterized by diluted absorption lines of CaII, MgI, etc., there appear to be three different regions, each generating its own spectral imprint. There is a low density region of ionized gas, analogous to the NLR seen in most active galaxies. One should be careful to note, however, that a clear diagnosis of the ionization mechanism has not been made from our data because of the difficulty of measuring the important weak lines such as HeII λ 4686 and [OIII] λ 4363.

There is a broad permitted line-emitting region whose temporal behaviour has not yet been well defined. This can be seen in the optical Balmer lines and in an IUE observation of broad Lyman-α reported by Danziger et al. (1983). It has been suggested by Ulrich (1981) that the broad-line spectrum had developed during the period between the observations of Danziger et al. (1979) and her own, at an epoch several years later. The equivalent widths have certainly changed during this period, since there has been a dramatic decrease in continuum radiation. There is, however, evidence that the broad lines have increased relative to the forbidden line spectrum. There are no observations to our knowledge which show the complete absence of broad lines. Broad-line variability in Seyfert and radio galaxies is now a well-established phenomenon with many reports in the literature, and detailed observations can be used to place extremely useful constraints on size scales and nuclear masses. An example of the optical spectrum, when the blue continuum was weak, is shown in Fig. 2.

The BL Lac nature of the nucleus is manifested through the variability of this blue continuum and through optical polarization reported by Angel and Stockman (1980). Danziger et al. (1979) decomposed the stellar and power-law components to give a spectral index of approximately −1. Using IUE observations, Danziger et al. (1983) combined UV, optical and IR data, at an epoch when the nucleus was about one magnitude fainter, to give a spectral index of about −1.5 for the non-stellar continuum. This implied steepening of the spectrum with decreasing luminosity needs to be checked at other epochs.

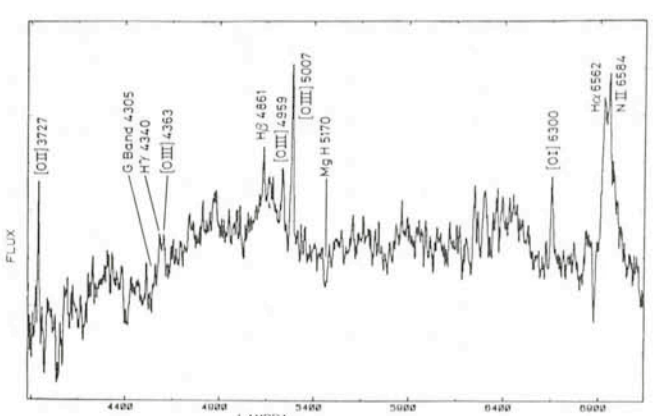

Fig. 2: *A low-resolution IDS spectrum of PKS 0521-36 taken when the nucleus was in a low luminosity state in August 1981. Note the broad Hα and Hβ emission.*

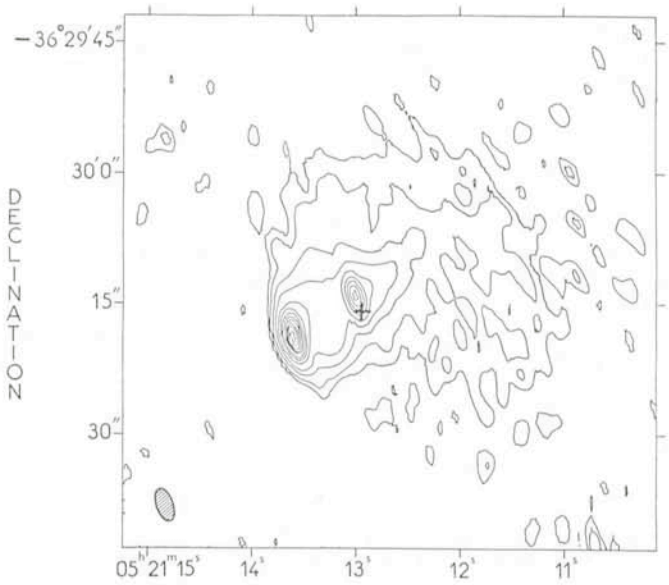

Fig. 3: *A 1.4 GHz continuum map of PKS 0521-36 made with the VLA in New Mexico. The optical nucleus is marked with a cross; the offset is probably due to the poor astrometric reference frame in the south.*

Radio Structure

Since its discovery, PKS 0521-36 was known to be an extended radio source (Mills, Slee and Hill, 1960). VLA observations have provided a much more detailed picture of its complex structure. A 1.4 GHz continuum map is shown in Fig. 3. It appears to be a triple source with the outer lobes of very unequal intensity. The south-eastern lobe is resolved with a size of about 1 arcsecond while the much weaker north-west component follows closely, in direction and extent, the optical jet. An unresolved, flat spectrum source is positioned at the nucleus of the galaxy. The apparent offset between the radio and optical nuclei is within the range of uncertainty due to the poorly known positions of SAO reference stars in the southern hemisphere. Such comparisons will, in the future, be greatly facilitated by the new Cape catalogue in the process of preparation (Nicholson et al., 1984). The radio nucleus has been resolved at approximately 1 milliarcsecond using VLBI measurements.

A correlation of the radio and optical structures reveals another interesting coincidence. That is between the steep south-east edge of the radio source and the eastern emission-line filament. This is reminiscent of a similar coincidence in Coma A reported by van Breugel (1981) and seen in a number of other galaxies with radio jets (Balick and Heckman, 1982; Danziger et al., 1984; Fosbury et al., 1984). The possible transfer of energy between the radio plasma and the thermal, emission-line gas is of great interest in the physics of radio sources.

The VLA map also shows the extended, low brightness emission having a steep spectrum and a diameter of about 30 arcseconds. The nature of this halo might be associated with the similarly sized structure hinted at by the Hα CCD picture. If this association were real, it would be of great interest.

X-ray Emission

PKS 0521-36 is an X-ray source (Schwartz and Ku, 1983) as are most BL Lac objects. We do not yet know anything about

variability although in the near future EXOSAT observations will provide information. More importantly we do not know whether it is an extended source or not. It could be extended up to a diameter of ~2 arcminutes and would not have been resolved by the one IPC observation from the Einstein Observatory. An extended source might point to a cooling flow giving rise to the condensing filaments that we see as low-excitation filaments and conceivably the diffuse Hα and radio halo.

From our spectroscopy of the filaments alone we can provide an estimate of the total Hβ emission = 9×10^{39} ergs/sec. Under the assumption that each hydrogen atom in the cooling flow recombines only once, this estimate converts into an accumulating mass flow of approximately 500 solar masses/year. This is of the same order of magnitude as Fabian and Nulsen (1977) obtained for NGC 1275 (Perseus A). In fact, a number of the other radio and optical properties of PKS 0521-36 remind one of NGC 1275.

At present we cannot assert strongly that the wider environment of PKS 0521-36 supports the idea of an X-ray cooling flow. Certainly it does not belong to a rich group or cluster. There are in the neighbourhood, however, other fainter galaxies whose redshifts are not yet known. And of course we know nothing at all about the possible existence of intergalactic gas clouds in this region.

Summary

There are many phenomenological details associated with PKS 0521-36, some suggestive ideas and not many clear-cut answers. It is clear, however, that new generations of observing facilities can shed further light on many of the problems alluded to here. The Space Telescope will have imaging capabilities that provide spatial resolution of PKS 0521-36 equivalent to that currently possible for M87 with large ground-based telescopes. It will also provide extended wavelength coverage for studying the jet. Future high-resolution X-ray imaging observations will be necessary and possible.

VLA observations to study the spectral and polarization properties of the various resolved components in this source are under way.

All of this may mean that PKS 0521-36 will in the future attract as much attention as the popular, relatively nearby active galaxies.

Acknowledgements

We thank Holger Pedersen for the Hα CCD image and Alec Boksenberg, Keith Shortridge, John Fordham and the La Silla technical staff for getting the IPCS operating on the 3.6 m telescope.

The VLA is operated by the Associated Universities Inc. under contract with the National Science Foundation.

References

Angel, J.R.P., Stockman, H.S., 1980. *Ann. Rev. Astron. Astrophys.* **18,** 321.
Balick, B., Heckman, T.M., 1982. *Ann. Rev. Astron. Astrophys.* **20,** 431.
Bolton, J.G., Clarke, M.E., Ekers, R.D., 1965. *Aust. J. Phys.* **18,** 627.
van Breugel, W., 1981. Optical Jets in Galaxies, Proc. of Second ESO/ESA Workshop, p. 63.
Danziger, I.J., Fosbury, R.A.E., Goss, W.M., Ekers, R.D., 1979. *Mon. Not. R. Astr. Soc.* **188,** 415.
Danziger, I.J., Bergeron, J., Fosbury, R.A.E., Maraschi, L., Tanzi, E.G., Treves, A., 1983. *Mon. Not. R. Astr. Soc.* **203,** 565.
Danziger, I.J., Fosbury, R.A.E., Goss, W.M., Bland, J., Boksenberg, A., 1984. *Mon. Not. R. Astr. Soc.* **208,** 589.
Eggen, O.J., 1970. *Astrophys. J.* **159,** L95.
Fabian, A.C., Nulsen, P.E.J., 1977. *Mon. Not. R. Astr. Soc.* **180,** 479.
Fosbury, R.A.E., 1982, *Extragalactic Radio Sources,* IAU Symposium **97,** 65.
Fosbury, R.A.E., Tadhunter, C.N., Bland, J., Danziger, I.J., 1984. *Mon. Not. R. Astr. Soc.* **208,** 955.
Mills, B.V., Slee, O.B., Hill, E.R., 1960. *Aust. J. Phys.* **13,** 676.
Nicholson, W., Penston, M.J., Murray, C.A., de Vegt, C., 1984. *Mon. Not. R. Astr. Soc.* **208,** 911.
Schwartz, D.A., Ku, W.H.M., 1983. *Astrophys. J.* **266,** 459.
Searle, L., Bolton, J.G., 1968. *Astrophys. J.* **154,** L101.
Sol, H., 1983. Astrophysical Jets, Proceedings of Torino Workshop Oct. 1982. D. Reidel. p. 135.
Ulrich, M.-H., 1981. *Astron. Astrophys.* **103,** L1.
Westerlund, B.E., Stokes, N.R., 1966. *Astrophys. J.* **145,** 354.

Observations of High Redshift Mg II and Fe II Absorption Lines in QSO Spectra

P. Boissé, Ecole Normale Supérieure, Paris, and J. Bergeron, Institut d'Astrophysique, Paris

Introduction

When the first absorption system was discovered in the spectrum of 3C191 by Burbidge et al. (1966) it was immediately realized that the analysis of QSO spectra could bring a lot of information on the large-scale content of the universe. The path length to high redshift QSOs is so large that the line of sight towards such objects is likely to intersect galaxies and intergalactic clouds which will leave their signature in the spectrum. Although many questions remain yet unsolved today, some conclusions emerge from the increasing amount of data. It seems now well established that among all systems, those containing sharp metal-rich absorption lines can be associated with intervening galactic haloes. Arguments are mainly of a statistical nature and come from a detailed study of the redshift distribution of the systems. This function appears to be compatible with absorption by randomly distributed clouds and, moreover, the systems tend to cluster in the same manner as galaxies (Young et al. 1982).

In standard Friedmann cosmological models and in the absence of cosmological evolution of the absorbers, the mean number of systems per unit redshift interval, dN/dz, is expected to be of the form

$$\frac{dN}{dz} = \frac{C \times n_0 \times \sigma_0}{H_0} \times \frac{1+Z}{\sqrt{1+2 \times q_0 \times z}}$$

where n_0 is the number density of absorbers and σ_0 their cross section at the present epoch. The knowledge of dN/dz is of great interest since in principle it could yield the value of q_0. In fact, over a large redshift range cosmic evolution effects could

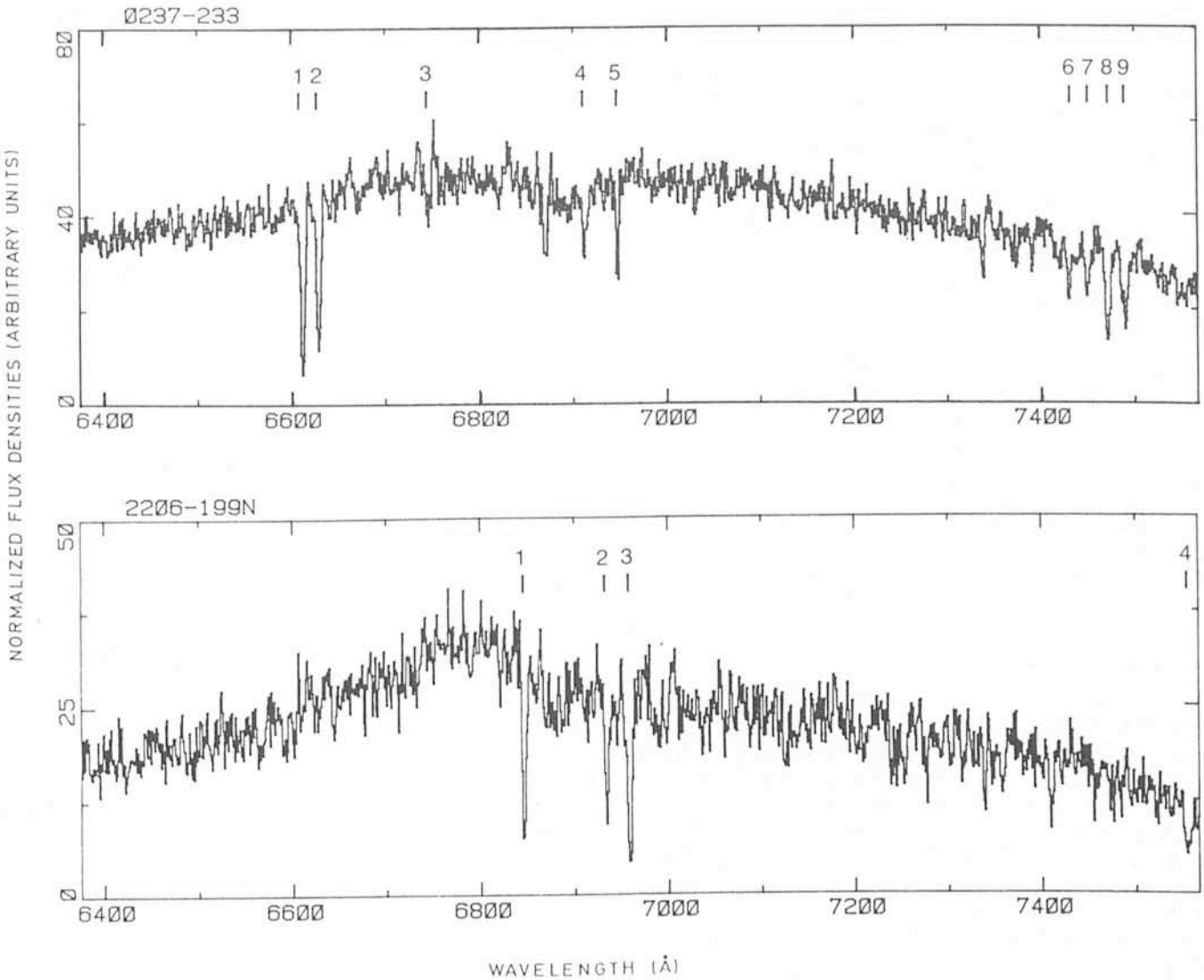

Fig. 1: *Two spectra obtained with the IDS on the 3.6 m telescope at La Silla. In the first one (0237–233) Mg II doublets are observed at z = 1.365, 1.657, 1.672 (lines 1–2, 6–7, 8–9). Other lines are also detected from Mg I at z = 1.365 (3) and Fe II at z = 1.672 (4–5). In the spectrum of 2206–199N a strong Fe II system is found at z = 1.920 (lines 1–2–3–4). In both spectra the absorption near 6870 Å is due to atmospheric oxygen.*

dominate, as found for the Lyα forest systems (very metal-poor population of absorbers).

Moreover, we have to face severe observational constraints which limit the size of the available samples. The identification of absorption lines is sometimes a difficult task and doublets such as those of C IV ($\lambda\lambda$ 1548–1551) and Mg II ($\lambda\lambda$ 2796–2803) which yield unambiguously the absorption redshift must be resolved. As a consequence, the rather large resolution required (e.g. R $\simeq$ 1500 for C IV) limits the wavelength interval observed per instrumental setting and a reasonable redshift coverage requires a very large amount of observing time. In practice, as most of the observations have been made in the blue, the value of dN/dz at low ($0.2 < z < 0.8$) and high ($1.2 < z < 3.0$) redshifts is mainly derived from the Mg II and C IV doublets respectively.

What Relationship Between C IV and Mg II Systems?

One puzzling question related to absorption systems is the well-known difference between C IV and Mg II lines, the former being about four times more numerous. This difference could be understood if some cosmological evolution were present with for instance a larger size of the C IV clouds at higher redshift. The present data suggest indeed a positive evolution for the C IV absorbers (Bergeron and Boissé, 1984) although larger samples would be needed to give a more definite answer. Another possibility is the existence of different populations of narrow-line absorption systems. C IV and Mg II lines could sample distinct regions and in this case we would not necessarily expect a strict correspondence between these systems. Using all available data we have built the rest equivalent width (W_r) distribution of C IV and Mg II lines. These two functions look quite different: the C IV distribution is rapidly increasing as W_r decreases whereas no such accumulation is found for Mg II systems at low W_r values (Bergeron and Boissé, 1984). This strongly suggests the existence of two distinct populations or phases. Another way to clarify the relationship between Mg II and C IV lines is to look at systems where both doublets have been observed. There are few such cases and they tend to strengthen the arguments coming from the comparison of the equivalent width distributions.

In order to investigate in more detail the existence of two separate populations of absorbers we have undertaken an observing programme including QSOs with C IV doublets of

various strengths already detected in the blue and with MgII (or FeII) lines expected in the red (Boissé and Bergeron, 1985). The observations were made with the Image Dissector Scanner (IDS) attached to the Cassegrain Boller and Chivens spectrograph on the 3.6 m telescope with a spectral resolution R = 1700 or FWHM = 4.0 Å. Sixteen QSOs brighter than $m_v = 18.0$ have been observed in the wavelength range 6370–7600 Å. This interval corresponds to a redshift range of 1.18–1.70 for the MgII doublet and 1.72–2.17 for the FeII UV 1, 2, 3 lines.

A Low Excitation Line Sample

The spectrum of two QSOs in our sample, 0237–233 and 2206–199N, is presented in Fig. 1. 0237–233 was known to have a very rich absorption spectrum with 4 CIV systems detected at z = 1.365, 1.596, 1.657, 1.672 (Sargent et al., 1980; Young et al., 1982). Three of them show clear MgII absorption with some additional lines from MgI and FeII. For 2206–199 a strong CIV doublet was previously reported by Robertson et al. (1983) at z = 1.920 and we observe an even stronger FeII counterpart.

The two spectra discussed above are by no means representative of our overall results, as illustrated in Fig. 2, since in most cases MgII or FeII lines were not present at an equivalent width limit $W_{obs.,\ lim.} \simeq 0.5$ to 1 Å (depending on the QSO apparent magnitude). More specifically, we observe that: 1) in the 5 systems with rest equivalent width W_r (CIV λ 1548) > 1 Å the low excitation lines are always present and in 4 cases stronger than CIV lines; 2) for the remaining 9 systems with weaker CIV absorption (0.5 < W_r (CIV) < 1.0 Å), there are only two MgII or FeII detections with W_r (MgII λ 2796)/W_r (CIV λ 1548) < 0.5. Thus, there appears to be a relationship between the strength of the absorption lines and the degree of ionization of the system.

Velocity Dispersions Inside MgII – FeII Clouds

Another characteristic property of the absorbing clouds is their velocity dispersion possibly different for regions of distinct ionization degree. For our observations, the resolution is unfortunately not large enough to give the true profile of the lines and only a curve of growth analysis can be performed. Then, the velocity distribution law has to be assumed a priori. This may lead to large systematic errors, especially in the estimation of the column densities, if several clouds with different opacities are present on the line of sight.

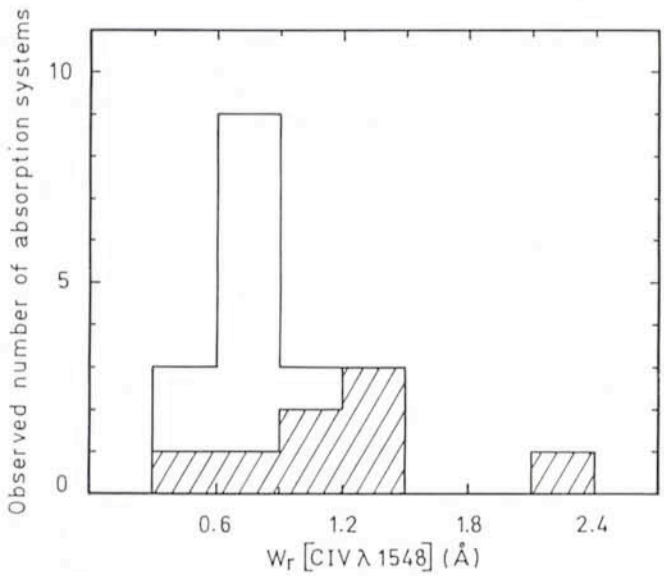

Fig. 2: *The number of CIV systems in the sample as a function of the rest equivalent width of CIV λ 1548 for which MgII or FeII lines were expected. The hatched area shows the distribution of the systems for which MgII or FeII lines have been detected.*

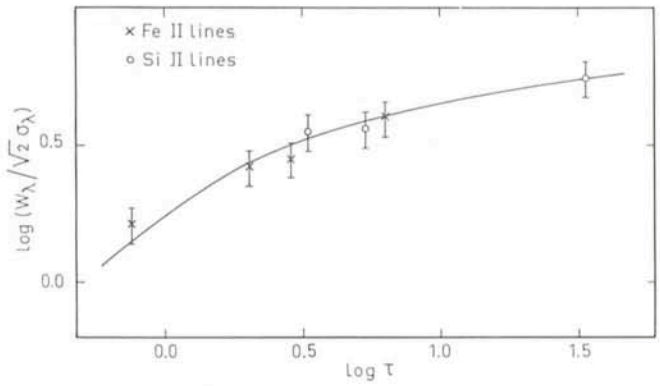

Fig. 3: *Curve of growth for the z = 1.9615 system in 0551–366. A single cloud model with a gaussian velocity distribution has been considered. In addition to the three FeII lines observed some data on FeII λ 1608 and on SiII lines have been used. The best fit is obtained with a velocity dispersion of 110 km/s. Each error bar corresponds to a relative uncertainty of 15 % on W.*

For the very strong system at z = 1.9615 in 0551–366 we have added data from Young et al. (1982) to ours and 4 FeII and 3 SiII lines could be included in the analysis to derive the velocity dispersion of the low-excitation region. The two sets of lines yield consistent results $\sigma_v = 100$ and 120 km/s respectively. When considering the FeII and SiII lines altogether, as has been done in Fig. 3, the best σ_v value is found to be about $\sigma_v \simeq 110$ km/s. As multiple components could be present, this number represents only an upper limit. The velocity dispersion of the higher excitation region can be derived from the CIV and SiIV doublets and we get a similar estimate as the previous one. For the other low excitation systems we obtain σ_v closer to the standard values of 20–40 km/s.

An Upper Limit on the Number Density of MgII Systems

In order to determine the true number density of systems per unit redshift interval, one has to be very careful not to include in the sample QSOs with a priori knowledge on the existence of absorption lines, otherwise dN/dz will be overestimated. As our observing programme is biased in that respect, we can only get from our results an upper limit on dN/dz for MgII–FeII systems. In the assumption of an empty universe ($q_0 = 0$) and no cosmological evolution the observed number density dN/dz (z) may be extrapolated to z = 0 with

$$\frac{dN}{dz}\ (z = 0) = \frac{dN}{dz}(z)/(1 + z)$$

From our number of observed systems (at an average redshift of 1.75) we get

$$\frac{dN}{dz}\ (z = 0) = 0.13 \pm 0.07$$

a value which is to be compared with the one obtained by Tytler et al. (1984) from unbiased observations at lower redshift (< z > = 0.53):

$$\frac{dN}{dz}\ (z = 0) = 0.19\ ^{+\ 0.12}_{-\ 0.08}$$

The assumed absence of cosmological evolution thus appears to be compatible with present data even if it is clear that the statistical significance of our results is severely limited by the smallness of the samples.

Conclusion

The comparison between high and low excitation lines in the same absorption systems has strengthened our previous suggestion of the existence of a well-defined class of "low excitation absorbers". In these systems C IV and Mg II (or Fe II) lines are very strong with W_r (C IV λ 1548 or Mg II λ 2796) > 1 Å.

In our Galaxy, high latitude gas has been observed by IUE in front of Magellanic Cloud stars (Savage and de Boer, 1981). It shows an excitation degree very similar to that of the low excitation systems, although the components observed in our Galaxy are generally much weaker. Thus, it seems reasonable to think that these low excitation systems are associated with thick galactic disks. Their physical state (excitation degree, ...) would then be determined mainly by the local starlight radiation field. On the other hand, weaker C IV systems of higher excitation could be related to extended haloes, a phase which would be more sensitive to the external UV radiation field (integrated emission of the QSOs) and therefore more easily subject to cosmological evolution effects.

References

Bergeron, J., Boissé, P.: 1984, *Astron. Astrophys.* **133,** 374.

Boissé, P., Bergeron, J.: 1985, *Astron. Astrophys.*, to be published.

Burbidge, E.M., Lynds, C.R., Burbidge, G.R.: 1966, *Astrophys. J.* **144,** 447.

Robertson, J.G., Shaver, P.A., Carswell, R.F.: 1983, XXIV Colloque International de Liège, ed. J.-P. Swings, p. 602.

Sargent, W.L.W., Young, P.J., Boksenberg, A., Tytler, D.: 1980, *Astrophys. J. Suppl.* **42,** 41.

Savage, B.D., de Boer, K.S.: 1981, *Astrophys. J.* **243,** 460.

Tytler, D., Boksenberg, A., Sargent, W.L.W., Young, P., Kunth, D.: 1984, preprint.

Young, P.J., Sargent, W.L.W., Boksenberg, A.: 1982, *Astrophys. J. Suppl.* **48,** 455.

Nova Muscae 1983: Coordinated Observations from X-rays to the Infrared Regime

J. Krautter[1], K. Beuermann[2], H. Ögelman[3]

[1] *Landessternwarte Heidelberg-Königstuhl*

[2] *Astronomisches Institut der TU Berlin*

[3] *Max-Planck-Institut für Extraterrestrische Physik, Garching*

During recent years, coordinated observations in different wavelength regions with different instruments have turned out to be a very efficient means of studying variable objects. However, scheduling of such observations is a tricky problem, and one has to plan them well in advance. Difficulties increase, if facilities of several ground-based observatories and astronomical satellites have to be used. But what, if one wants to study a nova outburst? Nova outbursts are absolutely unpredictable and so rare that one does not have any meaningful chance to observe a nova during a normal observing run. There is only one solution for this problem: As soon as a nova outburst is announced, one has to organize an ad-hoc observing campaign. But for that one has to have luck. And that we had.

Let us now explain how we came by lucky circumstances to initiate an ad-hoc observing campaign on Nova Muscae 1983. Two of us (K.B. and J.K.) were on La Silla to carry out simultaneous IR and Walraven photometry of cataclysmic variables. A particular purpose of our programme was to observe dwarf novae in outburst. Since dwarf novae are numerous enough and the quasi period of their outburst short enough, one has statistically a very good chance to observe several of them in outburst during a seven-night run. For this purpose we had a collaboration with F. Bateson, the head of the amateur astronomers of the Royal Astronomical Society of New Zealand (RASNZ). He was to inform us via telex about dwarf nova outbursts detected by his amateurs. In fact, his first telex contained very valuable information; not on a dwarf nova outburst but rather a nova outburst, Nova Muscae 1983. This information from New Zealand reached us via a small detour: Nova Muscae had been discovered more than two days ago (January 18) by W. Liller in the Chilean town Viña del Mar which is about 500 km away from us in La Silla. W. Liller had sent the news of the outburst to the IAU bureau in Cambridge, Mass. From there it was transferred to New Zealand and then to us. The information had to travel 35,000 km, almost once around the earth, to reach us.

We immediately started preparations to observe the nova. At dinner we could persuade spectroscopists to take a spectrum of Nova Muscae. Problems arose due to the brightness of the object which could have damaged the detectors. The

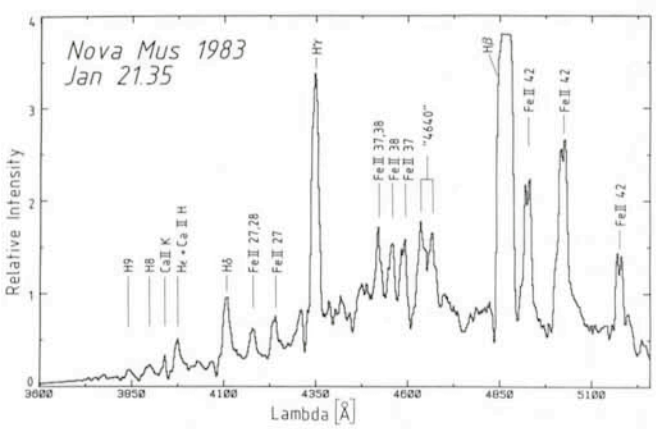

Fig. 1: *Image tube spectrum of Nova Muscae 1983 taken on January 21. The strong emission lines are heavily saturated. From Krautter et al. (1984).*

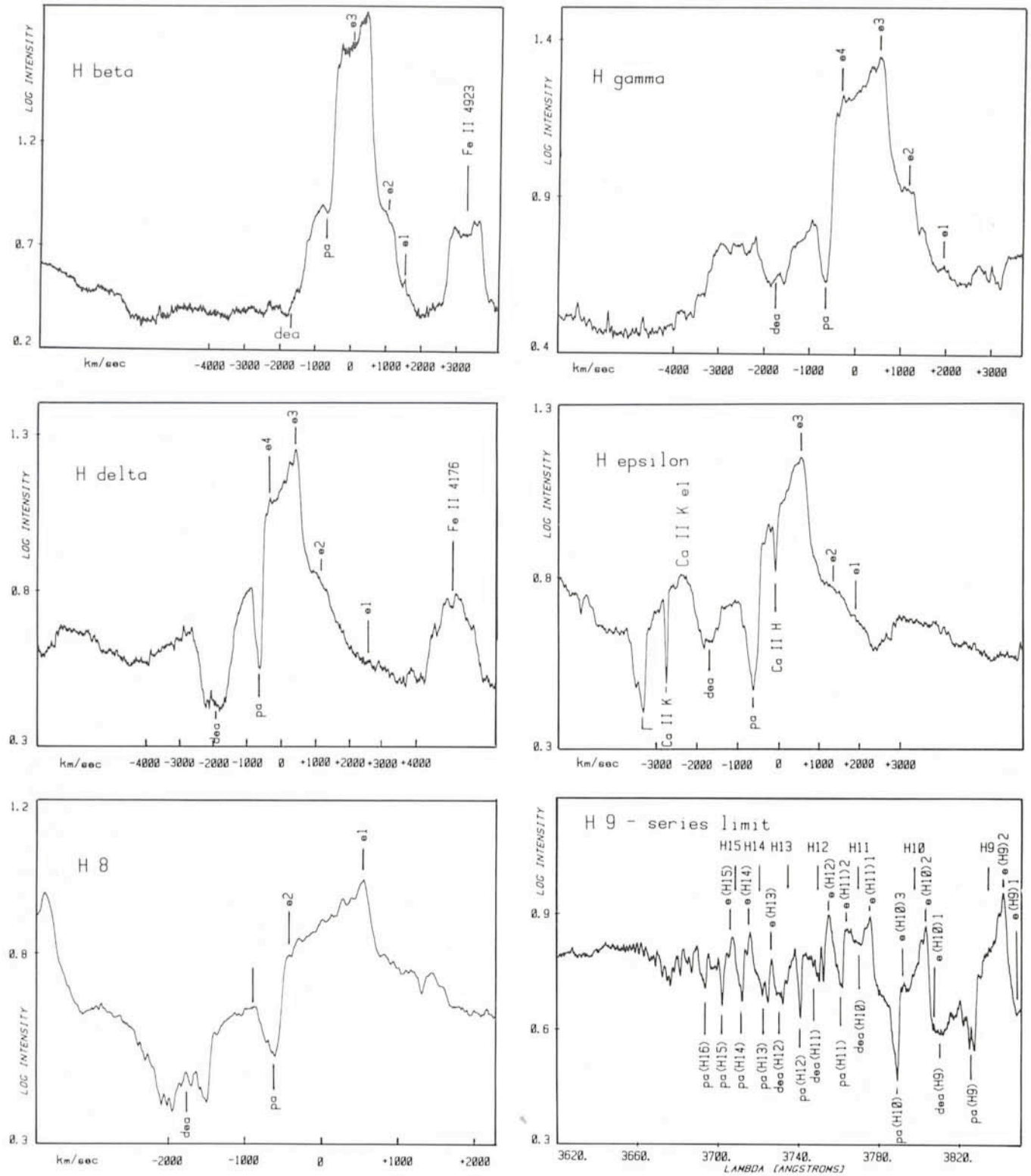

Fig. 2: *Balmer-line profiles of Nova Mus 83. Each profile is from a superposition of 5 coudé spectrograms. From Krautter et al. (1984).*

3.6 m observer solved the problem in a very simple way: he defocussed the telescope! This was the beginning of an extensive observing campaign of Nova Muscae, to which, eventually, some 25 astronomers, 8 telescopes on La Silla, and two satellites, IUE and EXOSAT, contributed. The main goal of this article is to show how the results from different spectral regions and different instruments interacted and complemented each other, and how we could, on the basis of these results, establish the fundamental parameters of Nova Muscae.

We started our spectroscopic observations of Nova Mus on January 21, 3 days after discovery, with 3 telescopes. Fig. 1 shows the first spectrum taken with the EMI image tube attached to the Boller and Chivens spectrograph at the 1.5 m telescope. The spectrum is dominated by strong emission lines of hydrogen and singly ionized metals which show two emission components at $v \approx -400$ km s^{-1} and +500 km s^{-1}. The Balmer lines show pronounced P Cygni profiles. More details can be seen in Fig. 2 which shows the Balmer line profiles on a superposition of 5 high-resolution coudé spectra

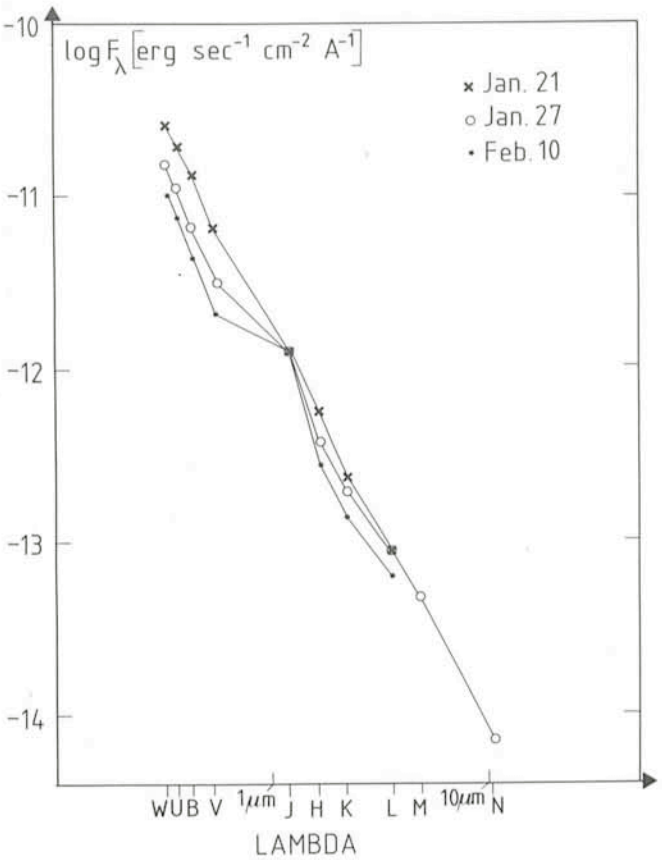

Fig. 3: *Flux distribution of Nova Mus 83 at different epochs. For dereddening E_{B-V} = 0.45 has been used. From Krautter et al. (1984).*

taken between January 25 and 29. No significant spectral changes took place between the first image tube spectrum and the last coudé spectrum. Two absorption systems are present: The principal absorption (v_{pa} = −588 km s^{-1}) and the so-called diffuse enhanced absorption system (v_{dea} = −1753 km s^{-1}). These velocities are typical for fast novae. The speed class of a nova (fast or slow nova) is defined by the lifetime t_3 which is the time it takes for the nova to decline from visual maximum by 3 magnitudes. If t_3 is less than 100 days a nova is called a fast nova. The knowledge of t_3 is important since a well defined relation between this parameter and the absolute magnitude exists.

But back to the spectra. When we did our first observations on January 21, Nova Mus had already undergone some evolution since its maximum brightness. The diffuse enhanced spectrum is characteristic for an advanced stage in a nova's life. Our next spectra taken on February 21 showed Nova Mus to be in the next phase of a nova's evolution, the so-called "Orion" stage. This stage is characterized by a new absorption system with the highest velocity (v = −1980 km s^{-1}) and the appearance of typical emission lines like HeII, NII, etc. The 4640 Å CII–NIII feature reaches maximum strength.

Our photometric observations (visual + IR) enabled us to determine the spectral energy distribution (SED) which is shown in Fig. 3 for 3 different epochs. For dereddening we used E_{B-V} = 0.45 which we derived from the 2200 Å feature in the UV spectrograms taken with the IUE. Generally the flux increases towards shorter wavelengths obeying a power law $F_\lambda \propto \lambda^{-\alpha}$ with $2 \leq \alpha \leq 2.3$. The overall intensity dropped by about a factor of 1.5 from January 21 to February 10. This spectral energy distribution is characteristic of free-free emission of an optically thin gas clearly showing that our first observations were after maximum brightness. General wisdom tells us that the free-free phase is already the second phase in the evolution of a nova's SED which is at maximum that of blackbody radiation from an optically thick pseudo-photosphere. The onset time ot the ff radiation depends on the speed class. For Nova Cyg 75, the fastest nova ever observed, the ff phase onset was 4.2 days after maximum. For other fast novae the ff phase began later, for instance for Nova Cyg 78, 8 days after maximum. It is therefore highly improbable that Nova Muscae was at maximum brightness at its detection on January 18, 3 days before our first observations.

But how does one get the visual maximum brightness which is crucial for determining the absolute magnitude via the luminosity lifetime relation? Fortunately, there are relations between the appearance and disappearance of spectral features and the change in the magnitude compared to the maximum brightness. Using these relations, we derived a most probable $V_{max} \approx 7.0$ mag.

Next we investigated the visual light curve in order to determine t_3. Fig. 4 shows the visual light curve till January 1, 1985. Since our photoelectric measurements cover 40 days only, this light curve has been prepared by using exclusively the visual data published by the amateur astronomers of the RASNZ. The extrapolation of the light curve back to V = 7.0 suggests that maximum brightness was reached around January 14–15, 3–4 days before the discovery. This enabled us to determine t_3 as 40 days which is turn gave M_V = −7.75 and a distance D = 4.8 ± 1 kpc. With this distance we could derive lower limits for the luminosity which are of the order of one Eddington luminosity for a 1 $M_\odot$ white dwarf.

What did we learn from the spectroscopic observations in the infrared and ultraviolet spectral regimes? The IR results are already described in a *Messenger* article by E.Oliva and A.Moorwood (1984, *The Messenger* **33,** 30). Additionally, we inferred from the IR spectra that the lower limit of the helium abundance is slightly above solar abundance. Fig. 5 shows a low resolution IUE spectrum of Nova Muscae taken on March 4, 1983. We have already mentioned that we could determine the interstellar extinction from the 2200 Å feature. The UV spectrum shows a wealth of emission lines. Dominant are those from neutral or low ionized atoms. Lines from highly ionized and/or excited levels are present too, but are generally weaker than the other lines. Very conspicuous are intercombination lines like NIII], NIV], CIII], SiIII], and OIII]. From the strength of the CNO lines we were able to derive crude abundances of these elements relative to each other. The results are N/C = 20 and N/O = 2.4 showing that nitrogen is strongly overabundant with respect to carbon and oxygen. This high nitrogen abundance is entirely consistent with the thermonuclear runaway models of nova outbursts with hydrogen being burnt via the CNO cycle. This conclusion is also supported by the luminosity of Nova Mus of about one L_{Edd}.

From March 1983 to March 1984 we did not continue our observations of Nova Muscae. However, other observations revealed some peculiarities which we summarize below.

– From April 1983 to February 1984 the visual magnitude was nearly constant (apart from the short flare around September 1). The decline rate is very low. This is very unusual for a fast nova.

– IUE observations carried out on June 13 showed a second outburst in the UV range (A. Cassatella, private communication). No indication for this outburst is found in the visual light curve nor in spectra taken in the visual spectral range on June 14 and 15 (W. Liller and M.T. Ruiz, private communication).

In spring 1984 we continued our observations of Nova Muscae which had now entered its last phase of evolution, the nebular stage. Again spectroscopic and photometric observations on La Silla and with IUE were carried out. For the time

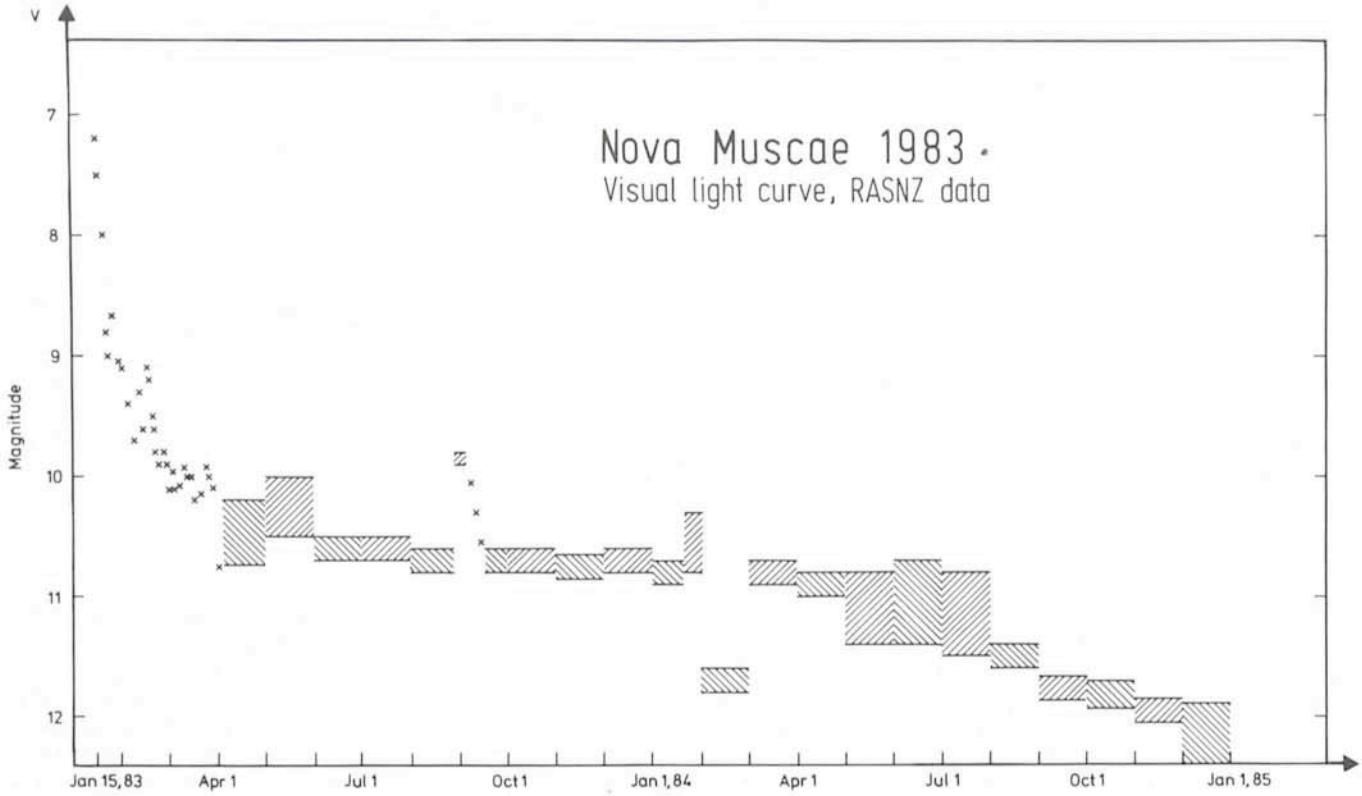

Fig. 4: *Visual light curve of Nova Mus 83 from January 18, 1983 to January 1, 1985. Only visual data published by the variable star section of the RASNZ have been used. Crosses denote individual observations. The shadowed areas show the monthly bandwidths of the visual measurements as published in the information bulletins of the RASNZ.*

being we can only present preliminary results of these observations. Figs. 6 and 7 show the same low-resolution spectrum taken with the IDS at the ESO 1.5 m telescope on two different scales in order to account for the large differences in emission-line intensities. The spectrum is dominated by strong nebular emission lines. Many highly excited lines are present, the strongest being [FeVII] λ 6087. A particularly interesting result is that we could also identify the coronal lines [FeX] λ 6074 and [FeXIV] λ 5303. Coronal line emission has been reported for several other novae, but to our knowledge [FeXIV] has been found only in one other nova yet, DQ Her.

By now, we had collected observations of the nova from 1200 Å to 10 μm. But what about X-ray emission? Why not look with EXOSAT for the X-ray emission? Among previous novae a few had been observed with earlier X-ray satellites

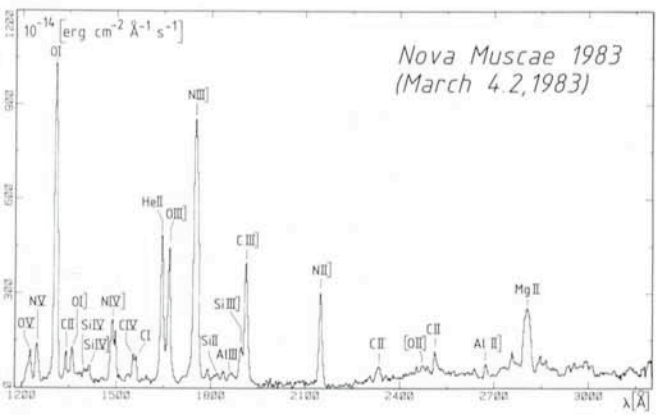

Fig. 5: *Combined SWP and LWR UV spectrograms taken with IUE on March 4, 1983. The more significant emission lines are indicated. From Krautter et al. (1984).*

during outburst or decline from outburst. But none of them was detected in X-rays. One reason for these negative results may be that the X-ray observations were carried out in the very early outburst phases soon after maximum brightness. In the beginning the envelope has a high density and the soft X-ray radiation is absorbed. In the case of Nova Muscae more than one year had passed since its maximum brightness. An estimate showed that the envelope should have been expanded enough to be transparent to soft X-rays. This encouraged us to propose Nova Muscae as target of opportunity for EXOSAT observations. The case was convincing enough for Dr. A. Peacock, the project scientist of EXOSAT, to declare Nova Mus as target of opportunity, and allocate observing time. On our first EXOSAT observation on April 20, 1984, we detected Nova Mus in the soft X-ray range (.04–2 keV) in two broadband filters: Lexan and Al-Parlene. The count rates were 3.4 ± 1.2 10^{-3} cs^{-1} (Lexan) and 3.7 ± 1.2 10^{-3} (Al-Parlene). Both observations taken together give a 4.5 σ statistical significance. This observation constitutes the first detection of X-rays from classical novae during outburst, including the decline stage.

Subsequently we were granted further observing time on EXOSAT, and we carried out two more observations on July 15, and December 22, both times with the Lexan filter only. The count rates were 3.0 ± 0.6 10^{-3} and 3.4 ± 0.9 10^{-3} c s^{-1} respectively. The X-ray flux has, within the error limits, been constant during the last 9 months. On the other hand, the visual brightness has significantly declined, as Fig. 4 shows.

Unfortunately, the low-energy data did not allow to determine the spectral characteristics with any meaningful accuracy because of the errors in the counting rates and the large overlapping bandwidths of the two filters. In order to gain physical insight into the nature of the X-ray emission we had to compare our measurements to models of nova outbursts. There are in principle two possible regions that may be

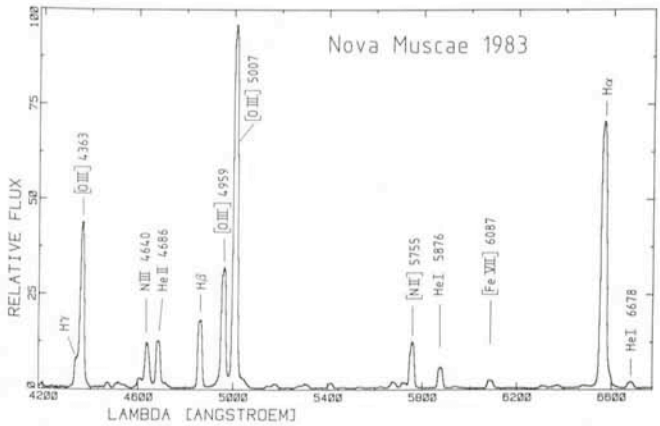

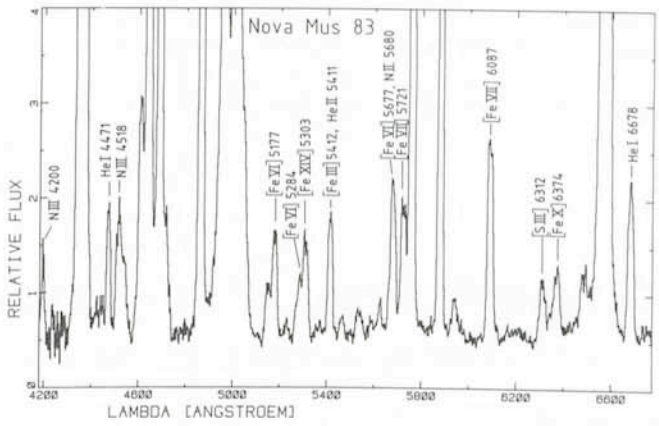

Figs. 6 + 7: *IDS spectrum of Nova Mus 83 taken on March 29, 1984 shown on two different ordinate scales. The most prominent emission lines are indicated.*

associated with the X-ray emission: the expanding shell or the white dwarf remnant. For the emission associated with the expanding shell, Brecher et al. (*Astrophysical Journal* **213,** 1977) have suggested a model in which it is predicted that as the ejected nova shell moves through circumstellar gas it will heat it to characteristic temperatures around 1 keV and produce thermal bremsstrahlung in the X-ray region. Our measurements are consistent with this type of emission provided that the temperature is less than 3 keV and the total unabsorbed low energy X-ray luminosity is about 10^{35} erg s^{-1}. The model predicts that the X-ray flux should decay as t^{-1}.

The alternative for the origin of the detected X-ray emission is the white dwarf itself. In hydrodynamic models of nova outbursts it was found that after several per cent of the hydrogen envelope is ejected during the hydrodynamic phase of the outburst, the velocity in the deeper zones drops quickly and hydrostatic equilibrium is established. The further evolution of the remnant is on nuclear burning time scale and thus may last for many years. For more details of these models we refer to e.g. Truran (in: *Nuclear Astrophysics,* ed. Barnes, Clayton, Schramm, Cambridge 1982).

In order to compare the measured soft X-ray flux with the parameters of the hydrostatic remnant, we have drawn in Fig. 8 the lines of constant luminosity that will give the measured X-ray counting rate under different values of kT and N_H for a blackbody type emission spectrum at 4.8 kpc distance. N_H is the column density of the interstellar hydrogen which causes the absorption of the soft X-rays. The range of the acceptable N_H was determined from $E_{B-V} = 0.45 \pm 0.15$ we derived from the UV spectra. Also drawn in Fig. 1 are lines of constant radius objects that will give the observed soft X-ray counting rates under the assumption that they radiate like a blackbody at temperature T and subsequently the radiation suffers an absorption corresponding to the value of N_H on the figure. It is immediately apparent from the figure that in the acceptable range of N_H values an object radiating at L_{Edd} (10^{38} erg s^{-1}) has to have a temperature around 0.025 keV (280,000 K) and its radius has to be less than 5×10^9 cm. Conversely, if we assume that the object radiating the X-rays is the white dwarf itself, then the implied luminosity would be about 10^{37} erg s^{-1} with a corresponding temperature around 0.03 keV (350,000 K).

At present we cannot decide between either of these models. A crucial test would be the determination of the spectral characteristics. At present, our time base is too short and/or the accuracy of the data not sufficient enough, to really exclude a t^{-1} dependence. A possible verification of the white dwarf origin would be the first direct observational proof of the nuclear shell burning predicted by the thermonuclear runaway models of nova outbursts.

This, at present, concludes the story of Nova Muscae 1983 which started in La Silla two years ago. We hope we have been able to stress the importance of observations in different spectral regions for variable objects like novae. Part of the results described here and additional information can be found in Krautter et al. (1984, *Astronomy and Astrophysics* **137,** 307) and Ögelman, Beuermann, and Krautter (1984, *Astrophysical Journal* Letters **287,** L31). We want to thank all colleagues who kindly contributed to the observations and spent part of their observing time on Nova Muscae: L. Bianchi, J. de Bruyn, E. Deul, H. Drechsel, R. Häfner, A. Heske, G. Klare,

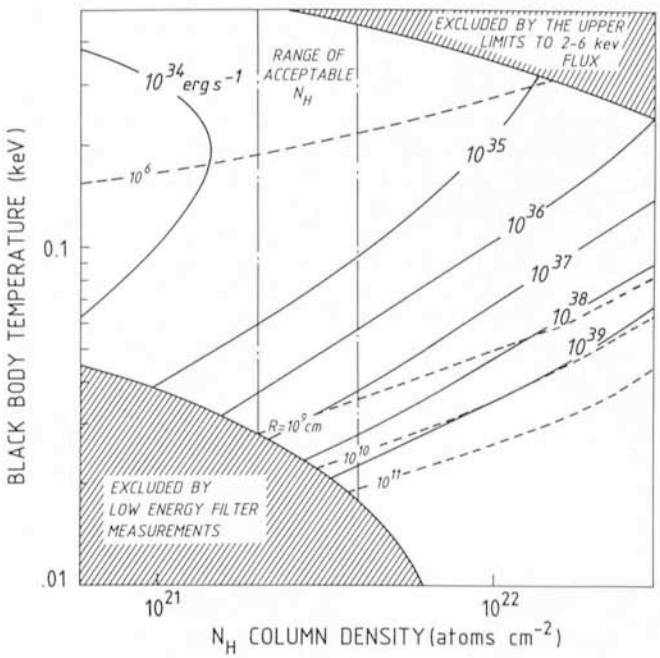

Fig. 8: *Summary of the observed X-ray flux from Nova Muscae 1983 for various N_H and kT combinations. The source spectrum was assumed to be that due to a blackbody at temperature T and at a distance of 4.8 kpc. The contours of constant source luminosity (in erg s^{-1}) that gives the observed soft X-ray counting rates are shown. Also shown in the figure are the radii (in cm) contours of objects that will radiate the required luminosity under the assumption that they are radiating as a blackbody at temperature T (dashed lines). From Ögelman, Beuermann and Krautter (1984).*

L. Kohoutek, C. Leitherer, J. Manfroid, A. Moorwood, Th. Neckel, E. Oliva, M. Pakull, W. Schlosser, R. Schulte-Ladbeck, O. Stahl, B. Stenholm, J. van Paradijs, N. Vogt, W. Wargau, B. Wolf, and F. J. Zickgraf. We also thank A. Peacock for granting observing time on EXOSAT, and, last not least, we cordially acknowledge the very valuable work F. Bateson and his amateur astronomers of the RASNZ did for Nova Muscae 1983.

On the Problem of the Luminous Emission Line Stars

R. Viotti, Istituto di Astrofisica Spaziale, Frascati, Italy

Introduction

Emission-line spectra are frequently observed among stars of high intrinsic luminosity. They provide evidence for the presence of extended stellar atmospheres, probably resulting from intense mass outflows. However, the physical relation between the strength of the emission lines and other stellar parameters, such as luminosity, gravitiy, temperature, rate of mass loss, rotation, binarity, etc. is far from clear. This situation is probably the result of the poor knowledge that we have of their basic physical parameters, and of the mechanisms of line formation in extended atmospheres. One major problem for galactic objects is the determination of their distance and interstellar reddening because of their position near the galactic plane. Many objects are also affected by a considerable amount of circumstellar extinction, and these problems make the determination of their intrinsic (bolometric) luminosity even more difficult. Another problem is the correct estimate of their temperature (or radius). In fact, as discussed for instance by de Jager (1980), these superluminous stars generally display a very tenuous stellar atmosphere so that both the brightness temperature and the radius at optical depth equal to unity largely vary with wavelength. The result is that for the most interesting objects their position in the Herzsprung-Russell diagram is quite uncertain, and it is therefore difficult to discuss them in the framework of the current evolutionary theories.

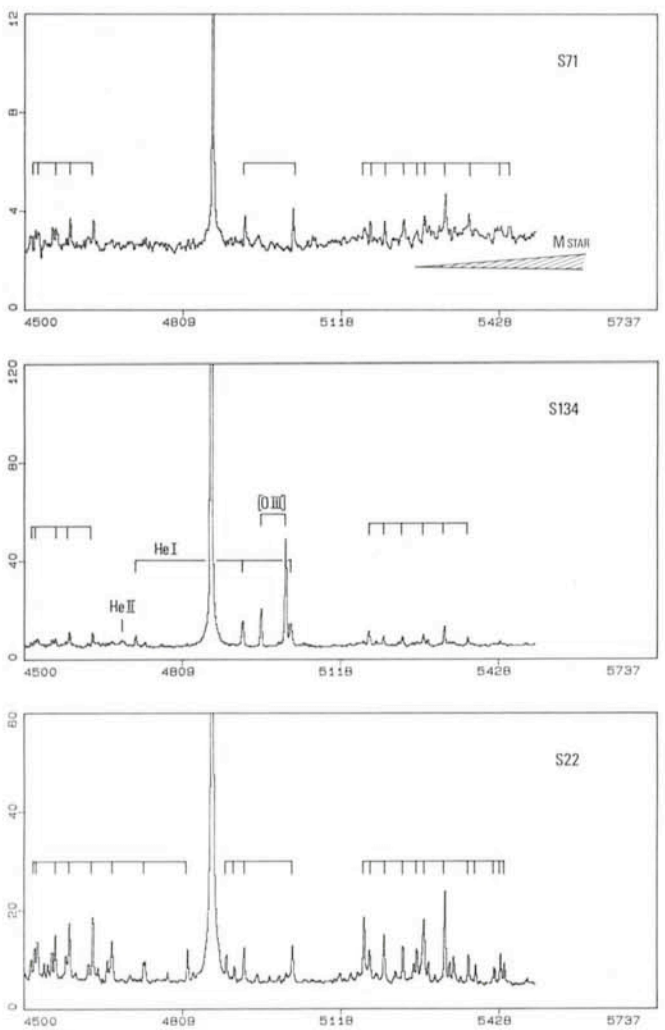

Fig. 1: *The low-resolution spectrum of three LMC emission-line stars: (a) S71, a VV Cep star characterized by low excitation emission lines and an M-type spectrum in the red. The Fe II emission lines are marked. (b) S134 (HD 38489) with both low and high ionization emission lines. (c) S22 (HD 34664) with one of the richest Fe II emission spectra. Both S22 and S134 are known to have circumstellar dust shells (Bensammar et al. 1981, Stahl et al. 1984). Spectra taken by R. Gilmozzi on November 21–22, 1983 (ESO 1.5 m + IDS). Fluxes are in units of* 10^{-14} *erg cm*$^{-2}$ *s*$^{-1}$ *Å*$^{-1}$.

On the other hand, the interest in these stars has recently increased, as they may represent a phase, or different phases of the evolution of massive stars after having left the main sequence (see e.g. the Proceedings of the ESO 1981 Workshop on "The Most Massive Stars"). Because of their high intrinsic luminosity, they can be identified also in distant galaxies, and this has been improved by the wide use of the new astronomical techniques. Obviously, the presence of prominent emission lines makes their identification with wide-field cameras easier than for the more normal early-type supergiants.

The Magellanic Clouds may represent the best laboratory for the study of the behaviour of luminous emission-line stars, since their distance is well known and the interstellar extinction is in general low. In addition, the difference in metallicity and stellar content among the clouds makes them an ideal case to study chemical composition effects. For this reason many projects of systematic investigation of the emission-line stars in the MCs are now under way (e.g. Shore and Sanduleak 1984, Stahl et al. 1985, Gilmozzi et al. 1985), with the aim of determining the main physical characteristics of these objects. In the following we shall illustrate some results obtained from the analysis of the optical (ESO) and ultraviolet (IUE) spectra of galactic and MC superluminous stars.

Spectroscopic Observations

The luminous emission-line stars show a large variety of optical spectra, with different degrees of line excitation and intensity. Fig. 1 shows three examples of Magellanic Cloud stars with emission lines. In general the emission lines are more prominent and more numerous in the brighter objects, while the *photospheric* (not P Cygni) absorptions are weak or not observable at all. Besides hydrogen and helium, Fe II is the most frequently observed ion in the optical spectrum of

superluminous stars and is represented by a large number of prominent emission lines (see Fig. 1). Generally, the emission spectrum becomes weaker towards shorter wavelengths, and in the IUE ultraviolet it is replaced by strong absorption features mostly due to singly ionized iron lines. The importance of the study of Fe II in the spectra of emission line stars has only recently been recognized, and many important results have already been obtained from both the observational and theoretical points of view. Emission lines of Fe II have been identified in the optical spectra of many different kinds of objects, including Be stars, symbiotic variables, stellar chromospheres, novae, active galactic nuclei, etc. In the case of the luminous stars, empirical methods for line analysis such as the *Self-Absorption Curve* method have been developed by M. Friedjung and collaborators to derive information about the physics of line formation in expanding stellar envelopes from the optical spectra. When only low-resolution spectra are available, as in the case of the IUE spectra of distant stars, one must attempt to compare the observations with *synthetic spectra* as described for instance by Muratorio et al. (1984). This is illustrated in Fig. 2 where the ultraviolet spectrum of the LMC star R 66 is compared with a synthetic spectrum computed using the Fe II level population and column density derived from the intensity of the optical emission lines.

The Hubble Space Telescope will enable us to observe luminous stars in very distant galaxies. We expect that their ultraviolet spectrum will be dominated by prominent (and variable) absorption features of Fe II and of other ionized metals formed in their extended expanding atmospheres. It is clear from the above arguments, that only the use of spectral synthesis techniques will allow us to derive physical information on these faint objects.

High Resolution Hα Profile

Hα is the most prominent emission line in the optical spectra of these stars. Frequently its equivalent width is so large as to significantly affect broad-band R photometry. For instance, in the two LMC stars S 22 and S 134 the flux in the R filter is about 60 per cent larger than by interpolation of the fluxes from the nearby V and I bands (see Stahl et al. 1985). In such objects the Hα profile can be easily studied at high resolution also in faint objects, including MC stars. In Fig. 3 we show the Hα profiles of three luminous emission-line stars. The observations were made with the CAT-CES system which is in principle limited to the 5th magnitude. S 22 is a LMC star with V = 11.75, but its faint luminosity has not prevented us to observe its Hα line with a resolving power of R = 50,000.

At high resolution Hα displays a complex profile which is different from star to star. For instance, in the three stars in Fig. 3 the Hα profile corresponds to the Beals' P Cygni types I, III and V in AG Car, S 22 and η Car respectively. In the galactic P Cyg star AG Car the narrow absorption is accompanied by very broad wings, probably formed by electron scattering as in the case of P Cyg itself, and by a blue-shifted absorption with a sharp edge which should be related to the terminal velocity of the stellar wind. This profile is variable, sometimes showing a second lower velocity absorption line (Bensammar et al. 1981) which could be attributed to the formation of a dense shell or to a transitory change of the atmospheric structure of AG Car. In S 22 the Hα profile is different with a narrow absorption and

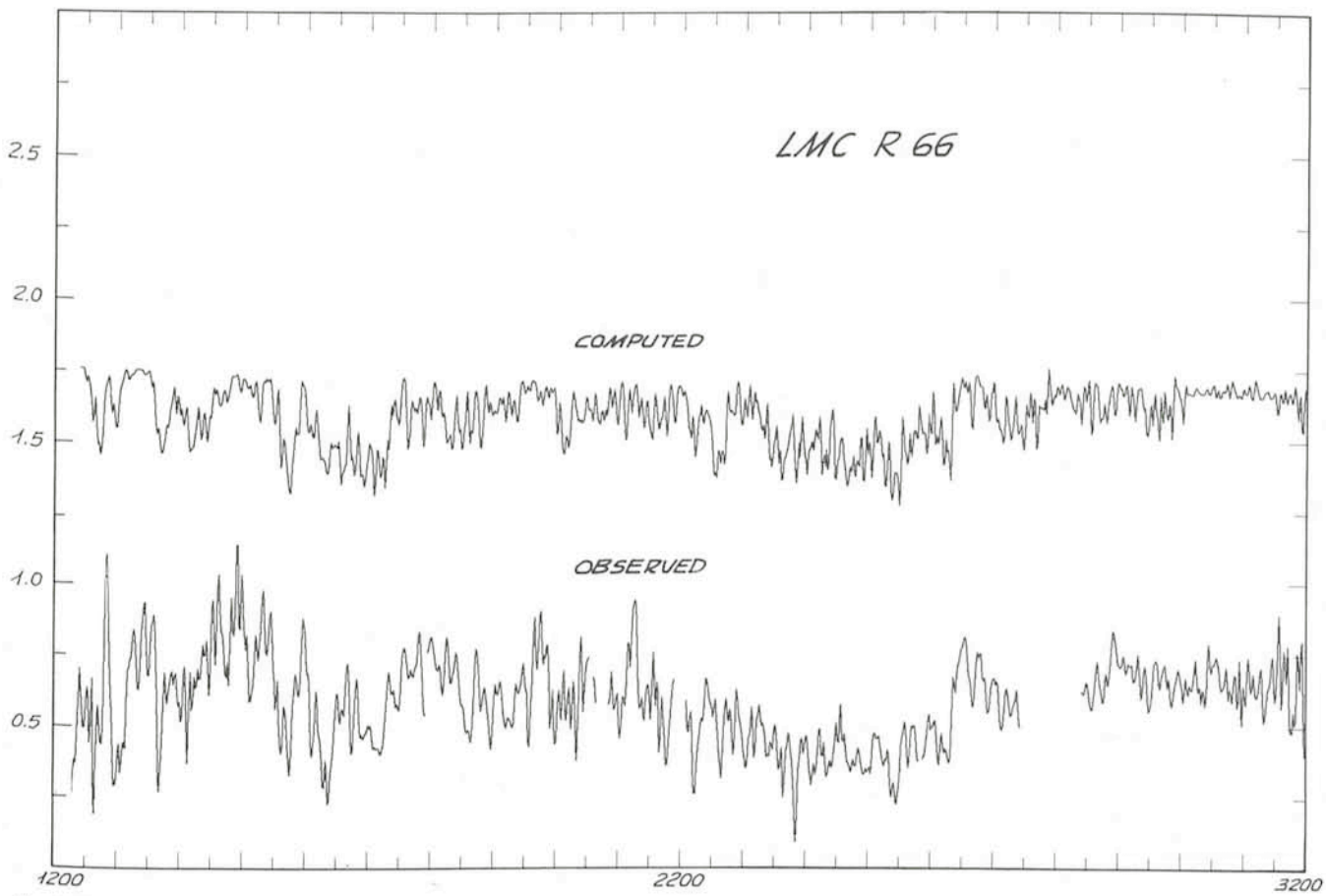

Fig. 2: *The dereddened low-resolution IUE spectrum of the LMC star R66 compared with a computed synthetic spectrum. A constant vertical shift is applied to the computed fluxes. Courtesy of G. Muratorio.*

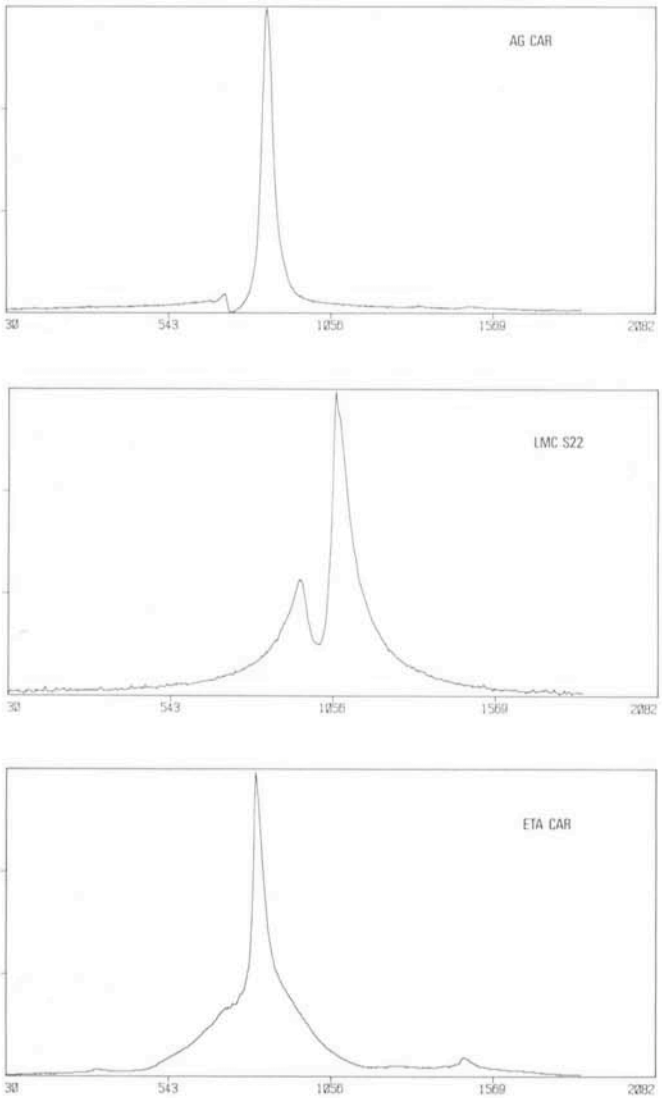

Fig. 3: *The high resolution Hα profile in three luminous emission-line stars: (a) AG Car (M_{bol} = –8.3, Viotti et al. 1984), (b) S22 (M_{bol} = –8.5, Bensammar et al. 1983), (c) η Car (M_{bol} = –12.0, Andriesse et al. 1978). Spectra taken by A. Altamore and C. Rossi on February 3–8, 1984 with the CAT-CES. The spectral resolution is 50,000 for S22 and 100,000 for the Carina stars (spectral range 6536 to 6593 Å).*

intense wings which look like damping wings. In η Car the line is characterized by a sharp central emission, with a blue absorption which is only marginally visible in February 1984, but was stronger in July 1981 (Melnick et al. 1982), and broad asymmetric wings. A similar bi-component structure is also present in the strong emission lines of HeI and FeII, and may indicate the coexistence near the central star of the high velocity dense wind and of a low velocity region.

Variability

Variability is one major characteristic of the brightest emission-line stars. It is known since a long time that irregular small amplitude photometric variations are present in most supergiant stars. The extreme case is represented by the so-called *Hubble-Sandage* or *S Dor* stars showing large photometric and spectroscopic changes on time scales from months to several years. The origin of these variations is still unclear, but in general stars appear bluer at minimum.

An interesting galactic case is represented by the southern variable AG Car whose light curve is characterized by large luminosity variations from V = 6 to 8 mag on time scales of months to years (Mayall 1969). The optical spectrum of this star has been extensively studied by Caputo and Viotti (1970) who found large changes of the excitation of the P Cygni lines. More recently, Viotti et al. (1984) found that during minimum luminosity (V = 7–8) the star displays a *hot* optical spectrum which closely resembles that of its northern counterpart P Cyg. But at maximum luminosity—when V is close to 6 mag—the helium P Cygni lines disappear and the equivalent spectral type is much cooler (A-type). Similar spectral variations are seen in the ultraviolet, and are accompanied by a large increase of the far-UV (IUE, SWP) flux during the phases of low visual luminosity. Viotti et al. and Wolf and Stahl (1982) have found that in spite of the large optical variability, the bolometric magnitude of AG Car remained nearly constant. This behaviour is very similar to that of the S Dor variables. The Large Magellanic Cloud contains a number of such interesting objects (e.g. R71, R127 and S Dor itself) extensively studied by the Heidelberg group, showing large spectral and luminosity variations. Also in these objects there is a clear indication that the variations occur at nearly constant bolometric luminosity (e.g. Wolf and Stahl 1983). One is therefore brought to the conclusion that *the variability is only apparent* and most probably caused by changes of the structure of the expanding atmosphere. This causes a flux redistribution of the stellar radiation, so that at minimum luminosity more energy is emitted in the ultraviolet and the star appears bluer and fainter. At maximum the UV flux is lower and the visual flux larger, while the bolometric luminosity remained the same. As we shall show later, a different situation holds in the case of the galactic variable η Car where the large luminosity variations are due to the circumstellar dust.

Apart from the rather spectacular variations of the S Dor variables described above, there are also smaller transient phenomena characterized by changes of the line strength and profile without large photometric variations. The classical example is P Cyg—the prototype of the superluminous emission-line stars—whose spectrum displays a stable absorption at –206 km s^{-1}, representing a shell at large distance from the star, and a variable absorption component at lower velocity formed in a transient shell moving (and accelerating) outwards (Lamers et al. 1984). Similar transient phenomena have also been observed in the peculiar star η Car by Viotti (1969) and Zanella et al. (1984). Again these observations indicate structure changes of the stellar atmospheric envelope, possibly originating by an increase of the mass loss rate, or by ejection of denser shells, so that a kind of perturbation moves outwards across the envelope, causing transient changes of the density

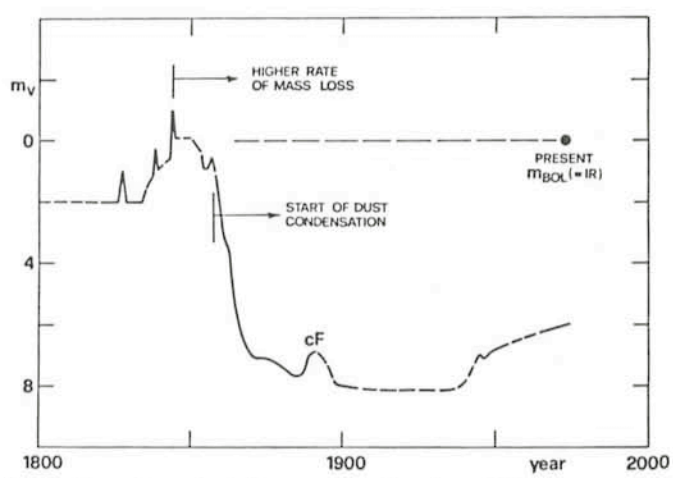

Fig. 4: *The schematic light curve of η Car since 1800.*

and temperature distribution. It is worth noting that if this perturbation is small, one could in principle use the observed spectral variations as a probe of the physical conditions in the outer stellar atmospheres.

Circumstellar Dust

Variability of a peculiar star may also be caused by other physical processes, such as extinction by circumstellar dust regions with variable thickness. The typical case is represented by the galactic superluminous star η Car. This is presently a sixth magnitude star, but 150 years ago it was one of the brightest stars in the sky (Fig. 4). Since 1856 the stellar magnitude gradually decreased, and this suggested the (uncorrect) classification of η Car as a very slow nova. The star is presently a very bright infrared source. Andriesse et al. (1978) found that the bolometric magnitude derived from the infrared energy distribution is close to the estimated bolometric magnitude during the bright phase of last century. This suggests that the large fading after 1856 is due to the start of the dust-condensation process. The optical and ultraviolet radiation of the central star is more and more absorbed by the expanding envelope, and reemitted in the infrared. Presently, the star is in fact surrounded by a small dusty nebula whose total mass is a few solar masses, formed by matter ejected during the past 150 years.

Circumstellar dust is not exceptional among the most luminous emission-line stars. For instance, recent infrared surveys of the Magellanic Clouds have disclosed several stars with IR excess attributed to thermal emission from dust heated by the stellar radiation (Stahl et al. 1984, 1985, Glass 1984). The question is still open whether this dust is protostellar, or formed from the stellar wind in the present or in a previous evolutionary stage of the star. Anyhow, we cannot exclude that in the extreme conditions which cloud be present in the atmospheres of the S Dor and Hupple-Sandage variables, dust grains could be formed and/or accreted in their stellar winds, causing a considerable attenuation of the stellar light. Subsequent changes in the physical conditions of the stellar atmosphere might destroy the grains, or dissipate the dust envelope, resulting in an apparent brightening of the star. It is therefore attractive to conclude that these processes could be at least partly at the origin of the large brightness variations observed in the Hubble-Sandage variables, and that *these variations occur at probably constant bolometric luminosity*, as in the case of η Car.

It is clear from the above arguments that the study of the (variable) structure of the envelopes of luminous emission-line stars is crucial to understand their nature. The problem of the *circumstellar dust* is a particularly interesting one and should deserve more investigation in the future. However, although the most luminous stars have been the subject of a large number of studies in the last years, it is far from clear what is their role in the evolution of massive stars, and, in particular, which are their basic physical parameters, such as temperature, luminosity, chemical abundance, mass and mass-loss rate. More systematic studies are required of a number of representative individual objects in our Galaxy, as well as in the MCs and in external galaxies, in order to provide a more *complete* and *homogeneous* set of observational data which could be useful for making appropriate theoretical models.

I am very grateful to Aldo Altamore, Roberto Gilmozzi, Gerard Muratorio and Corinne Rossi for their collaboration in this investigation, and for providing me with unpublished data, and to Michael Friedjung for discussions and comments on the manuscript.

References

Andriesse, C.D., Donn, B.D., Viotti, R.: 1978, *Mon. Not. R. Astr. Soc.* **185,** 771.
Bensammar, S., Guadenzi, S., Johnson, H.M., Thé, P.S., Zuiderwijk, E.J., Viotti, R.: 1981, *Effects of Mass Loss on Stellar Evolution*, C. Chiosi and R. Stalio eds., D. Reidel, Dordrecht, 67.
Bensammar, S., Friedjung, M., Muratorio, G., Viotti, R.: 1983, *Astron. Astrophys.* **126,** 427.
Caputo, F., Viotti, R.: 1970, *Astron. Astrophys.* **7,** 266.
de Jager, C.: 1980, *The Brightest Stars,* D. Reidel, Dordrecht.
Glass, I.S.: 1984, *Mon. Not. R. Astr. Soc.* **209,** 759.
Gilmozzi, R., Viotti, R., Wolf, O., Zickgraf, F.-J.: 1985, in prep.
Lamers, H.J., Korevaar, P., Cassatella, A.: 1984, *Fourth European IUE Conference,* ESA SP-218, 315.
Mayall, M.W.: 1969, *J.R. Astr. Soc. Canada* **63,** 221.
Melnick, J., Ruiz, M.T., Maza, J.: 1982, *Astron. Astrophys.* **111,** 375.
Muratorio, G., Friedjung, M., Viotti, R.: 1984, Proc. *Fourth European IUE Conference,* Rome, 15–18 May 1984, ESA SP-218, p. 309.
Shore, S.N., Sanduleak, N.: 1984, *Astrophys. J. Suppl. Series* **55,** 1.
Stahl, O., Leitherer, C., Wolf, B., Zickgraf, F.-J.: 1984, *Astron. Astrophys.* **131,** L5.
Stahl, O., Wolf, B., de Groot, M., Leitherer, C.: 1985, *Astron. Astrophys. Suppl.,* in press.
Viotti, R.: 1969, XV Liège Colloquium *Les Transitions Interdites dans les Spectres des Astres,* Université de Liège, Vol. **54,** 333.
Viotti, R.; 1976, *Astrophys. J.* **204,** 293.
Viotti, R., Altamore, A., Barylak, M., Cassatella, A., Gilmozzi, R., Rossi, C.: 1984, *NASA IUE Conference.*
Wolf, B., Stahl, O.: 1982, *Astron. Astrophys.* **112,** 111.
Wolf, B., Stahl, O.: 1983, *The Messenger,* No. **33,** 11.
Zanella, R., Wolf, B., Stahl, O.: 1984, *Astron. Astrophys.* **137,** 79.

Rotation and Activity of T Tauri Stars

J. Bouvier and C. Bertout, Institut d'Astrophysique de Paris

T Tauri stars are late-type, pre-main-sequence stars that, although at present quite active, will evolve in time into stars resembling the Sun. They are emission-line variables with strong ultraviolet and infrared excesses. They display flare-like X-ray emission, and a few can be detected in the radio range as well. Mass-loss rates estimated for these objects reach about $10^{-8} M_\odot$ /yr, and some T Tauri winds drive anisotropic, often bipolar, high velocity molecular outflows. A question which naturally arises when studying T Tauri stars is therefore what makes these objects so different from the main-sequence stars they are likely to become. In other words, is the T Tauri phenomenon due to a specific and as yet undetermined physical process, or is it only an exaggerated form of solar-type activity?

Stellar evolution theory might have been able to offer an answer to this question, at least in a first approximation, since pre-main-sequence evolution in spherical symmetry has been computed by various groups. But the T Tauri phase corresponds to the transition between the protostellar and main-sequence stages, and little understood magnetic and convective phenomena are expected to influence the evolution and spectral appearance of the star during this phase. Since the

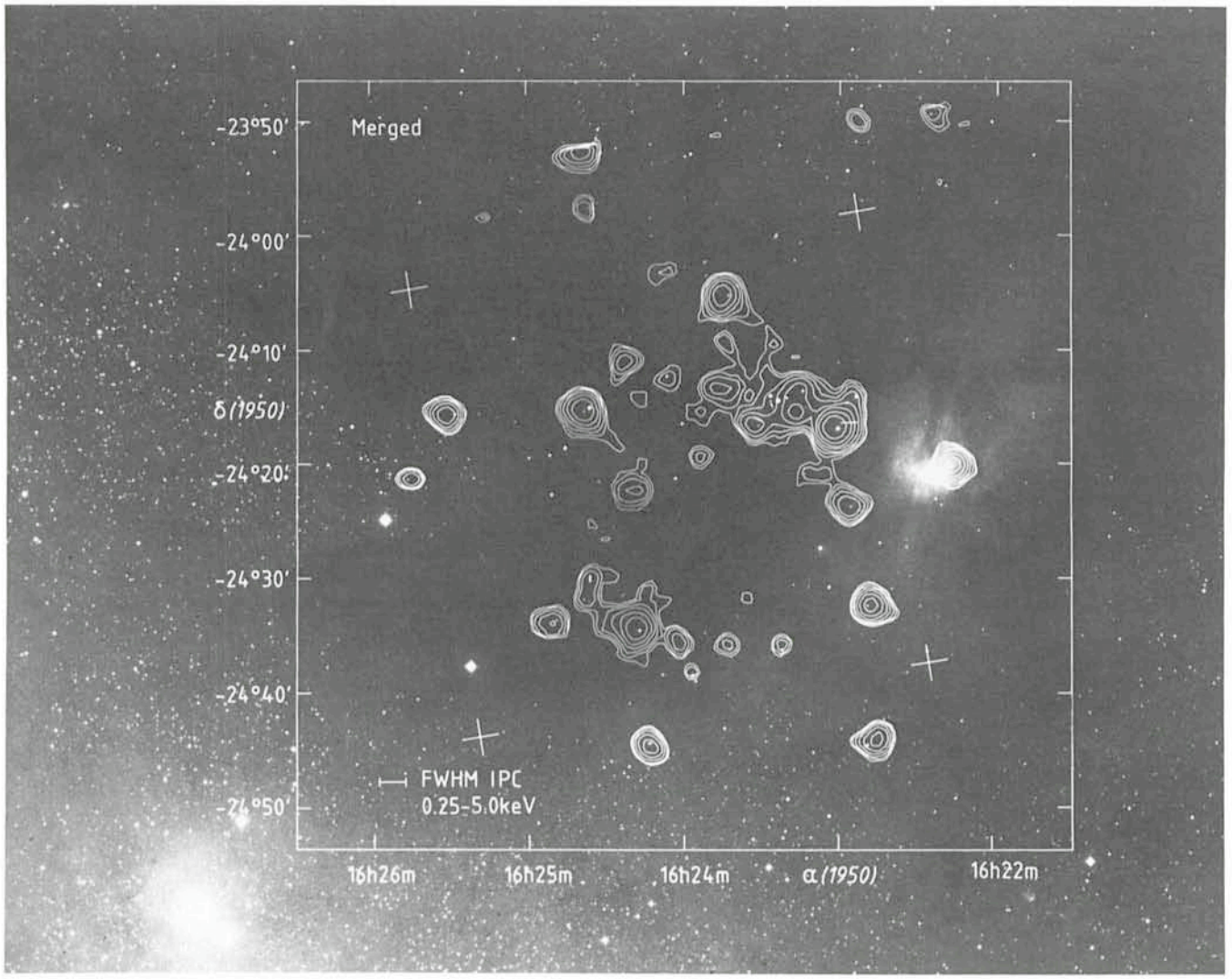

Fig. 1: *X-ray map of the ϱ Ophiuchi dark cloud from Montmerle et al. (1983,* Ap. J., ***269,*** *182). The contour levels show the detected X-ray sources, most of which are pre-main-sequence stars.*

physics of these phenomena cannot be taken into account in evolutionary codes, several empirical models have been proposed which shed light on particular properties of T Tauri stars; but to date none has been able to account for enough aspects of the T Tauri phenomenon to have gained widespread acceptance. Theory's inability to answer our question leads us to try an observational study of the similarities between T Tauri stars and other late-type stars.

Magnetic fields drive the surface activity of late-type dwarfs via dynamo processes resulting from the interaction between rotation and the deep convective zones present in these stars. While details of stellar dynamos are still in question, strong support to the dynamo hypothesis is given by the observed relationship (also predicted by dynamo models) between the stellar rotation rate and indicators of atmospheric activity, such as the X-ray flux and the flux in the CaII H and K line emission cores. Recent progress in these matters has been reviewed by Pallavicini in *The Messenger* No. **35,** p.5. By studying rotation in T Tauri stars, we might thus find out if dynamo processes are at work in these stars. We might also discriminate between those properties of T Tauri stars which are the result of magnetic activity and those which result from other physical processes. Identifying these unknown processes will indeed be easier when the role of magnetism in T Tauri activity will be clearly defined. All these reasons have led us to study the relationships between rotation and various activity criteria in T Tauri stars.

We chose to concentrate on the ϱ Ophiuchi region because it has been well studied in X-rays (cf. Fig. 1) and because it is easily observed from La Silla. But deriving accurate rotation velocities for T Tauri stars, which are rather faint objects, typically of the twelfth magnitude and higher, is not an easy task. We first describe below the different ways of doing this, and then summarize in the last part of this article our first results.

Measuring Rotational Velocities in Faint Stars

The spectral lines of a fast-rotating star appear broader than those of a slow-rotating one. In the ideal case where the axis of rotation is perpendicular to the line of sight, this broadening is a measure of the star's equatorial velocity. In reality, however, the rotation axes are randomly orientated relative to the line of sight so that the broadening is a measure of the projected rotational velocity, v.sini, where i is the angle between the rotation axis and the line of sight. V.sini is thus a lower limit of the true equatorial velocity, and spectroscopic determinations of stellar rotation have only a statistical meaning.

An example of rotational broadening appears in Fig. 2, which shows a selected spectral region of two T Tauri stars,

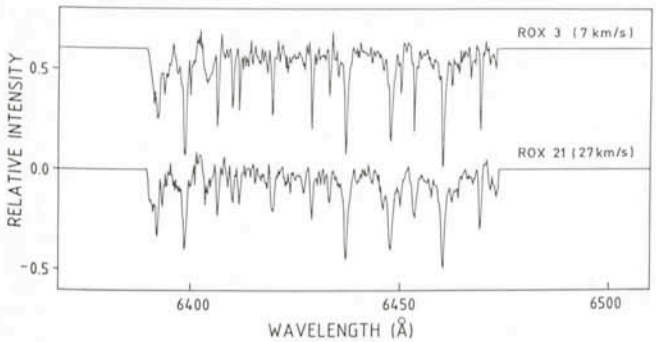

Fig. 2: *A selected spectral region for two T Tauri stars of the ϱ Ophiuchi cloud. Both stars are of spectral type M 1. Broader absorption lines in the spectra of ROX 21 are due to higher rotational velocity.*

both of spectral type M 1 and located in the ϱ Ophiuchi dark cloud. The spectrograms were obtained at the ESO 3.6 m telescope with CASPEC at a resolution of 20,000 in February 1984. Although these two objects are quite faint (V = 13.2 and 13.4), a good signal-to-noise ratio was reached in one hour of exposure time. Comparison of the broader photospheric absorption lines of the lower spectrum (v.sini = 27 km/s) to the upper one (v.sini = 7 km/s) illustrates the effect of rotation.

Recent progress in instrumental techniques and in the sensitivity of detectors now allows the use of powerful methods to measure v.sini that take into account the changes caused by rotation both in line width and in line profile shape. Behind these methods lies the principle that a rotationally broadened spectral line can be described as the convolution of the rotationally unbroadened line with a given rotation function. Under certain assumptions which remain valid for moderate rotators (v.sini $<$50 km/s, typically), this rotation function is easily calculated and only depends upon rotation rate and wavelength. Fourier analysis then becomes a powerful means to study rotational broadening, since convolution converts to ordinary product in Fourier space. Some results obtained by this method are shown in Fig. 3. In Fig. 3a, the Fourier transform of a CASPEC spectrogram of the T Tauri star LH_{α} 332-20 is shown as a solid line. The reference star, HR 1136, is a main-sequence star of the same spectral type and rotating at 2.2 km/s. Its Fourier transform was multiplied by the Fourier transforms of rotation functions corresponding to rotational velocities of 30, 35 and 40 km/s, and the results are shown as squares. We then search for the best fit in the frequence region comprised between 0.15 and 0.8 $Å^{-1}$ since large-scale continuum variations affect the Fourier transform

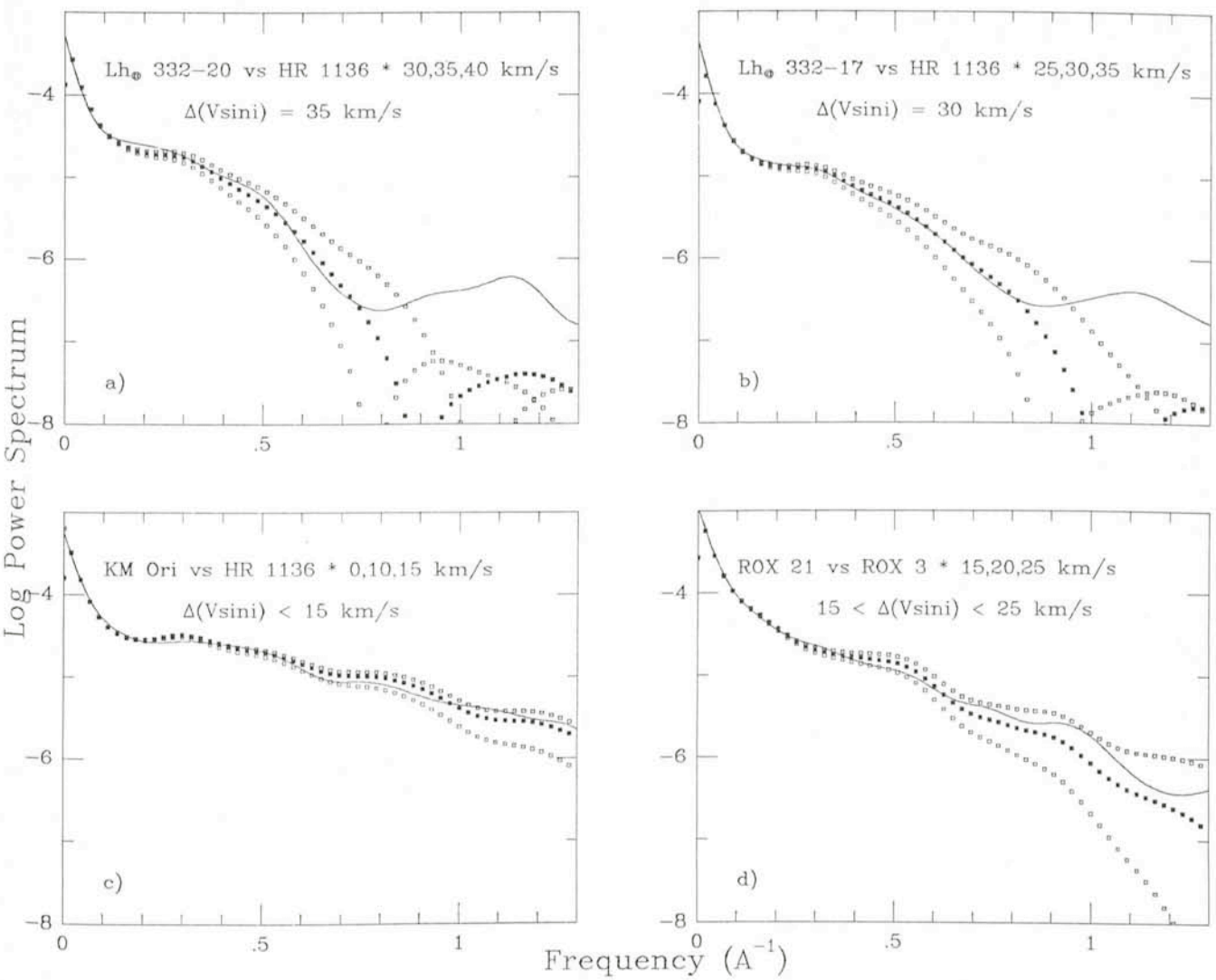

Fig. 3: *The Fourier transform method is applied on 4 T Tauri stars located in the Chameleon, Orion and Ophiuchus regions (see text). Reference stars are HR 1136 (v.sini = 2.2 km/s) in a), b) and c) and ROX 3 (v.sini = 7 km/s) in d). In each figure, the Fourier transform of the studied spectrum is shown as a solid line, and the artificially broadened transforms of the reference spectra as squares.*

below 0.15 $Å^{-1}$ and noise dominates the transform above 0.8 $Å^{-1}$. As seen in Fig. 3a, the best fit arises for v.sini (LH_{α}332-20) – v.sini (HR 1136) = 35 km/s, giving a rotational velocity of 37 km/s for LH_{α}332-20. Figs. 3b to 3d show similar analyses for 3 other T Tauri stars.

Although this method is very powerful, accurate results can be obtained only from both very high signal-to-noise ratio (S/N = 300) and high resolution spectrograms. As a rule-of-thumb, the lowest rotational velocity which can be measured by this method is given by:

$$\text{v.sini (km/s)} = 1.0 \times \text{dispersion (Å/mm)}.$$

Since T Tauri are relatively faint objects it is difficult to fulfill both conditions except with large telescopes and state-of-the-art detectors. Indeed, Vogel and Kuhi, who used this method in 1981 (*Astrophysical Journal* **25,** 960) to determine the rotational velocity of pre-main-sequence stars could derive only upper limits of the rotational velocity for as much as 80 % of their sample. The most suitable instrument at La Silla for this method would be the CES on the CAT telescope owing to its very high resolution (R = 100,000). However, even with exposure times as long as 3 hours, a signal-to-noise of 300 cannot be reached for stars fainter than the sixth magnitude.

A less stringent method based on cross-corelation techniques can be used successfully for fainter stars. Cross-correlation works by shifting two spectrograms one relative to the other and calculating at each step a correlation coefficient which shows the degree of similarity between the two. For example, if both spectra are exactly the same, the correlation coefficient will be 1 when the spectrograms overlap and will decrease smoothly as the spectrograms are shifted. This will result in a correlation peak with a maximum value of 1. Fig. 4 shows the results obtained by applying this method to the two CASPEC spectrograms presented in Fig. 2. The spectrogram of ROX 21 was correlated with that of ROX 3 as reference, and the resulting correlation peak is shown as filled squares in Fig. 4. Then the spectrum of ROX 3 was artificially broadened by convolving it with rotation functions corresponding to different rotation values. The broadened spectra were correlated with the spectrum of ROX 3, and the resulting peaks are shown as broken and solid lines in Fig. 4. The full-widths at half-maximum of the latter and of the observed peak are then compared, with the best fit occurring for v.sini = 20 km/s.

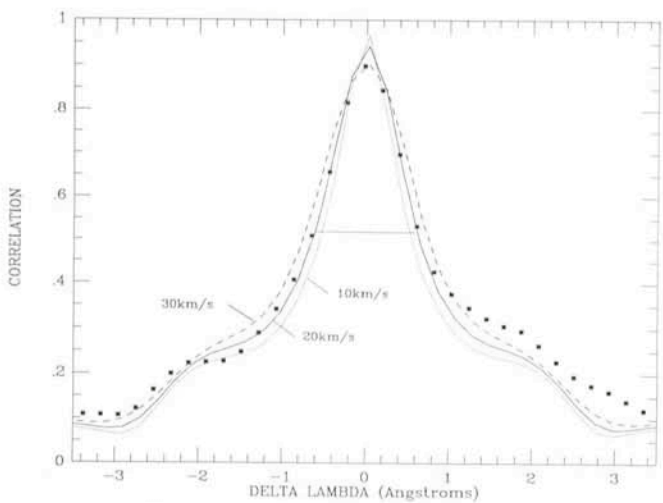

Fig. 4: *The observed correlation peak of the two spectrograms displayed in Fig. 2 is shown as filled squares and fitted by artificially broadened peaks for different values of the rotational velocity (see text). The best fit occurs for v.sini = 20 km/s. The large wings of the peak are caused by blends.*

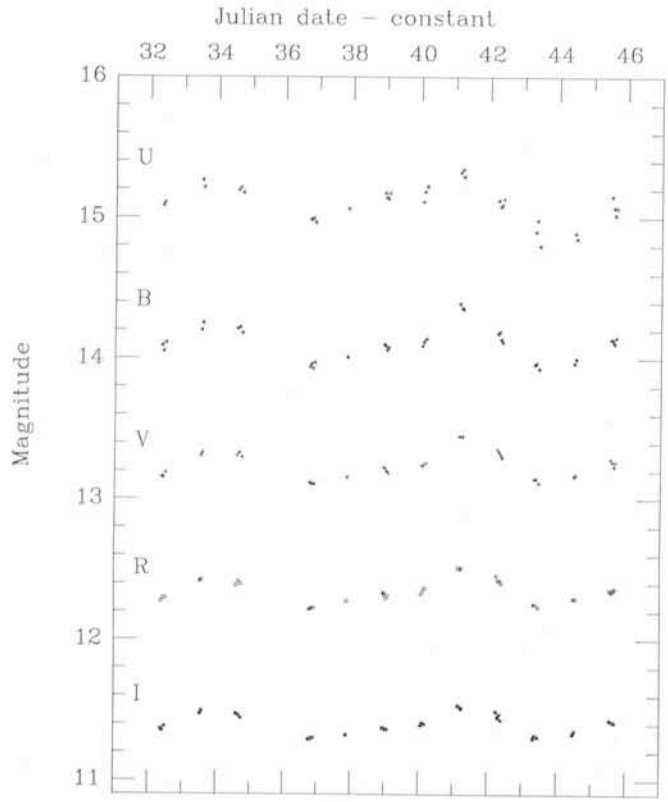

Fig. 5: *Light variations in five photometric bands of the T Tauri star SY Cha during 14 nights. The period of the variations is 6.12 days.*

Since ROX 3 is rotating at 7 km/s, we obtain 27 km/s for ROX 21. This is a more suitable method for studying T Tauri stars than are Fourier techniques since it can be used even in the case of relatively low signal-to-noise ratios (S/N = 50). However, high resolution is still necessary to measure slow rotators. For example, with CASPEC a signal-to-noise of 50 can be achieved on a 13th-magnitude star in one hour of exposure time, and its resolution of 20,000 allows one to determine rotational velocities as low as 10 km/s.

While the method just described is to be used for previously recorded spectrograms, a similar correlation technique is used on-line in the CORAVEL instrument, described in some detail by W. Benz and M. Mayor (1981, *Astronomy & Astrophysics* **93,** 235). Typical integration time on a 13th-magnitude T Tauri star with CORAVEL is 30 minutes and the detection limit is 2 km/s.

As mentioned above, all these spectroscopic methods will lead to a determination of the projected rotational velocity. Direct determination of equatorial velocities is possible for some late-type stars which possess large dark spots on their surfaces (cf. Rydgren et al., 1984, *Astronomical Journal* **89,** 7). Since these surface spots are cooler than the surrounding photosphere and are rotating with the stellar surface, the star will appear successively brighter and fainter as it rotates, depending on whether the spot is located on the hidden or the visible part of the stellar surface. This rotational modulation results in quasi-sinusoidal variations in the light curve of the star. The period of these variations will then allow the derivation of the true stellar equatorial velocity if the radius of the star is known, whatever the orientation of the rotation axis. It is a method which can determine the rotational velocity of slow as well as fast rotators, provided one gets enough observing time to follow the light curve of the slow stars during at least 1.5 periods and as long as the sampling of the light curve is narrow

enough for the fast stars. Moreover, this method can be applied to very faint objects since accurate photometry can be achieved at the 1 m telescope for stars as faint as m = 16.

Some T Tauri stars show periodic light curves that are interpreted in this manner. Among them is SY Cha, which was observed during 14 nights in February 1984 at the La Silla 1 m telescope equipped with the UBVRI photometer. Fig. 5 shows the light variations displayed in each photometric band during the observing run. Although the variations are not sinusoidal, meaning that the spot covers a non-negligible portion of the stellar photosphere, a periodicity of about 6 days can clearly be seen. Applying a period-finding algorithm developed on the VAX computer at La Silla by E. Zuiderwijk, we found a rotation period of 6.12 days which leads to a rotational velocity of 21 km/s if the radius equals 2.5 $R_\odot$. This method is only applicable to stars for which rotational modulation due to surface spots is not hidden by the apparently random photometric variations exhibited by most active T Tauri stars. Uncertainties about radii of T Tauri stars also remain a problem for this method's accuracy.

Rotation and X-ray Emission

Applying the different methods described above, we were able to derive rotational velocities for 12 T Tauri stars, 6 of them located in the ϱ Ophiuchi region. In doing so, CORAVEL proved to be best for our purposes, and we wish to thank both M. Mayor for kindly proposing the use of this instrument for this programme and W. Benz for conducting the CORAVEL observations on the 1.5 m Danish telescope at La Silla in June 1984. The following discussion is based on rotation rates of 20 T Tauri stars, 8 of which were available in the literature.

In Fig. 6 we plot X-ray luminosity versus projected rotational velocity for late-type main-sequence stars (G to M), for T Tauri stars and for RS CVn systems. Late-type main-sequence stars are represented by empty symbols, RS CVn systems by star symbols and T Tauri stars by filled triangles. Vertical bars associated with T Tauri stars represent the observed range of variability in X-ray luminosity, and horizontal bars are the uncertainties on the projected rotational velocities.

RS Canis Venaticorum systems are active late-type spectroscopic binaries. Their large rotational velocities arise from the synchronization of their angular and orbital motions. That they are located higher in Fig. 6 than T Tauri stars is only the result of a selection effect since accurate rotational velocities are known only for the most active systems; X-ray surveys including T Tauri stars and RS CVn systems show that they display the same range of X-ray luminosities. A least-square fit performed on the data of Fig. 6 shows that the X-ray luminosity scales approximately as the square of the rotational velocity. Pallavicini found the same relationship for a sample of late-type main-sequence stars, and showed its consistency with predictions of stellar dynamo models.

It thus appears likely that the mechanism responsible for X-

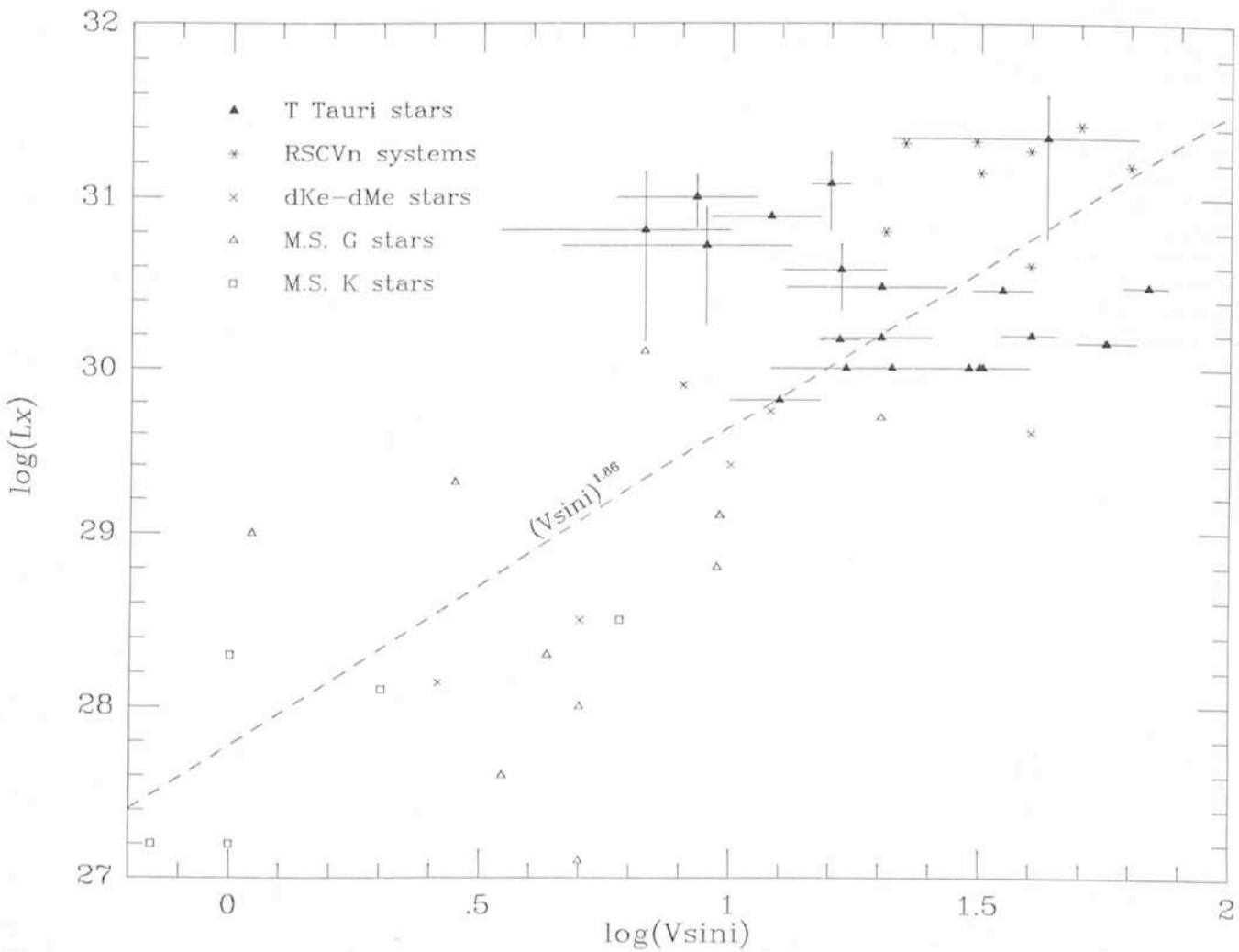

Fig. 6: *X-ray luminosity versus projected rotational velocity for late-type main-sequence stars, RS CVn systems and T Tauri stars (see text for details).*

ray emission is the same in late-type main-sequence stars, RS CVn systems and T Tauri stars. The enhanced X-ray emission displayed by T Tauri stars and RS CVn systems compared to main-sequence stars can be accounted for by their higher rotational velocities. Since X-rays originate from coronae in main-sequence late-type stars and RS CVn systems, this result suggests the presence around T Tauri stars of coronae responsible for a relatively low-level X-ray emission (of the order of 10^{30}erg/s) onto which strong flare-like eruptions are superimposed. The existence of coronae around T Tauri stars has been a topic of controversy in recent years, and this result may represent the best, albeit indirect, piece of evidence for coronae to date.

Conclusions and Prospects

An important aspect of our results is that the RS CVn class can be used as a "stick" to measure magnetic surface activity in T Tauri stars. Since RS CVn stars are not fully understood yet, it is not a perfect measuring stick; but it is a definite help, since by comparing the different properties of T Tauri stars to those of RS CVn systems, we can, at least in principle, find out which are due to magnetic activity and which must be accounted for by other physical mechanisms.

To reach this goal, various activity indicators in both T Tauri and RS CVn stars must be observed systematically, and their relationship with rotation studied. For example, we plan to follow chromospheric indicators such as the Ca II H and K lines over at least one rotation period to find out the range of variation of their flux and to study possible correlations with phase. We already know that Hα emission strength is not correlated to rotation rate, which means that Hα emission is probably not directly related to magnetic activity, but a detailed study of Hα variability would be needed to confirm this result. Also, more data are needed on the rotation rates of T Tauri stars in order to improve statistics and to allow us to study correlations within the T Tauri class. But thanks to the friendliness of our Swiss colleagues and to CORAVEL's excellence, we know now that this is possible even for faint T Tauri stars.

Double Emission and Line Absorption Doubling in Mira Stars: A New Approach

D. Gillet and P. Bouchet, ESO
R. Ferlet, Institut d'Astrophysique de Paris
E. Maurice, Observatoire de Marseille

The spectra of Mira variables present a large number of emission and absorption lines which vary in strength and profile with phase. According to current models, these lines are the consequence of strong shock waves propagating through the stellar atmosphere. However, the dynamics of the shock propagation is so far not completely understood, and the interpretation of the emission and absorption line variability can only be made through semi-empirical models. Extensive studies during a whole variability period (Hinkle, Scharlach and Hall, 1984; Gillet, Maurice, Bouchet and Ferlet, 1985; hereafter: GMBF) can provide fundamental clues to the knowledge of the underlying physics. In the present note, through two examples, we show that it is possible to know the dynamical and physical conditions of the line emitting regions, using high resolution optical observations with modern detectors. All observations presented hereafter have been obtained with the Coudé Echelle Spectrometer (CES) of ESO equipped with a 1872-diode Reticon. The 1.4 m Coudé Auxiliary Telescope (CAT) or 3.6 m telescope were used to feed the CES. The resolving power was between 80,000 and 100,000. In the case of the 3.6 m telescope, the observations were obtained through a fiber optic link whose details are given in Lund and Ferlet (1984).

The Double Hα Emission Line: A Fundamental Geometric Effect

It is a classical result that the Balmer emission profiles in cool Mira stars present strong mutilations very likely due to absorptions by atoms and molecules of the upper atmosphere, i.e. above the shock wave (Joy, 1947). In o Ceti, these absorptions disappear before the luminosity minimum (phase ~0.36) when the shock reaches the low density part of the atmosphere (Gillet, Maurice, Baade, 1983; hereafter: GMB and Fig. 1a). In S Car, the effective temperature is too high during the luminosity maximum, and the profile does not show any mutilations (GMBF and Fig. 1b).

The wavelength scale in these two figures is given in the rest frame of the stars. It is obvious that there is a strong absorption centred at the laboratory wavelength. For o Ceti, it appears clearly around phase 0.4 when the redshifted emission component is fully developed, whereas it is already visible at the luminosity maximum for S Car.

We suggest that this large absorption is intrinsically different from the narrow absorptions observed in the blueshifted emission component of o Ceti around the luminosity maximum and discussed above. This absorption is only apparent and is the consequence of a geometrical effect. Indeed, if one assumes that the front velocity is high (70–80 km/s), the shock will reach already around phase 0.4 a layer far from the photosphere. The observer would then begin to receive the emission from the part of the shock propagating away from him, previously occulted by the stellar disk, and corresponding to the redshifted component. In this frame, the large absorption is not real, contrary to what was previously assumed in the literature.

This interpretation is consistent with the high shock front velocities deduced from the detailed Hα profile studies by GMB and GMBF, and with the jump velocities derived from the fluorescent lines by Willson (1976). Note that the presence of both emission components already at the luminosity maximum in the hot Mira star S Car is explained by the absence of a dense molecular atmosphere contrary to o Ceti (see GMBF).

The True Nature of the Absorption Line Doubling Phenomenon

It is another classical result that around the luminosity maximum many absorption lines in the near-infrared and infrared ranges are observed double. The current interpretation assumes the existence of two atmospheric regions with different velocities (two-component model), as a consequence of the propagation of the shock through the atmosphere (Wing, 1980).

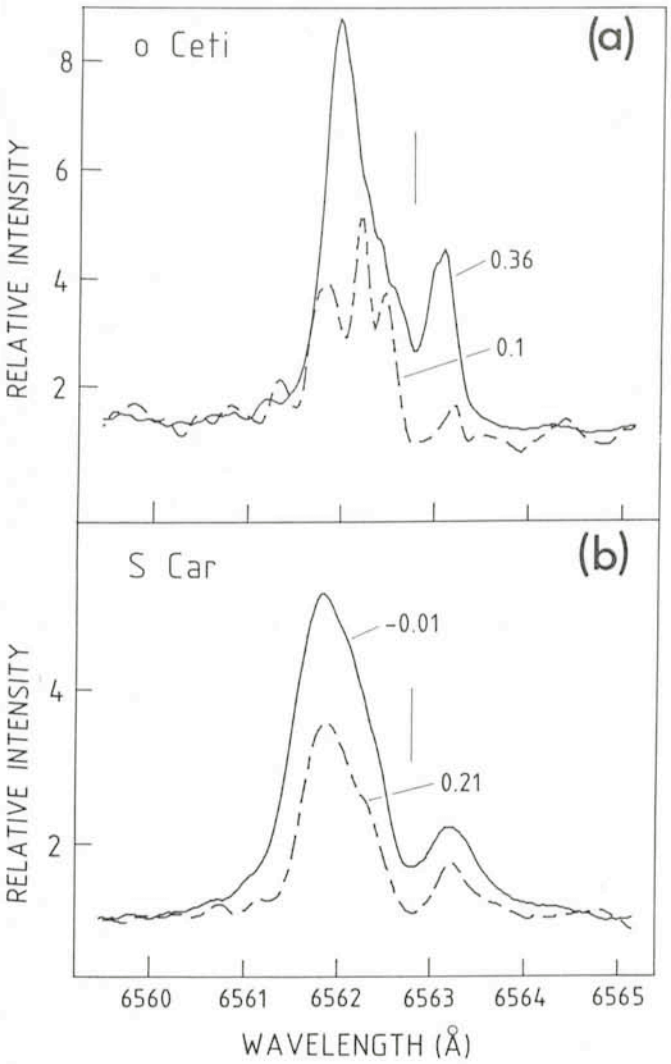

Fig. 1: *CES-Reticon spectra of Hα emission profiles in two Mira stars observed with a resolution of 66 mÅ. The wavelength scales are in the rest frame of the stars and the Hα laboratory wavelength is indicated by a vertical line.*

(a) in o Ceti at phases 0.1 and 0.36 (0.0 is the luminosity maximum). At 0.10, there are large mutilations within the profile due to molecular absorptions. These absorptions are virtually absent at 0.36, but the emission shows a blueshifted and a redshifted component.

(b) in the hot Mira star S Car at phases −0.01 and 0.21. There are no mutilations, but the two emission components are already well visible from luminosity maximum.

This phenomenon is well observed in the infrared (0.8–5 μm) because, in the blue, spectra of Mira stars are extremely blended. S Car offers a further advantage because its effective temperature is so high at luminosity maximum (3,600 K or K5e type) that the profiles are practically free of blend (compare Figs. 2 and 3). Fig. 2 shows the two bluest lines of the CaII infrared triplet, along with some FeI and TiII lines, observed at phases 0.05, 0.13 and 0.20. The result is striking at first glance: inverse CaII P-Cygni profile on top of a broad absorption; both P-Cygni and inverse P-Cygni characteristics for TiI at the same phases (0.05 and 0.13); the classical double absorption for FeI (Figs. 2b and 2c).

However, the FeI profile at phase 0.05 (Fig. 2a) presents a central emission above the continuum. Its relative intensity decreases from phases 0.05 to 0.20 to become weaker than the continuum, thus giving the classical double absorption profile. This strongly suggests that the FeI line doubling is only apparent, the real profile corresponding to an emission superposed on an underlying otherwise normal photospheric absorption.

On the other hand, the CaII, TiI and FeI emission intensities decrease together during the phase interval of Fig. 2. This variation is not due to the effect of the variation of the continuum because its intensity decreases. Therefore, one may think that these lines are affected by the same physical phenomenon and thus could be produced within the same emitting region.

Consequently, as the FeI lines are produced close to the photosphere, the CaII and TiI P-Cygni type are only apparent. They can be understood also by an emission superposed on an underlying photospheric absorption.

We propose that these different kinds of profiles might be formed during the ballistic motions of the atmospheric matter previously driven by the shock wave propagation (see Fig. 4). The large rate of thermal energy transferred from the front to the gas is realized during the ballistic motion which is by this fact not adiabatic. When the gas is in the ascending branch, the emission is blueshifted with respect to the laboratory wavelength, giving rise to an apparent double absorption line with a blue component weaker than the red one. When the

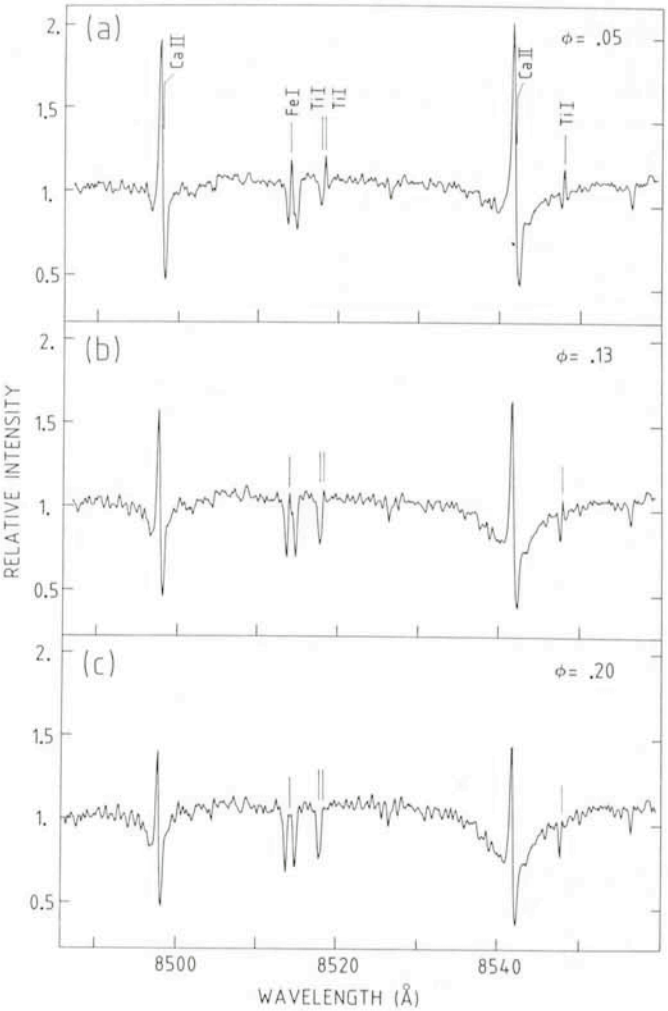

Fig. 2: *Near-infrared, CaII, FeI and TiII profiles in S Car just after the luminosity maximum. All these lines originate near the photosphere and their profiles are explained by ballistic motions due to the shock wave propagation. The P-Cygni types (CaII, TiI) and the double absorption lines are only apparent. Note that the majority of small features on the continuum are present on each spectrum and are certainly of stellar origin.*

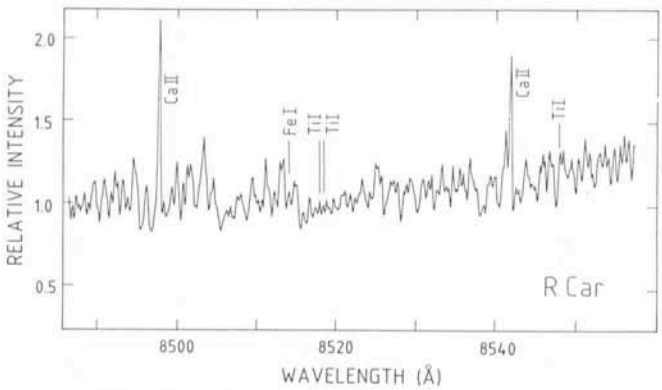

Fig. 3: *Approximately the same wavelength range, resolution (85 mÅ) and signal-to-noise ratio (~200) as in Fig. 2 but for a typical Mira star (R Car) also near the luminosity maximum. Here, the molecular blends do not permit observation of the intrinsic line profiles.*

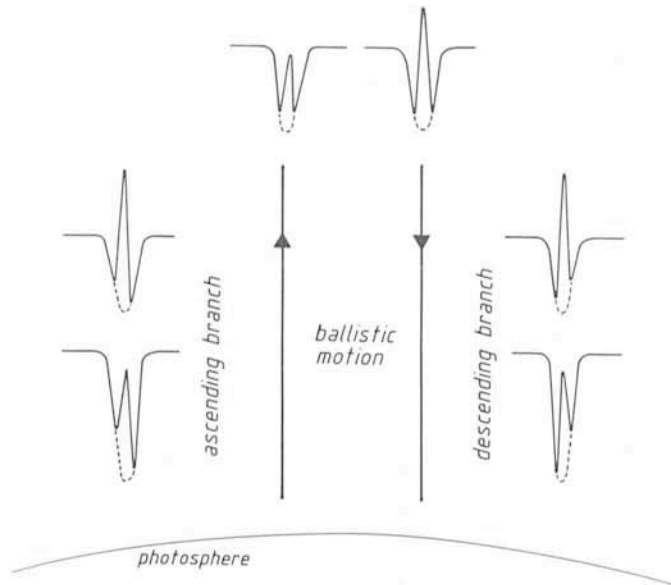

Fig. 4: *Schematic diagram showing the different types of profile expected to form during a ballistic motion close to the photoshere. Apparently like double absorption or P-Cygni types, these profiles are in fact made of an emission superposed on an underlying broad photospheric absorption (see text).*

matter reaches its maximum altitude, the emission is centred on the photospheric absorption and the two absorption components are equal. During the descending branch, one gets the symmetrical profiles to those of the ascending branch (Fig. 4).

A complete study of this line doubling phenomenon observed in S Car can be found in GMBF. Further high resolution, high signal-to-noise observations of other Mira stars are needed before generalizing our interpretation. It is not even yet established if all double absorption lines (like molecular ones) observable in S Car can be explained by the same mechanism.

Conclusion

Optical high resolution, high signal-to-noise ratio spectroscopy is well suited to tackle the atmospheric dynamical state of Mira stars. More generally, significant progress concerning our knowledge of all pulsating stars can be rapidly reached by using recent resources of line profile analysis.

We have shown here such examples, related to o Ceti and S Car. Their Hα profiles seem to indicate that the shock wave does not stay close to their photospheres. Also, the varying profiles observed in the near-infrared region of S Car seem incompatible with the classical interpretation of the so-called line doubling phenomenon (two-component model).

References

Gillet, D., Maurice, E., Baade, D.: 1983, *Astron. Astrophys.* **128,** 384.
Gillet, D., Maurice, E., Bouchet, P., Ferlet, R.: 1985, *Astron. Astrophys.,* submitted.
Hinkle, K.H., Scharlach, W.W.G., Hall, D.N.: 1984, *Astrophys. J. Suppl.* **56,** 1.
Lund, G., Ferlet, R.: 1984, *The Messenger* **36,** 2.
Joy, A.H.: 1947, *Astrophys. J.* **106,** 288.
Willson, L.A.: 1976, *Astrophys. J.* **205,** 172.
Wing, R.F.: 1980, *Current Problems in Stellar Pulsation Instabilities,* Eds. Fischel, D., Lesh, J.R., Sparks, W.M., p. 533.

W Serpentis Stars—A New Class of Interacting Binaries

W. Strupat, H. Drechsel and J. Rahe, Remeis-Sternwarte, Bamberg

Introduction

In August 1978, Plavec and Koch made the first IUE satellite observations of a group of eclipsing binaries known for their complex photometric and spectroscopic behaviour in the optical range, namely W Serpentis, RX and SX Cassiopeiae, W Crucis, and AR Pavonis.

The UV spectra were very conspicuous, showing a wealth of pronounced emission lines, e.g., resonance lines of relatively high ionization stages like NV, CIV, SiIV, OIII, AlIII or FeIII as well as intercombination and forbidden lines of, e.g., CIII, NIV, and OIII, while no absorptions could be detected at all.

The remarkable similarity of the IUE spectra suggested comparable physical conditions at the place of origin of these lines, especially in the circumbinary region, where a large amount of circumbinary matter must exist.

The presence of high ionization lines in both UV and optical ranges is surprising, since neither of the two binary components is apparently hot enough to supply the ionizing photons; except for AR Pav, all objects are of spectral type later than A5. All members of the considered object class have semi-detached or contact configurations: in the case of, e.g., W Cru and RX Cas, the Wilson-Devinney approach was used to analyze their photometric light curves; convergence could only be achieved in the contact mode. Some features are similar to those observed in symbiotic stars and RS CVn binaries.

There are several further indications of a possible relationship between these stars, e.g., strongly distorted radial velocity and light curves and orbital period changes; one might conclude that these objects are presently in an active evolutio-

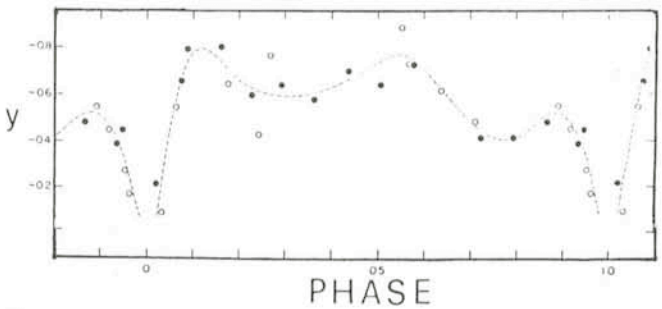

Fig. 1: *y-light curve of W Ser after Lynds (1957); open and filled circles refer to observations in different epochs.*

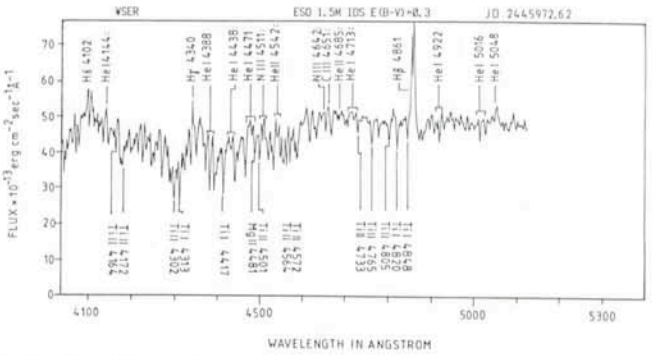

Fig. 3: *Blue IDS spectrum of W Ser, taken at orbital phase Φ = 0.16.*

nary stage, probably in the phase of rapid mass transfer or shortly after the reversal of the mass ratio, when mass loss through the Lagrangian points is expected. This overall similarity of physical properties and interaction processes and the fact that the observed common characteristics cannot fully account for the definition pattern of any subgroup of close binaries led Plavec to "invent" a new class of interacting binary systems, called "W Serpentis objects".

However, in spite of extensive observations, a precise definition of the actual evolutionary stage and of exact parameters of these highly interacting systems has not been possible so far. This was reason enough to establish a still ongoing programme to take a closer look at these objects, incorporating observations from different spectral ranges between the UV and IR regions.

In this article, we describe some results of recent ESO observations of the prototype W Serpentis, obtained by means of simultaneous spectroscopic (ESO 1.52 m telescope + IDS) and photometric (ESO 1 m telescope, UBVRI) measurements performed in September 1984.

Photometry

The light curve of W Serpentis is very unusual for an eclipsing binary: there are three maxima between two successive primary minima, due to appreciable light depression close to quadrature phases (see Fig. 1). Lynds (1957) gives for the elements of heliocentric primary minimum: HJD = $2435629^d.60 + 14^d.15667 \times E$; the period is increasing with the considerable rate of about 15 seconds per year.

The period increase is confirmed by a comparison of our recent photometric measurements with the data of Lynds

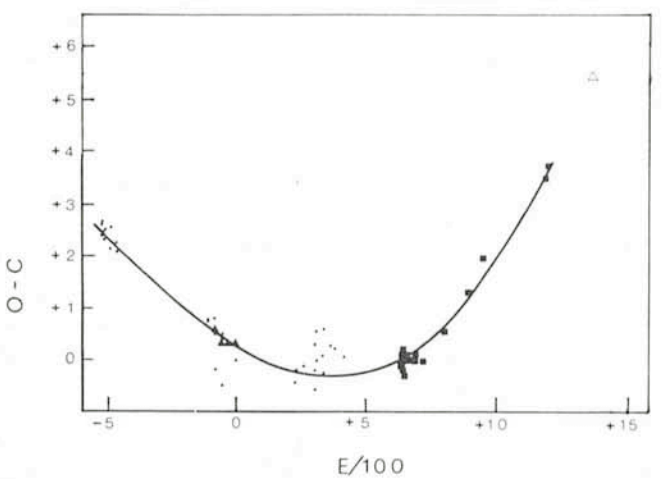

Fig. 2: *(O–C) diagram of W Ser according to Koch and Guinan (1978). (O–C) is given in days; the zero epoch corresponds to JD_o = $2426625^d.493$. The meaning of the symbols is explained in the text.*

yielding a phase difference of $\Delta\Phi = 0.445$. The resulting (Observed-Computed) value of $5^d.477$ fits well into the (O-C) diagram and is represented by an open triangle in Fig. 2. The least squares cubic polynomial fit of the data as a function of epoch is shown as a smooth line; photoelectric, photographic and visual observations are given as squares, circles and filled triangles, respectively.

Spectrophotometry

UBVRI magnitudes have been converted into absolute fluxes and used in combination with our optical and UV spectra to derive the absolute continuum flux distribution of W Ser (de-reddened with $E_{B-V} = 0.30$ mag) over a broad range. Close to quadrature phase, the spectrum is reasonably well represented by a blackbody of 6,600 K. During the primary minimum, however, when the secondary should contribute the largest relative fraction to the observed flux, the spectral distribution of the reduced light remains essentially unchanged. As the shape of the light curve indicates that the eclipse is not total, one can conclude that the residual intensity of the optical continuum at primary minimum still arises mainly from the primary component, while the contribution of the secondary is negligible in this spectral region.

The observed flux distribution agrees with spectral classification of the primary as F4III. Since the flux in the UBVRI region is steadily decreasing towards longer wavelengths, we conclude that the secondary must be a very cool object, which agrees with its spectroscopic undetectability in the optical and UV ranges. Assuming central eclipses, the depth of the primary minimum yields a value of about 0.7 for the ratio of radii R_2/R_1 of the two components. With a radius of the F4III primary of $R_1 \sim 5R_\odot$, we obtain $R_2 \sim 3.5R_\odot$; with an effective temperature of, say, 3,100 K for an M subgiant, its luminosity amounts to about $1L_\odot$, which is only a few per cent of the luminosity of the primary component, and thus explains that it has so far not been detected spectroscopically.

Spectroscopy

Figs. 3 and 4 show blue and red IDS spectra of W Ser in the range between 4000 and 5200 Å, and between 4500 and 6500 Å, respectively, obtained at orbital phases $\Phi = 0.16$ and $\Phi = 0.30$. The optical spectrum is dominated by strong Hydrogen Balmer, HeI and HeII lines, some of which are identified in the figures.

The profiles of the Balmer lines display broad emission components with superimposed central absorptions. The Hβ profile, as observed at orbital phase $\Phi = 0.16$, is shown in Fig. 5. An especially striking feature is the inverse P Cygni profile of the HeI triplet line at 5876 Å; a similar profile shape is also indicated at Hβ (see Fig. 4).

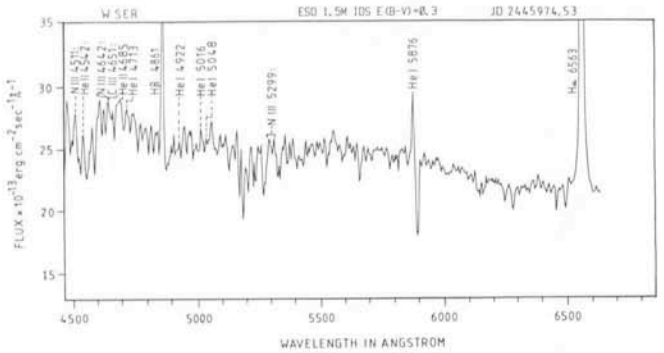

Fig. 4: *Red IDS spectrum taken at orbital phase Φ = 0.30.*

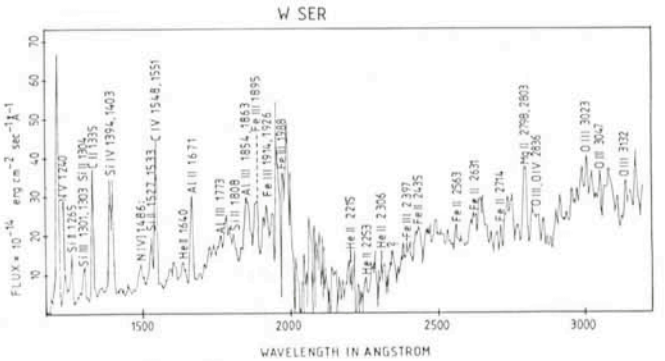

Fig. 6: *IUE spectrum of W Ser (SWP 22414 + LWP 2890) taken at the same orbital phase.*

The central absorption dips are conceivably due to a stream of matter transferred from the cool secondary contact component to the hotter primary; the double-peaked emission may also arise from a gaseous ring around a detached primary. The red-shifted absorption component of the inverse P Cygni profile of HeI (5876 Å) in a spectrum taken close to the quadrature phase 0.25 can be explained by the motion of the primary (with a velocity component in the direction of the observer) relative to a nearly stationary circumstellar envelope surrounding the whole binary system.

As a typical example for the W Ser class, the spectral appearance in the UV range of the prototype W Ser is illustrated in Fig. 6. Our combined SWP and LWP IUE spectra show a wealth of strong UV emission lines of partly semi-forbidden intercombination or forbidden transitions, as indicated in the figure.

Evolutionary Stage

Even with a very low effective temperature of $T_2 \sim 3{,}000$ K, the secondary still has approximately solar luminosity, and therefore appears overluminous for its mass, so that we are presumably dealing with an evolved M-type subgiant. This would imply that the system has already passed through the first phase of rapid mass transfer during which the mass ratio was reversed on a thermal Helmholtz-Kelvin time scale, and primary and secondary have interchanged their roles. In the course of this short-lived scenario, the originally more massive primary became an inconspicuous cool star—slightly evolved and probably close to the Hayashi limit—, while the mass gainer first moved up the main sequence and then evolved along the giant branch, where it can presently be observed.

Close binary evolution theory predicts that the previously more massive star is still in contact with its Roche lobe, and continues to transfer matter onto its companion at a rate which has been reduced as a consequence of re-establishment of thermal equilibrium and due to the fact that the evolution time scale of the original primary has now slowed down to a nuclear one.

The observed properties of W Ser are in qualitative agreement with what is expected in such a situation:

– mass transfer in a direction from the less massive to the more massive component can explain the observed increase of the orbital period;

– the continuing mass exchange is further assumed to be non-conservative, particularly in view of the present binary configuration as a near contact system, consisting of two evolved stars which fill their Roche limits;

– gaseous streams will arise and a large amount of circumstellar matter will accumulate around the binary, since the radiation pressure of only slightly evolved intermediate- and late-type stars is not effective enough to be the driving mechanism of a massive wind. Thus, the high ionization level can be explained in terms of accretion shock heating or acoustic wave dissipation in extended chromospheric regions.

It is too early to outline a more sophisticated model of these complex systems, which definitely deserve enhanced attention in the future, especially with respect to their importance for binary evolution theory.

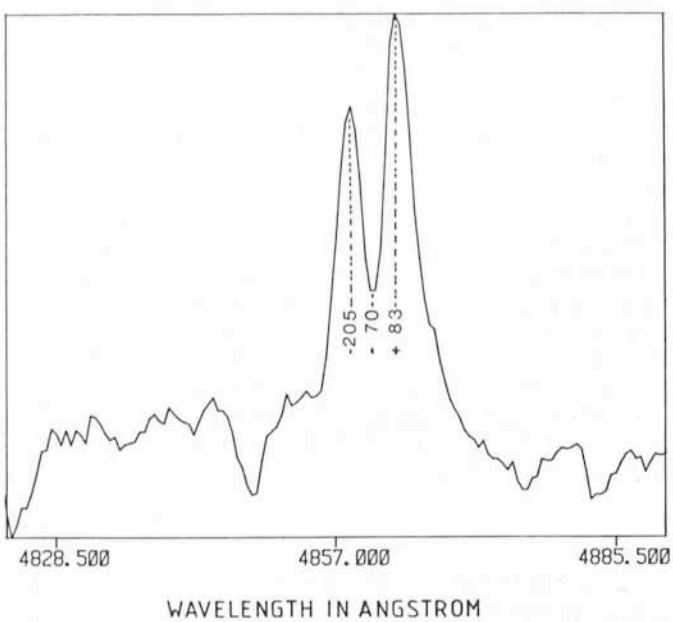

Fig. 5: *Hβ profile of W Ser at orbital phase Φ = 0.16; the numbers give the radial velocities in km sec^{-1}.*

References

Koch, R.H., Guinan, E.F.: 1978, *IBVS* **1483.**
Lynds, C.R.: 1957, *Ap.J.* **126,** 81.
Plavec, M., Koch, R.H.: 1978, *IBVS,* **1482.**

Visits to La Plata Observatory

La Plata Observatory will welcome visitors to ESO-La Silla that are willing to make a stop at Buenos Aires on their trip to Chile or on their way back. There is a nice guesthouse at the Observatory that can be used, for a couple of days or so, by astronomers interested in visiting the Observatory and delivering talks on their research work to the Argentine colleagues. No payments can, however, be made at present. La Plata is at 60 km from Buenos Aires. In the same area lie the Instituto de Astronomía y Física del Espacio (IAFE), in Buenos Aires proper, and the Instituto Argentino de Radioastronomía (IAR), about 40 km from Buenos Aires on the way to La Plata. Those interested should contact: Sr Decano Prof. Cesar A. Mondinalli, or Dr Alejandro Feinstein, Observatorio Astronómico, Paseo del Bosque, 1900 La Plata, Argentina. Telex: 31216 CESLA AR. *A. Feinstein*

STAFF MOVEMENTS

Arrivals

Europe

ADORF, Hans-Martin (D), Fellow, ST/ECF
BÜCHERL, Helmut (D), Electro-mechanical Technician
FONTANA, Silvana (I), Head of Personnel Service
MERKLE, Fritz (D), Optical Engineer/Physicist
OCHSENBEIN, François (F), Astronomer/Data Archivist
RUSSO, Guido (I), Fellow, ST/ECF

Chile

GOUIFFES, Christian (F), Cooperant
LACOMBE, François (F), Cooperant

Departures

Europe

DIEBOLD, Lothar (D), Photographer
MARGUTTI, Pietro (I), Programmer
VÉRON, Marie-Paule (F), Associate
VÉRON, Philippe (F), Associate

Chile

KAABERGER, Stig Ulf (S), Electro-mechanical Engineer

Émotion du docteur Véron se croyant poursuivi par un chien enragé

This issue of the "Messenger" is the last one prepared by P. Véron who is leaving ESO. For those who have not had the opportunity to meet him, we are publishing here a cartoon depicting him, drawn by the famous French cartoonist Honoré Daumier (1808–1879).

(In the meantime Dr. Véron has been appointed director of the Observatoire de Haute-Provence.)

Esta edición del «Mensajero» es la última preparada por P. Véron quien abandona ESO. Para aquellos que no tuvieron la oportunidad de conocerlo publicamos una caricatura que lo retrata, hecha por el famoso caricaturista francés Honoré Daumier (1808–1879).

(Entretanto el Dr. Véron fue designado director del Observatoire de Haute-Provence.)

VLT News

In the context of the VLT activities, the Director General of ESO has appointed the members of five working groups. The names of the persons appointed are listed below. The chairmen of these committees augmented with M.-H. Demoulin-Ulrich and P. Shaver (ESO) form the VLT Advisory Committee chaired by J.-P. Swings (Liège).

VLT WORKING GROUPS—LIST OF MEMBERS

SITE SELECTION

A. Ardeberg (Lund)
M. Sarazin (ESO)
H. van der Laan* (Leiden)
J. Vernin (Nice)
G. Weigelt (Erlangen)
H. Wöhl (Freiburg)

INTERFEROMETRY

O. Citterio (Milano)
D. Downes (IRAM)
A. Labeyrie (CERGA)
P. Lena* (Paris)
J.E. Noordam (Dwingeloo)
F. Roddier (Nice/NOAO)
J.J. Wijnbergen (Groningen)
R. Wilson (ESO)

HIGH RESOLUTION SPECTROSCOPY

I. Appenzeller* (Heidelberg)
D. Baade (ESO)
L. Delbouille (Liège)
S. D'Odorico (ESO)
D. Dravins (Lund)
P. Felenbok (Meudon)
M. Mayor (Genève)
P.E. Nissen (Aarhus)
J. Solf (MPI Heidelberg)

LOW RESOLUTION SPECTROSCOPY + IMAGING

H.R. Butcher* (Groningen)
J. Danziger (ESO)
M.-H. Demoulin-Ulrich (ESO)
M. Dennefeld (IAP)
S. di Serego Alighieri (ST/ECF)
B. Fort (Toulouse)
T. Gehren (Munich)
C. Jamar (Liège)
P. Shaver (ESO)

INFRARED ASPECTS

B. Carli (Florence)
E. Kreysa (Bonn)
D. Lemke (MPI Heidelberg)
A. Moorwood* (ESO)
G. Olofsson (Stockholm)
P. Salinari (Florence)
F. Sibille (Lyon)

* Chairman

ALGUNOS RESUMENES

Buscando estrellas de carbón . . . . . y encontrando un quasar de gran corrimiento al rojo

En el contexto de una investigación de estrellas de carbón en galaxias enanas esféricas que son satélites de nuestra galaxia, realizada por los profesores Lequeux y Westerlund y el Dr. Azzopardi, se observó la galaxia Carina (descubierta en 1977 por Cannon y sus colaboradores y la última de las ya siete conocidas) en Noviembre de 1983. Con el corrector de campo amplio en el foco primario del telescopio de 3.6 m se obtuvo una placa Grism de muy buena calidad. Esta placa, que muestra miles de espectros, fue investigada sistemáticamente con un microscopio y se descubrieron 5 nuevos candidatos a estrellas de carbón además de 6 estrellas de carbón ya conocidas. Estrellas de carbón son objetos estelares rojos muy luminosos y bastante escasos. Las capas externas de la atmósfera de estas estrellas viejas han sido altamente enriquecidas por el carbón formado en sus regiones centrales.

Durante las noches del 23 al 24 de Noviembre de 1984 y del 19 al 21 de Enero de 1985, estos cinco nuevos candidatos a estrellas de carbón fueron observados con el espectrógrafo Boller & Chivens y la cámara CCD en el foco Cassegrain del telescopio de 3.6 m. Durante estas observaciones, tres estrellas fueron positivamente identificadas

como estrellas de carbón y una fue clasificada como una enana M tardía. Sin embargo, el quinto objeto resultó ser un quasar con un gran corrimiento al rojo de Z = 3.09. Hasta ahora se han encontrado pocos objetos de esta clase (alrededor de un 2 % de los quasares registrados en el catálogo de quasares y núcleos activos hecho por Véron y Véron (1984) tienen un corrimiento al rojo superior a 3.0). Quasares o QSOs (Quasi Stellar Objects = objetos cuasi estelares) tienen propiedades muy extraordinarias. Las más notables son su gran luminosidad, variabilidad y pequeños tamaños. La gran luminosidad de los quasares permite a éstos ser vistos a muy lejanas distancias; por otro lado su gran corrimiento al rojo, el cual está relacionado a su velocidad, refleja la expansión del universo. Son probablemente los núcleos activos de galaxias.

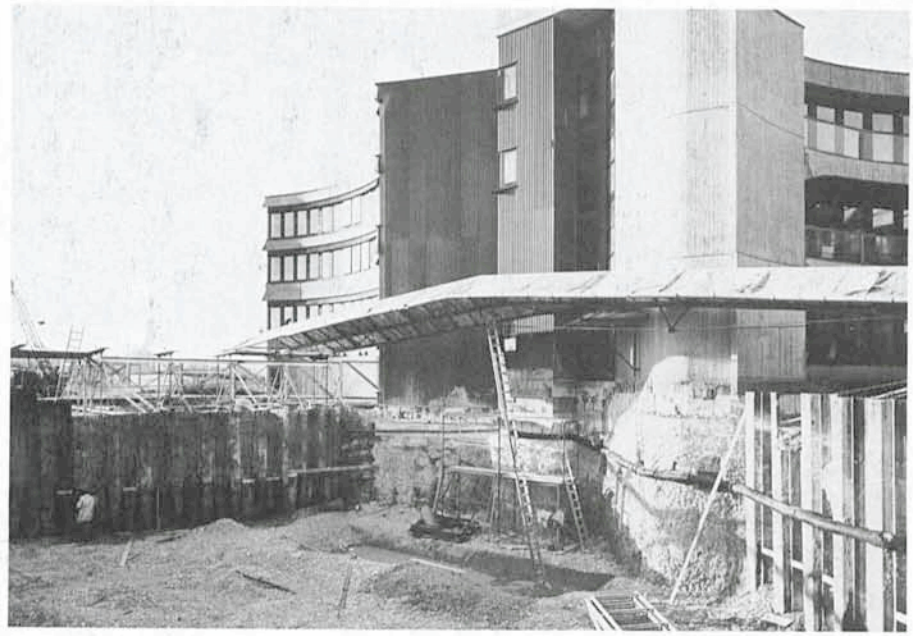

Extension of the ESO Headquarters building in Garching has become necessary. This picture shows that the work has already started; new office space should become available at the beginning of 1986.

Ha sido necesario ampliar el edificio principal de ESO en Garching. Esta fotografia muestra que los trabajos ya han comenzado; a principios de 1986 se deberá poder contar con nuevas oficinas.

Contents

ESO, the European Southern Observatory, was created in 1962 to . . . establish and operate an astronomical observatory in the southern hemisphere, equipped with powerful instruments, with the aim of furthering and organizing collaboration in astronomy . . . It is supported by eight countries: Belgium, Denmark, France, the Federal Republic of Germany, Italy, the Netherlands, Sweden and Switzerland. It operates the La Silla observatory in the Atacama desert, 600 km north of Santiago de Chile, at 2,400 m altitude, where thirteen telescopes with apertures up to 3.6 m are presently in operation. The astronomical observations on La Silla are carried out by visiting astronomers – mainly from the member countries – and, to some extent, by ESO staff astronomers, often in collaboration with the former. The ESO Headquarters in Europe are located in Garching, near Munich.
ESO has about 120 international staff members in Europe and Chile and about 120 local staff members in Santiago and on La Silla. In addition, there are a number of fellows and scientific associates.

The ESO MESSENGER is published four times a year: in March, June, September and December. It is distributed free to ESO personnel and others interested in astronomy.
The text of any article may be reprinted if credit is given to ESO. Copies of most illustrations are available to editors without charge.

Editor: Philippe Véron
Technical editor: Kurt Kjär

EUROPEAN
SOUTHERN OBSERVATORY
Karl-Schwarzschild-Str. 2
D-8046 Garching b. München
Fed. Rep. of Germany
Tel. (089) 32006-0
Telex 5-28282-0 eo d

Printed by Universitätsdruckerei
Dr. C. Wolf & Sohn
Heidemannstraße 166
8000 München 45
Fed. Rep. of Germany

ISSN 0722-6691